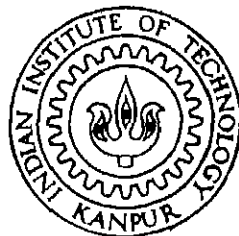


# BEHAVIOUR OF STEEL EMBEDDED PLATES IN R. C. C. STRUCTURES : A PARAMETRIC STUDY

by

Rajasekher Panisetty

CE  
1997  
M  
PAN  
BEH



DEPARTMENT OF CIVIL ENGINEERING

INDIAN INSTITUTE OF TECHNOLOGY KANPUR

March, 1997

# BEHAVIOUR OF STEEL EMBEDDED PLATES IN R.C.C. STRUCTURES : A PARAMETRIC STUDY

A THESIS SUBMITTED  
IN PARTIAL FULFILLMENT OF THE REQUIREMENTS  
FOR THE DEGREE OF  
MASTER OF TECHNOLOGY

By

Rajasekher Panisetty

*to the*

DEPARTMENT OF CIVIL ENGINEERING  
INDIAN INSTITUTE OF TECHNOLOGY  
KANPUR-208016 INDIA

MARCH 1997

24 APR 1997 / CE

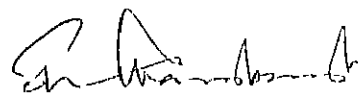
                      
123314  
Case No. A

CE-1997-M-PAN-BEH

dedicated  
to  
my Parents

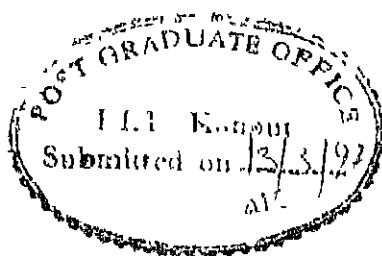
# Certificate

It is certified that this work entitled **BEHAVIOR OF STEEL EMBEDDED PLATES IN R.C.C. STRUCTURES : A PARAMETRIC STUDY**, by *Rajasekher Panisetty* has been carried out under my supervision and that this work has not been submitted elsewhere for a degree.



**(Dr. Sekhar K. Chakrabarti)**

Associate Professor  
Department of Civil Engineering  
Indian Institute of Technology  
Kanpur-208016 India



## Abstract

The Behavior and Capacity of Embedded Steel Plate-Anchor Assemblies in R C C Structures are studied with the help of the mathematical model developed for Non-linear Analysis. A detailed parametric study is performed varying the base and anchor stiffness for different plate thicknesses to observe the behavior of anchor both in compressive and tensile loading. The behavior of the assembly, when subjected to tensile and shear loading is studied. Interaction diagrams and moment-rotation charts useful for analysis/design of such assemblies, are developed for eccentric compressive and eccentric tensile loading at failure/collapse loads. A study has been made to evaluate the interaction diagrams developed for the cases of eccentric compressive loading, when shear loading is also present in combination.

# Acknowledgement

I take this opportunity to thank Dr S.K Chakrabarti for his invaluable guidance and encouragement at every stage of difficulty, throughout my stay. I extend my thanks to the family of Dr S.K.Chakrabarti for their kindness and affection. I am extremely grateful to all the Professors in Structural Engineering Department, for their concern and pleasant company. My special thanks to Dr C.V.R. Murthy for being very friendly and encouraging during my stay. I am extremely thankful to Dr R.C.Mishra for his co-operation and useful discussions during the course of thesis work.

I have no words to express the everlasting memories shared with Jaswant, Pradeep, Shubha, Ruchi, Bidisha, Rajaneesh, Gloverji, Bhabhiji and Silvi. I thank all of them for their affection, guidance and encouragement. My sincere thanks to Acharya for the discussions made in course of the thesis work.

I thank Chowdary and his family, Mishra and his family for being very considerate to me. I thank my seniors Aparna, Varsha, K.S.N., batchmates, hostelmates and all the juniors of Structures for making my stay a pleasant one in I.I.T Kanpur.

**Rajasekher Panisetty**

# Contents

Acknowledgement	ii
List of Figures	v
<b>1 INTRODUCTION</b>	<b>1</b>
1.1 Introduction . . . . .	1
1.2 Literature-Review . . . . .	8
1.2.1 Past Studies on Plates - . . . . .	9
1.2.2 Past Studies of Plates on Elastic Base . . . . .	9
1.2.3 Past Studies on Anchors . . . . .	11
1.2.4 Past Studies on Plate-Anchor Assemblies - . . . . .	11
1.3 Objectives and Scope of the Thesis . . . . .	14
1.4 Organisation of Present Study . . . . .	15
<b>2 MATHEMATICAL MODEL</b>	<b>16</b>
2.1 Introduction . . . . .	16
2.1.1 Common Modes of Failures:- . . . . .	17
2.1.2 Governing Equations of the Structure . . . . .	18
2.1.3 Details of the Mathematical Model Adopted.- . . . .	21
<b>3 Behavior of Assembly : A Parametric Study</b>	<b>27</b>
3.1 Introduction . . . . .	27
3.2 Study on Anchor Tension in Plate-Anchor Assemblies subjected to Eccentric Compressive loading . . . . .	28
3.3 Study on Anchor Tension and Assembly Capacity in Plate-Anchor Assemblies subjected to Tensile Loading . . . . .	39



3 4	Study on Assembly Capacity in Plate-Anchor Assemblies subjected to Shear Loading . . . . .	44
3 5	Study for the Development of Strength Interaction Diagrams and Moment-Rotation Charts for Plate-Anchor Assemblies subjected to Eccentric Compressive Loading . . . . .	47
3 6	Study for the Development of Strength Interaction Diagrams and Moment-Rotation Charts for Plate-Anchor Assemblies subjected to Eccentric Tensile Loading . . . . .	51
3 7	Study for the Evaluation of the Interaction Diagrams for Plate Anchor Assemblies subjected to Eccentric Compressive Loading and Shear Loading .	53
4	ANALYSIS OF RESULTS	60
4 1	Plate-Anchor Assemblies subjected to Eccentric Compressive Loading .	61
4 1 1	Interaction Diagrams . . . . .	61
4 1 2	Moment-Rotation Charts . . . . .	67
4 2	Plate-Anchor Assemblies subjected to Eccentric Tensile Loading . . . .	74
4 2 1	Interaction Diagrams . . . . .	74
4 2 2	Moment-Rotation Charts . . . . .	75
4.3	Evaluation of Interaction Diagrams for Eccentric Compressive Loading combined with Shear Loading . . . . .	87
4 4	Deflected Shapes and Stress Contours . . . . .	87
5	Summary and Conclusions	90
5.1	Summary . . . . .	90
5 2	Conclusions . . . . .	91
5.3	Future Scope of Work . . . . .	93
	Bibliography	94

# List of Figures

1 1	Some typical cast-in-place steel embedded plates . . . . .	2
1 2	General Arrangement of Plates on elastic base . . . . .	4
1 3	General Arrangement of Plate-Anchor Assemblies . . . . .	5
1 4	Deflected shape and forces in Plate-Anchor Assemblies . . . . .	6
2 1	Embedded Plate-Anchor Assembly Model . . . . .	18
2.2	Typical Grid Pattern and 9 Noded Mindlin Element . . . . .	22
2.3	Moment-Curvature Relationship for Plates . . . . .	24
2 4	Idealised Stress-Strain Curve for Concrete Base . . . . .	25
2.5	Idealised Stress-Strain Curve for Anchors . . . . .	26
3 1	Variation of Anchor Tension for Anchor No. 1 with Anchor Stiffness at Collapse . . . . .	31
3 1	Variation of Anchor Tension for Anchor No. 1 with Anchor Stiffness at Collapse . . . . .	32
3 2	Variation of Anchor Tension for Anchor No. 1 with Base Stiffness at Collapse . . . . .	33
3 2	Variation of Anchor Tension for Anchor No. 1 with Base Stiffness at Collapse . . . . .	34
3 3	Variation of Anchor Tension for Central Anchor with Anchor Stiffness at Collapse . . . . .	35
3.3	Variation of Anchor Tension for Central Anchor with Anchor Stiffness at Collapse . . . . .	36
3 4	Variation of Anchor Tension for Central Anchor with Base Stiffness at Collapse . . . . .	37
3.4	Variation of Anchor Tension for Central Anchor with Base Stiffness at Collapse . . . . .	38
3 5	Anchor Tension at Collapse for Axial Tensile Load . . . . .	40
3 5	Anchor Tension at Collapse for Axial Tensile Load . . . . .	41

3 6	Assembly subjected to Shear Loading	45
3 7	Rotation of Assembly	50
3 8	Assembly Capacity at Collapse Vs H/P Ratio	55
3 9	Assembly Capacity at Collapse Vs H/P Ratio	56
3 10	Assembly Capacity at Collapse Vs H/P Ratio	57
3 11	Assembly Capacity at Collapse Vs H/P Ratio	58
3 12	Assembly Capacity at Collapse Vs H/P Ratio	59
4 1	Interaction Diagram for Eccentric Compressive loading at Failure	63
4 2	Interaction Diagram for Eccentric Compressive loading at Collapse	64
4.3	Interaction Diagram for Eccentric Compressive loading at Failure	65
4 4	Interaction Diagram for Eccentric Compressive loading at Collapse	66
4 5	Moment-rotation Charts for Eccentric Compressive loading ( $A_{atch}/A_{plate} = 0.1$ )	68
4 5	Moment-rotation Charts for Eccentric Compressive loading ( $A_{atch}/A_{plate} = 0.1$ )	69
4 5	Moment-rotation Charts for Eccentric Compressive loading ( $A_{atch}/A_{plate} = 0.1$ )	70
4 6	Moment-rotation Charts for Eccentric Compressive loading ( $A_{atch}/A_{plate} = 0.2$ )	71
4 6	Moment-rotation Charts for Eccentric Compressive loading ( $A_{atch}/A_{plate} = 0.2$ )	72
4 6	Moment-rotation Charts for Eccentric Compressive loading ( $A_{atch}/A_{plate} = 0.2$ )	73
4 7	Interaction Diagram for Eccentric Tensile loading at Failure	76
4 8	Interaction Diagram for Eccentric Tensile loading at Collapse	77
4 9	Interaction Diagram for Eccentric Tensile loading at Failure	78
4 10	Interaction Diagram for Eccentric Tensile loading at Collapse	79
4 11	Moment-rotation Charts for Eccentric tensile loading ( $A_{atch}/A_{plate} = 0.1$ )	81
4 11	Moment-rotation Charts for Eccentric tensile loading ( $A_{atch}/A_{plate} = 0.1$ )	82
4 11	Moment-rotation Charts for Eccentric tensile loading ( $A_{atch}/A_{plate} = 0.1$ )	83
4 12	Moment-rotation Charts for Eccentric tensile loading ( $A_{atch}/A_{plate} = 0.2$ )	84
4 12	Moment-rotation Charts for Eccentric tensile loading ( $A_{atch}/A_{plate} = 0.2$ )	85
4 12	Moment-rotation Charts for Eccentric tensile loading ( $A_{atch}/A_{plate} = 0.2$ )	86
4.13	Moment-rotation Chart for Eccentric Compressive and Tensile Loading	86
4 14	Typical Deflected Shapes of Embedded Plate	88
4 15	Typical Contours for Equivalent Stress	89

# List of Notation

The following symbols are used in this thesis:

- $A_1$  = area of the base plate in contact with base at failure
- $A_2$  = area of the base
- $A_c$  = tributary area of base
- $b_x, b_y$  = half the dimension of the attachment,
- $E$  = modulus of elasticity of the plate material,
- $E_c$  = modulus of elasticity of concrete,
- $f_{ck}$  = characteristic compressive strength of concrete,
- $f_x, f_y$  = dimensionless factors associated with maximum negative,
- $f_u$  = maximum permissible pressure on base at failure;
- $k_a$  = dimensional anchor stiffness,
- $k_b$  = dimensional base stiffness,
- $L$  = effective depth of concrete base,
- $l$  = short span of the plate;
- $l_x, l_y$  = half the dimensions of rectangular plate;
- $M_p$  = Plastic moment capacity of the plate;
- $M_{yt}$  = yield moment capacity of the plate;
- $M_x, M_y$  = externally applied moment on the plate about y and x axes, respectively;
- $N_i$  = isoparametric interpolation functions,
- $\Phi$  = Strength reduction factor;
- $P$  = point load on the plate,
- $q$  = uniformly distributed load on the plate,
- $t$  = thickness of the plate,
- $w$  = downward displacement of the plate;
- $x, y$  = cartesian coordinates;
- $\theta$  = Assembly rotation at the attachment ;

- $\beta_x, \beta_y$  = rotations of normal to undeformed midplane of the plate in  
                   = x-z and y-z planes respectively,  
 $\epsilon_{xx}$  = normal strain in x-direction,  
 $\epsilon_{yy}$  = normal strain in y-direction,  
 $\epsilon_{zz}$  = normal strain in z-direction,  
 $\sigma_{xx}$  = normal stress in x-direction;  
 $\sigma_{yy}$  = normal stress in y-direction,  
 $\sigma_{zz}$  = normal stress in z-direction;  
 $\tau_{xy}$  = shear stress in y-direction in x-plane,  
 $\tau_{xz}$  = shear stress in z-direction in x-plane,  
 $\tau_{yz}$  = shear stress in z-direction in y-plane,  
 $\gamma_{xy}$  = shear strain in y-direction in x-plane,  
 $\gamma_{xz}$  = shear strain in z-direction in x-plane,  
 $\gamma_{yz}$  = shear strain in z-direction in y-plane;  
 $\Theta$  = Curvature of the beam section,  
 $\theta_{x,i}, \theta_{y,i}$  = plate rotations at node i in y and x directions, respectively;  
 $\Pi$  = Potential Energy,  
 $\nu$  = Poisson's ratio of the plate material,  
 $A_{atch}$  = Area of Attachment,  
 $A_{base}$  = Area of Concrete Base,  
 $A_{anc}$  = Area of a single Anchor;  
 $s_1, s_2$  = spacing of anchors in long and short directions of plate,  
 $f_y$  = Yield Strength of Plate;  
 $f_y'$  = Yield Strength of Anchor,  
 $\pi$  = dimensionless term,  
 $h$  = height at which shear load is applied,  
 $e$  = eccentricity at which the load is applied;  
 $d'$  = edge distance of anchors from boundary of plate;  
 $b, d$  = dimensions of attachment,  
 $B, D$  = dimensions of plate,

# Chapter 1

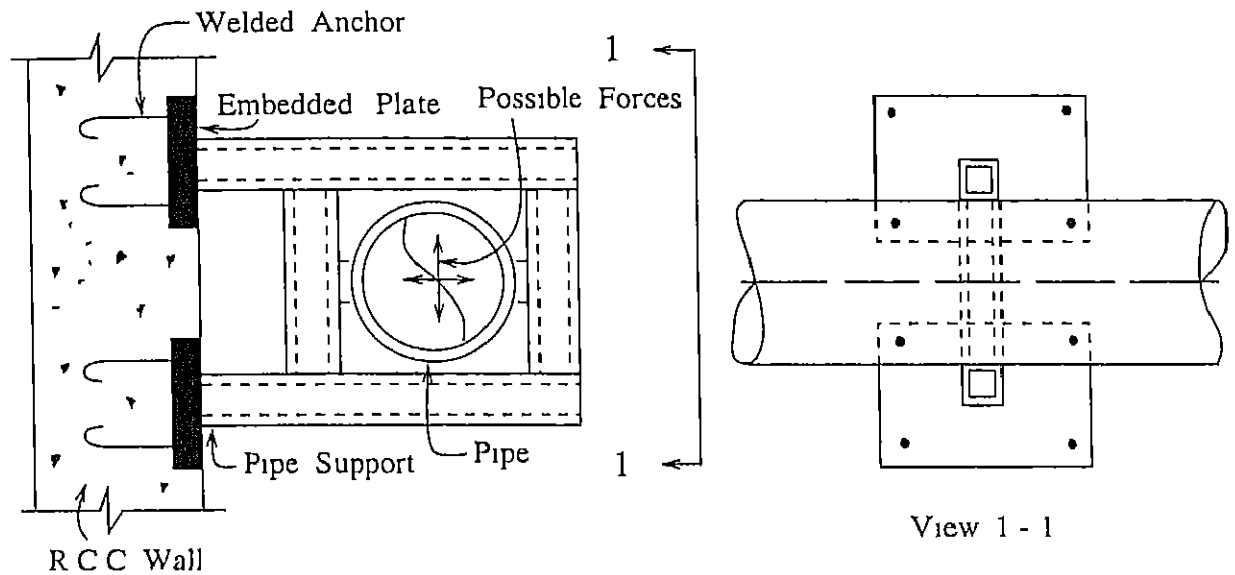
## INTRODUCTION

### 1.1 Introduction

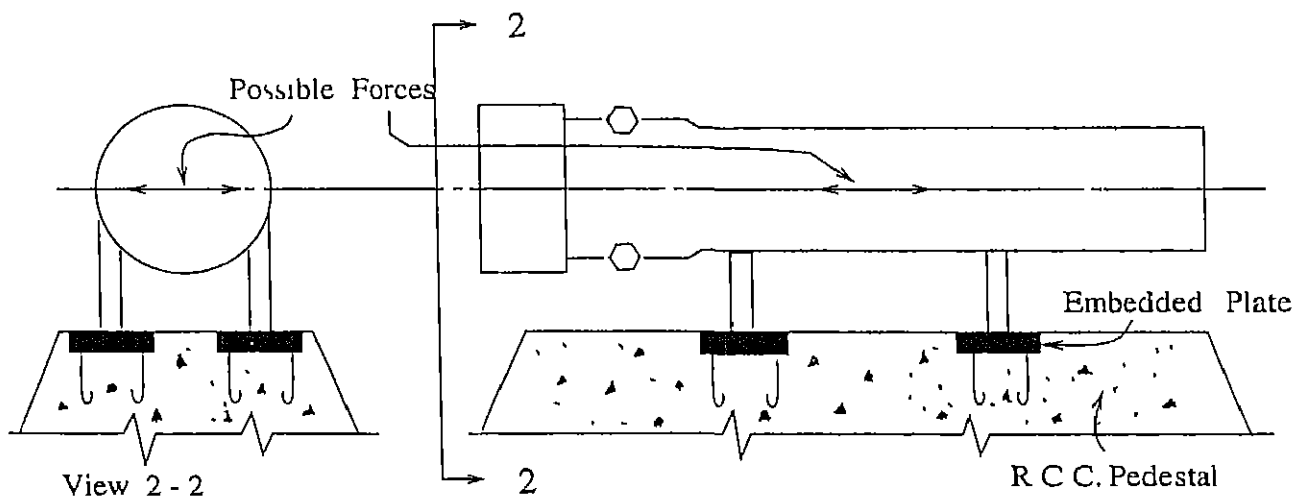
In many Engineering applications, the cast-in-place Embedded steel plates (with or without anchors) are used to support machine, equipment, pipelines etc , from the reinforced concrete members. The embedded steel plates are considered as important elements in the design and construction of industrial structures like thermal power plants, nuclear power plants etc. They perform a key role for the compliance of safety regulations of these industries. Generally, the embedded plates are the assemblies consisting of

- Steel Plate
- Anchors
- Concrete Base

The plate is made of steel to which the steel anchors are connected at desired locations. These plate-anchor assemblies are placed in the form- work prior to concreting in such a manner, that pouring and compaction of concrete does not disturb their desired locations. Anchors are available in various forms like bolts, angles, studs, and mild steel bars. The anchors are generally bent in J-shape at the end so as to provide adequate anchorage. Some typical cast-in-place steel embedded plates are shown schematically in Fig. 1.1.



Embedded Plates for Pipe Supports



Embedded Plates for Vessel Supports

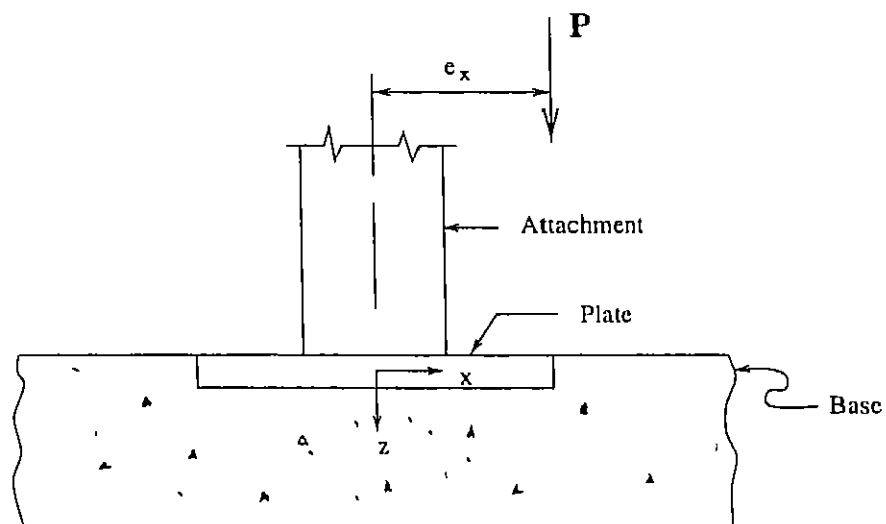
Figure 1.1. Some typical cast-in-place steel embedded plates

An attachment, normally welded to the exposed face of the plate is used to support the loads from pipes, equipment etc and transfer the load to the main reinforced concrete structures through plate-anchor assembly. The various forces likely to act on the support system are due to the dead loads, thermal movements, seismic forces, fluid dynamic forces or combination thereof. The plate-anchor assembly in its regular form consists of a plate resting on a tensionless elastic concrete base with anchors at certain locations. It is very common in practice to have plates resting on tensionless elastic foundations such as pavement slabs etc, and one such plate is shown in Fig 1.2. The general arrangement of plate-anchor assembly is shown in Fig 1.3.

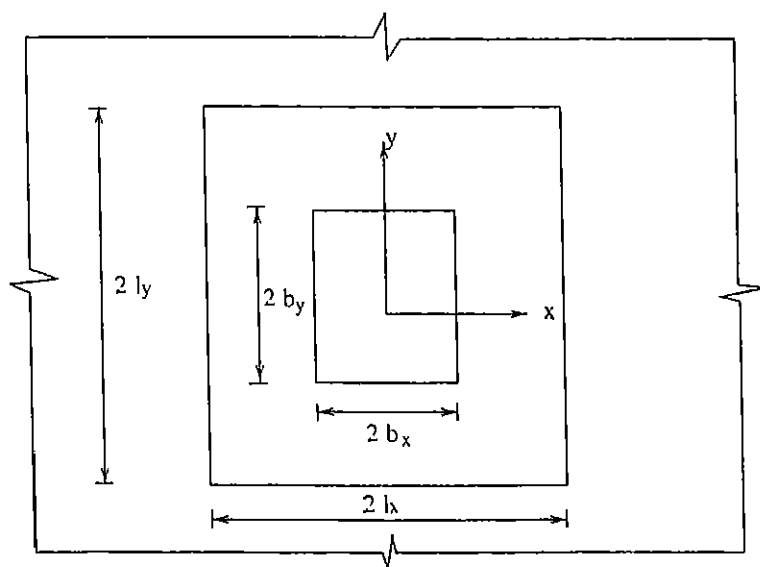
Most of the studies made on plates resting on tensionless elastic foundation are based on classical thin plate theory as presented by Timoshenko [38]. Rectangular plates resting on tensionless foundation and subject to rotationally symmetrical loads, were studied by Weitsman [43], Kamiya [27], Villaggio [41] and Al-Kharat [5]. Celep [12] studied the behavior of rectangular plates resting on tensionless elastic foundations subject to uniformly distributed load, concentrated loads and moments, using numerical methods. Weitsman and Celep showed that regions of no contact can develop under plates that are supported on tensionless foundations and that the extent of no contact depends upon the ratio of loads in combined loading rather than the levels of these loads. This results in a non-linear pressure distribution in the foundation. Mishra et al [29] demonstrated the effect of transverse shear and attachment size on the behavior of the rectangular plates resting on tensionless foundations.

The behavior of plate-anchor assembly is dependent on number of parameters such as plate dimensions, material of plate, number of anchors, their size and location, base characteristics, size of attachment and combination of forces acting on the assembly. In Fig 1.4, possible deformed shape of the plate is shown when acted upon by axial load and uniaxial moment. When the moment is small, the pressure distribution under the plate is assumed to be linear and the plate is having full contact between the plate and base. As the moment increases relative to load, the plate starts uplifting on one side causing tension in anchors,





Sectional Elevation



Plan

Figure 1.2. General Arrangement of Plates on elastic base

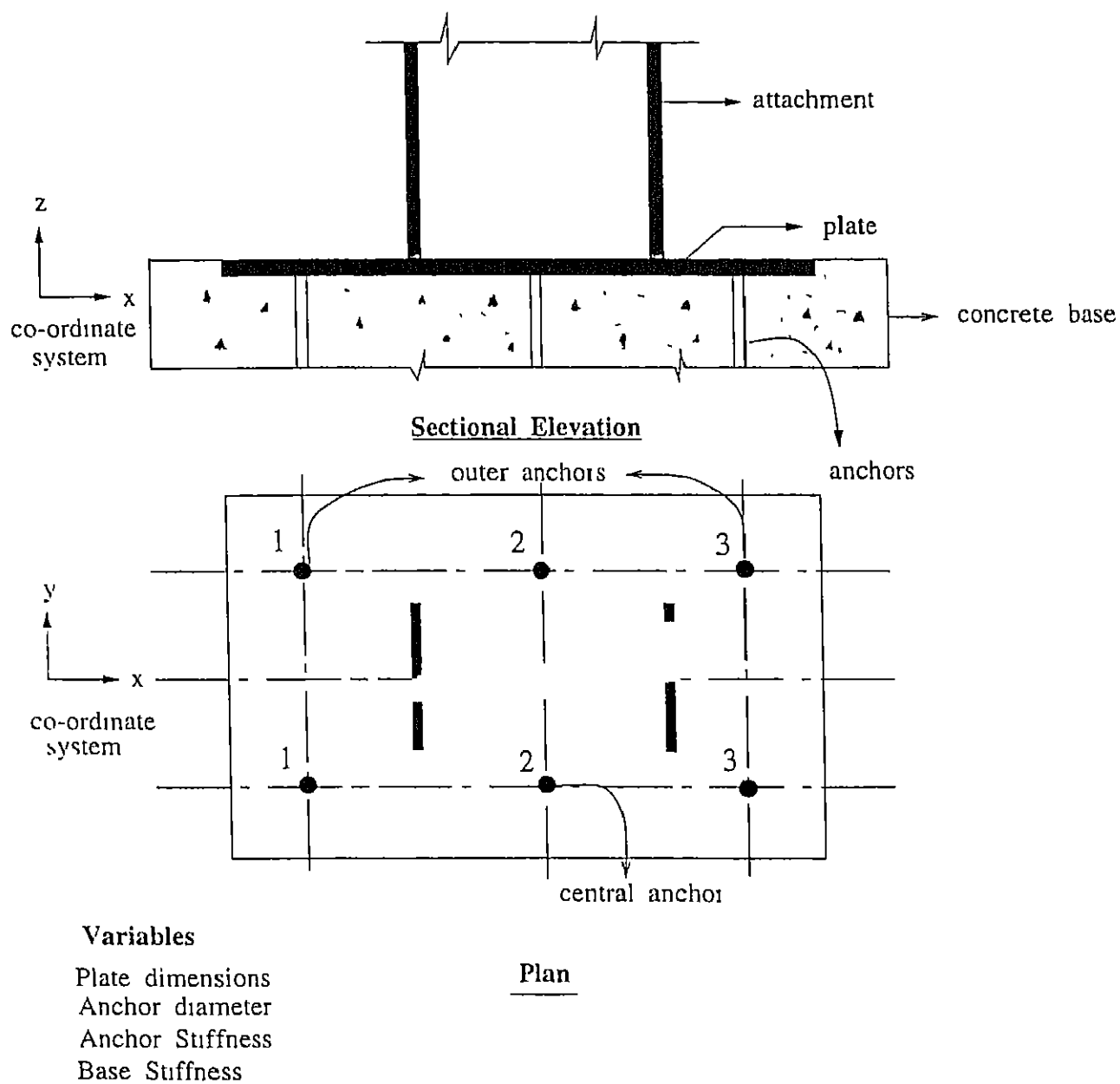
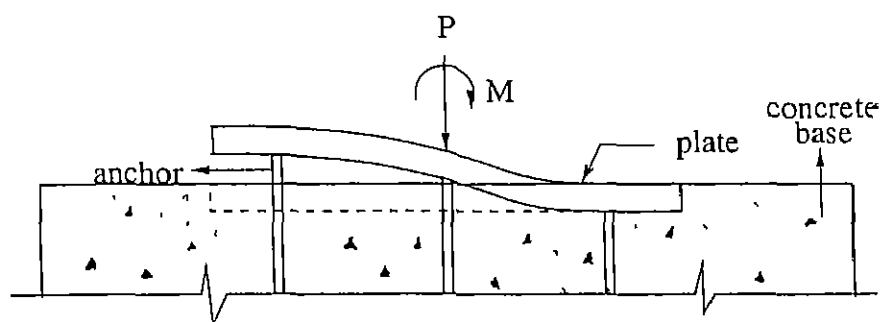
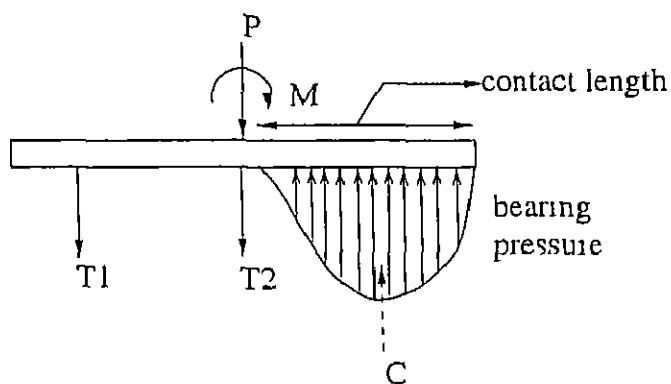


Figure 1.3 General Arrangement of Plate-Anchor Assemblies



Deformed Shape of the Plate



Forces acting on the Plate

- T1 - tension in anchor 1
- T2 - tension in anchor 2
- C - compressive reaction

Figure 1 4 Deflected shape and forces in Plate-Anchor Assemblies

while reducing the contact area. This causes the bearing pressure at the interface to become increasingly non-linear [28] due to bending of plate and base stress-strain characteristics. For relatively thicker plates, the plates may start rotating rigid-bodily about one of the edges (toe) with large reduction in contact area and resulting high pressure at toe, which may ultimately lead to premature failure of the assembly by crushing of the base [17]. Thus, the behavior of the plate-anchor assembly is seen to be dependent on several factors and the analysis and design of these assemblies, becomes a complicated affair. Simplified assumptions are made to design such structures. The simplest method commonly used for the analysis of embedded plate-anchor assembly is based on the assumption that the plate rotates rigid-bodily about toe. The pressure distribution is assumed to be linear in the working load design method and rectangular stress block similar to concrete beam design in ultimate load method. Thus the anchor tension can be computed by considering the static equilibrium of the system considering anchors and base independent. Finally, the plate thickness is obtained from bending requirements.

The primary limitation of all the existing methods is that the methods do not consider the flexibility of the plate, and, only predict the ultimate capacity assuming the plate to be rigid and that both anchors and base reach their ultimate capacities at failure simultaneously. Also these methods can not directly accommodate the shear forces and the bi-axial moments transferred through attachment, which are common in practice. For determining the maximum permissible bearing pressure at failure on concrete base, the current practice [1,3] is to use the ratio of total plate area to the concrete base area as the criterion, however, the allowable bearing pressure on concrete base has been shown to be dependent on the ratio of contact area of plate with base to the area of the base [17]. The uplifting of the plate, which is witnessed in case of plates resting on relatively stiff foundations [12,29,43], is not taken into account while determining the maximum permissible bearing pressure in concrete base. The contact area of the plate with base decreases with increase in the eccentricity of the load. The anchor response to combined tension and shear, has been shown to be governed by interaction law [15,30,32], where as in conventional design methods tension anchors are supposed to develop full tensile strength, an assumption which is far away from reality. In

the existing methods, the estimation of the capacity of the assembly is based on only one of the possible assumed stress distribution patterns at ultimate which may not be the case always. Hence, no exhaustive information regarding plate-stress, anchor forces, base pressure and mode of failure at collapse, is actually obtained. In fact, since limit analysis does not provide any information about the behavior of the structure during its loading history, the only meaningful result that can be obtained is the collapse load factor, the reliability of the method adopted can be evaluated only with respect to this quantity.

Considering the limitations of the existing methods, it appears worthwhile to go for non-linear analysis of the plate-anchor assemblies to account for plasticity effects of the materials. Such a non-linear analysis attempts to use the beneficial plasticity properties of materials in investigating the response and hence, deriving better rationale for analysis and design of these assemblies. This approach has the advantages of, firstly, by developing means to study material and structure response at advanced levels of loads and deformations, secondly, by (a) providing a physical basis for the fail-safe approach to engineering systems instead of the weakest-link approach (elastic limit of one component), (b) introducing the concept of gradual (ductile) deformation of the structure rather than its sudden (brittle) failure, and (c) making it possible to take advantage of the capacity and energy reserves of the structure, if and as appropriate.

## 1.2 Literature-Review

As explained in the earlier section, an embedded plate-anchor assembly consists of basically three components, viz: (1) the plate, (2) the elastic base and (3) the anchors. To understand the behavior of the complete assembly, it is necessary to understand the behavior of these three components individually. The abstracts from literature are presented below to give an over view of what has been done in the relevant areas till now.

### 1.2.1 Past Studies on Plates:-

A vast number of investigators have dealt with the bending and deflections of circular and rectangular plates. However a few selective studies which are relevant to the present work, are included here. Both analytical and numerical solution methods have been employed for analysis of plates assuming thin plate behavior [36,38]. Shull et al [34] have given procedure to estimate upper and lower bound on the load carrying capacity of simply supported rectangular plates. Save et al [33] have dealt with plastic analysis and design of plates. Hrabok et al [22] have reviewed plate bending finite elements and have presented a catalogue of these elements. Turvey [39] analyzed circular plates to study the effect of shear deformations on first yield. It was found that the effect of shear deformation was insignificant on first yield as compared to the results using classical thin plate theory for simply supported edges and clamped edges. However, the plate central deflections were found to be significantly higher for both edge conditions. Yuan et al [44] suggested the use of improved rectangular element for shear deformable plates and demonstrated the effect of shear in suspended plates with simply supported and clamped edges. The past studies indicate that for thick plates, the plate deformations obtained by classical thin plate theory are highly underestimated.

### 1.2.2 Past Studies of Plates on Elastic Base :

For the plates on elastic base, the important models generally taken for consideration are the Winkler's [42] model and Reissner [31] model. According to the supposition of Winkler, the base pressure at any point is proportional to the displacement at that point and the base is modelled consisting of independent elastic springs active in compression as well as tension. Reissner model includes the effect of transverse shear deformations but has a limited applicability due to its complexities in implementation as compared to Winkler model.

The study of the response of plates resting on elastic base using Winkler model was done by many investigators. Most of these studies are based on classical thin-plate theory [38]. Plates experiencing large deflections on elastic foundations for various boundary conditions, were studied by Sinha [35]. The behavior of base plate subjected to an axial load in the central area of plate was studied experimentally by DeWolf [17]. The important factors

which were affecting the base pressure of concrete are, the ratio of plate thickness to the distance between the edge of plate and column edge, compressive strength of concrete base and the ratio of areas of concrete base and plate. DeWolf et al [18] showed that the increase in depth of concrete base would increase the ultimate load capacity considerably for axially loaded plates.

Al-Khaiat et al [5] analysed plates on elastic foundations by initial value method. Circular and rectangular plates on tensionless foundations subjected to rotationally symmetric load was studied by Weitsman [43], Kamiya [27] & Villaggio [41]. Rectangular plates on tensionless foundations subjected to uniformly distributed load, concentrated load and moments were studied by Celep [12]. Finite element technique was used for the analysis and no assumptions were made regarding the shape of contact region. Weitsman and Celep showed that, an increase in the loading solely increases the displacements without changing the contact region, when subjected to one type of external load. When various types of loadings are present, the contact region depends on the ratio of the loadings. In all the above studies, the effect of transverse shear has been neglected, in considering thin plate behavior.

Mishra and Chakrabarti [29] studied the behavior of flexible rectangular plates resting on elastic base with any type of edge conditions and loading. They studied the effect of shear and attachment for realistic design conditions with the help of finite element model developed. A 9-noded Mindlin plate element was adopted to incorporate the transverse shear deformation. They concluded that the effect of transverse shear increases for small ratios of plate dimension to thickness of plate. They also observed that the deflections are highly under estimated when analysed using thin-plate theory and the contact region of plate and concrete base are dependent on the relative stiffness and plate thickness.

Mishra [45] has studied plates resting on tensionless elastic foundations using the model developed for Non-linear behavior. The author stated that the capacity of plate, mode of failure are dependent on parameters like characteristic strength of concrete and its stiffness, plate dimensions, thickness, attachment size and combination of external loads. The conclusions were that the failure is by cracking of concrete or yielding of plates for relatively thin plates and for thicker plates, the failure is mainly due to the cracking of concrete.

### 1.2.3 Past Studies on Anchors :

The design capacity of welded studs governed by ductile failure as well as concrete wedge failure subjected to direct tension, direct shear & their combination are available in PCI Handbook [30]. Klingner et al [25, 26] presented the nominal capacity of short anchor bolts and welded studs, when subjected to direct tension and direct shear. These values are compared with the available experimental results. Klingner has suggested the capacity reduction factor for various types of loads and failures. Load-deflection behavior of liner anchorage system used in steel-lined concrete containment structures of nuclear power plants has been studied by Armentrout et al [6]. The experimental study of J-shaped bolts embedded in concrete masonry have been done by Brown et al [9]. The various loading cases for the observation were direct tension, direct shear and a combination of tension & shear. Three modes of failure of bolts were discussed namely, the fracture of the bolt, pull out by straightening of bolt and the concrete wedge failure. Ueda et al. [40] has performed an experimental study of anchor bolts in unreinforced concrete, subjected to shear. The effect of spacing and edge distance of bolts are considered as very important aspects for single or group behavior of anchorage systems.

### 1.2.4 Past Studies on Plate-Anchor Assemblies:-

The determination of moment-rotation characteristics for common types of column anchorages were presented by Salmon et al [32]. Upper and lower bounds for maximum resisting moment and maximum rotation were developed. The consideration taken for column anchorage failure are, (a) failure in shear resistance, (b) failure in moment resistance and (c) failure in tensile resistance. The important variables taken for column anchorage were (a) the dimensions of the base plate, (b) dimension, location and stress-strain characteristics of anchor bolts; (c) dimension and stress-strain characteristics of concrete base and (d) the vertical loading. Extension of anchor, compression of concrete and bending of the base plate, were considered as the causes of rotation. The authors have suggested that for a long embedded steel bar pulled out of concrete, the bond is not effective over the entire length, but effective over an approximate length of 24 times diameter of bar. Shear was shown to have



little effect on ultimate resisting moment, but has significant effect on maximum rotation

The effect of plate flexibility on the behavior of base plate assembly was studied by Diluna and Flaherty [20]. They concluded that the anchor tension and bearing pressure distribution on concrete base depend on plate flexibility. As the plate becomes more flexible, the distance between the tensile reaction and centroid of compressive reaction tend to decrease thereby increasing the bolt tension. The prying effect caused by the flexibility of plate affect the anchor tension. It was observed that the increase in base stiffness by 10 times has only a minor variation in the base plate behavior, while keeping the other parameters constant.

Cannon et al. [10] prepared a guide for the design of anchor bolts and the steel embedments. The design guidelines developed were established from both experimental and analytical results.

ASCE Nuclear Structures and Materials Committee, Materials and Structural Design Committee [4] has presented a state-of-art report to review and discuss the issues of selection of embedment material, design and installation problems. The report also include discussions regarding the behavior of each type of embedment, their design criteria and design methods, common to nuclear industry.

DeWolf et al. [19] have studied experimentally the behavior of steel column base plates subjected to axial loads and moments. The experimental set-up consisted of lower half which is a mirror image of upper half. The variables considered for the experiments were the anchor bolt size, base plate thickness and load eccentricity. The authors concluded that the actual base-plate behavior is more closely modelled by Ultimate design method than Working stress method. The authors also concluded that the anchors do not attain their full capacity at low load eccentricities, when they are large in relation to the plate dimensions. They suggested the inclusion of the effect of confinement which occurs when the concrete area is greater than the base plate area. The authors also indicated that increase in the plate thickness beyond the value obtained in design methods can lead to decreased capacity.

Thambiratnam et al. [37] had also conducted experiments to study the behavior of base plates under the action of axial loads and moments. The main parameters of the study were thickness of the base plate and eccentricity of the load. They concluded that the failure of base plate assembly was due to cracking of concrete at low eccentricities and

for high eccentricities, the primary mode of failure was the yielding of base plate. It was also concluded that thick base plates tend to ride up (as rigid plate) on edge causing large bearing pressure and consequent premature failure due to crushing of concrete.

Cook et al [15] studied experimentally the behavior of anchor connection, subjected to various combinations of moment and shear. They used flexible and rigid base plates with steel attachments, connected to concrete with threaded cast-in-place or retrofit anchors. The authors concluded that the tension and shear force in anchors redistribute inelastically to maintain equilibrium, if the resistance offered by friction is more than the applied shear, anchors are not required to resist the shear; if the applied shear is more than the frictional resistance, the anchors in compression resist the shear force along with friction and the anchors in tension are assumed to develop full tension strength for moment resistance, if the shear resistance offered by friction and anchors in compression are not sufficient, then anchors in tension also resist the applied shear.

Cannon [11] in his study, observed that the location of compressive reaction, redistribution of load to anchors are effected by the plate stresses. The effect of preloading of anchors on performance and capacity of anchorage was also studied. The other observations made in the study were regarding the amount of redistribution that takes place between the lines of anchors, when subjected to shear and moment. The author concluded that the redistribution depends on the base plate flexibility and the strain capacity of anchors; the yielding occurs first in the base plate, when high strength anchors are used allowing redistribution to start at an earlier stage; the redistribution reduces the load in maximum stressed anchor and allows the base plate flexibility to dominate.

Chakrabarti and Tripathi [13] studied the significance of plate flexibility, anchor stiffness and concrete base stiffness on the behavior of plate-anchor assembly. An idealised model was prepared for a typical embedded steel plate-anchor assembly using finite element technique. The parameters considered for the analysis were the plate thickness, concrete base stiffness and anchor stiffness. The effect of tension in anchors, maximum bearing pressure in concrete base and maximum equivalent plate stress, due to variations of parameters, were presented. The results were compared with "Concrete Beam" analogy method and a set of design guidelines were suggested.

Kallolil [24] and Mishra [45] conducted experimental study on plate-anchor assemblies. Three full scale tests were conducted and the plan dimensions of plate; locations; number and size of anchors, concrete base dimensions, material properties of concrete, anchors and embedded plates were kept constant. They observed that the deformation of embedded plate during loading and just prior to failure are in agreement with the pattern predicted by existing methods for such plate-anchor assemblies. A distinct fold line was observed in each of the plate by the side of the compression face of the attachment, which gives a clear indication of plate yielding.

Mishra [45] has developed a mathematical model to study the Non-linear behavior of embedded plate-anchor assembly. The effect of transverse shear deformation has been incorporated in the model. The model can be used for any type of loading and boundary conditions. The results using the model have been found to be in reasonable agreement with the available experimental and analytical results in respect of prediction of behavior and capacity.

From the review of the past studies it has been observed that a definite need exists in undertaking a systematic investigation for knowing the pattern of variation of strength and serviceability characteristics of embedded plate-anchor assemblies based upon the realistic model developed by Mishra. It is expected that the results of such investigation will be of help in updating the design guidelines of such assemblies with better rationale.

### 1.3 Objectives and Scope of the Thesis

The main objective of the thesis is to study the realistic behavior of the plate-anchor assemblies with the help of the model developed by Mishra, and recommend design guidelines for common types of loading. It has been observed that limited research data are available regarding the behavior of such assemblies. Considering the importance of such embedded plates in respect of their industrial application, a definite need exists for knowing the behavior of these assemblies. The plate flexibility, attachment effect and material non-linearities, under any combination of loads, were taken into account for the development of the model. The effect of various parameters in the assembly have to be studied in order to understand

the behavior of the plate-anchor assembly

With this in view the scope of the thesis is to study the behavior of the plate-anchor assembly by varying different parameters of the plate-anchor assembly for different types of loading. The behavior of individual elements of the plate anchor assembly under different loading conditions will be studied. The moment-rotation characteristics of the assembly due to variation of parameters will be investigated. The capacity of the assembly at failure as well as at collapse, due to different loading conditions, will be observed. Finally, a set of design guidelines will be developed for the plate-anchor assembly.

## 1.4 Organisation of Present Study

In chapter 2, the development of the model, the modes of failure and the governing equations are discussed.

In chapter 3, a detailed parametric study is presented varying the base and anchor stiffness, for different plate thicknesses of plate-anchor assemblies subjected to compressive loading. The behavior of the assembly when subjected to tensile and shear loading are also studied. The dimensional analysis of all the design parameters in the plate-anchor assembly, performed to develop the interaction diagrams and moment-rotation charts is presented in Appendix-II. The behavior of the assembly when subjected to compressive loading in combination with shear loading, is also studied.

In chapter 4, the analysis of the results are presented. The interaction diagrams, which are used to obtain the load carrying capacity of the assembly are developed for compressive and tensile loading. The moment-rotation charts, which are used to obtain the rotation undergone by the assembly are developed. The evaluation of the interaction diagrams developed for compressive loading is presented for the cases, when the assemblies are subjected to shear loading in combination with compressive loading. Typical deflected shapes and stress contours are presented.

In chapter 5 Summary, conclusions and scope for future work are included.

# Chapter 2

## MATHEMATICAL MODEL

### 2.1 Introduction

The behavior of the embedded anchor-plate assembly is a complex phenomenon and depends upon a number of factors. The present investigation regarding the behavior of embedded plate-anchor assembly, has been conducted using the model developed by Mishra [45]. The model estimates the load carrying capacity of the assembly and also provides other pertinent information regarding the assembly behavior during its loading history.

The model has been developed in various stages and in each stage its reliability has been tested. The model was first developed for linear analysis (working stress), and then updated for non-linear analysis (ultimate load). A 9-noded Mindlin element was used to account for transverse shear deformations in the plate. Attachment size effect has been included by increasing the plate stiffness in the area in contact with the attachment. It has been assumed that anchor-characteristics are known either experimentally or can be predicted using available methods. The model can predict the stage-wise development of nodal displacements and resulting stress-resultants in each component. Out of the three main sources of non-linearity, contacting area (support conditions), material non-linearity and geometric non-linearity (due to large deformations), the first two are considered in developing the model.

A typical embedded plate assembly consists of three basic components, the plate, the anchors and the base. It was necessary to understand the behaviour of these components

separately and collectively, to model the system by making suitable assumptions. A brief account, of the various primary modes of failure observed in plate-anchor assemblies, is given in the section to follow.

### 2.1.1 Common Modes of Failures:-

In general a plate-anchor assembly is assumed to have failed if any of the three components has reached the limiting value of stress-resultants. The plate-anchor assembly may fail in any one or a combination of three possible types of failure modes as given below.

- *Concrete Failure* - This type of failure is encountered when the concrete base supporting the plate/plate-anchor assembly starts cracking at advanced level of loading which may lead to collapse of the structure due to crushing of the concrete or formation of a mechanism. This type of failure is brittle in nature and occurs when the base pressure developed on the interface of the plate and base exceeds the permissible bearing pressure of the base. The effect of confinement is considered for the resulting bearing pressure at ultimate capacity [1,19].
- *Plate Failure* - This type of failure occurs when the plate stresses reach yield limit in relatively thin plates and may lead to collapse of the structure by formation of a mechanism or crushing of concrete. This type of failure is ductile in nature.
- *Anchor Failure* - This type of failure is encountered in a plate-anchor assembly when the anchors fail first and may lead to collapse either by formation of a mechanism or crushing of the concrete. There are a number of factors which determine the behavior of the anchors [6, 9, 25, 26, 30, 40]. The anchor failure can be any of the three types :
  - a) *Anchor Material Failure* - This type of failure is due to yielding of anchor in tension or a combination of shear and tension at relatively large eccentricity of loads. The anchors attain their full capacity and the failure is ductile in nature.
  - b) *Concrete Wedge Failure* - This type of failure is a premature brittle failure and occurs when the characteristic strength of the concrete is low. The anchor comes out with a concrete wedge prior to attainment of its full capacity.
  - c) *Anchor Bond Failure* :- This type of failure is also a premature brittle failure and

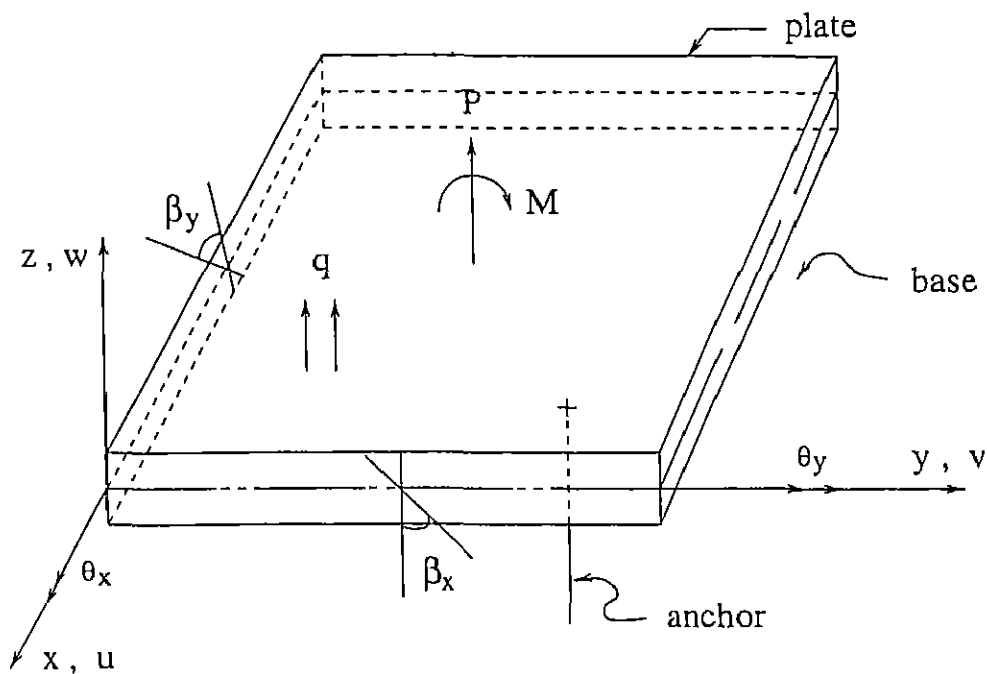


Figure 2.1. Embedded Plate-Anchor Assembly Model

is caused when sufficient bond length is not available for anchor to develop its full capacity

The brittle failure of the anchors can be avoided by proper use of bond length and high strength concrete, proper edge distance and distance between the anchors in a group. The model developed has the capabilities of finding both anchor ductile failure as well as brittle failure of concrete.

### 2.1.2 Governing Equations of the Structure

Considering the plate-anchor assembly model in Fig. 2.1, the bending strains in the plate  $\epsilon_{xx}$ ,  $\epsilon_{yy}$ ,  $\gamma_{xy}$  vary linearly through the plate thickness and are given by the curvatures of the plate using:

$u = z\beta_x(x, y)$ ,  $v = -z\beta_y(x, y)$  and  $w = w(x, y)$  where  $x, y, z$  are the coordinates of a point on the plate,  $u, v, w$  are the displacements in the directions of  $x, y, z$ , respectively and  $\beta_x, \beta_y$  are the rotations of the normal to the undeformed middle surface in  $x$ - $z$  and  $y$ - $z$  planes, respectively. It may be recalled that in Kirchhoff's plate theory, where shear deformations

are neglected  $\beta_x = \frac{\partial w}{\partial x}$  and  $\beta_y = \frac{\partial w}{\partial y}$

$$\begin{bmatrix} \epsilon_{xx} \\ \epsilon_{yy} \\ \gamma_{xy} \end{bmatrix} = z \begin{bmatrix} \frac{\partial \beta_x}{\partial x} \\ -\frac{\partial \beta_y}{\partial y} \\ \frac{\partial \beta_x}{\partial y} - \frac{\partial \beta_y}{\partial x} \end{bmatrix} = zB \quad (2.1)$$

whereas the transverse shear strains are assumed to be constant through the thickness and are given by.

$$\gamma = \begin{bmatrix} \gamma_{yz} \\ \gamma_{xz} \end{bmatrix} = \begin{bmatrix} \frac{\partial w}{\partial y} - \beta_y \\ \frac{\partial w}{\partial x} - \beta_x \end{bmatrix} \quad (2.2)$$

The state of stress in the plate corresponds to plane stress condition, i.e.,  $\sigma_{zz} = 0$ .

Considering an isotropic material we can thus write

$$\begin{bmatrix} \sigma_{xx} \\ \sigma_{yy} \\ \sigma_{xy} \end{bmatrix} = z \frac{E}{1-\nu^2} \begin{bmatrix} 1 & \nu & 0 \\ \nu & 1 & 0 \\ 0 & 0 & \frac{1-\nu}{2} \end{bmatrix} \begin{bmatrix} \frac{\partial \beta_x}{\partial x} \\ -\frac{\partial \beta_y}{\partial y} \\ \frac{\partial \beta_x}{\partial y} - \frac{\partial \beta_y}{\partial x} \end{bmatrix} \quad (2.3)$$

$$\begin{bmatrix} \tau_{yz} \\ \tau_{xz} \end{bmatrix} = z \frac{E}{2(1+\nu)} \begin{bmatrix} \frac{\partial w}{\partial y} - \beta_y \\ \frac{\partial w}{\partial x} - \beta_x \end{bmatrix} \quad (2.4)$$

Where E is modulus of elasticity and  $\nu$  is Poisson's ratio of the material

To establish the element equilibrium equations we now proceed with principle of virtual displacement or minimum potential  $\Pi$ . If  $q$  is the transverse loading per unit area,  $P_i$ ,  $M_{xi}$ ,  $M_{yi}$  are concentrated loads, moments in x and y directions, respectively, at points  $(x_i, y_i)$ ,  $k_b$  is base stiffness and  $k_a$  are anchors stiffnesses, located at points  $(x_a, y_a)$ , the total potential  $\Pi$  is given as below

$$\begin{aligned} \Pi = & \frac{1}{2} \int_A \int_{-t/2}^{t/2} \begin{bmatrix} \epsilon_{xx} & \epsilon_{yy} & \gamma_{xy} \end{bmatrix} \begin{bmatrix} \sigma_{xx} \\ \sigma_{yy} \\ \tau_{xy} \end{bmatrix} dz dA + \frac{k_b}{2} \int_A w^2 dA \\ & + \frac{k_s}{2} \int_A \int_{-t/2}^{t/2} \begin{bmatrix} \gamma_{yz} & \gamma_{xz} \end{bmatrix} \begin{bmatrix} \tau_{yz} \\ \tau_{xz} \end{bmatrix} dz dA + \frac{k_s}{2} \int_A w^2 \delta(x - x_a) \delta(y - y_a) dA \\ & - \int_A w P_i \delta(x - x_i) \delta(y - y_i) dA - \int_A M_{xi} \beta_x \delta(x - x_i) \delta(y - y_i) dA \\ & - \int_A M_{yi} \beta_y \delta(x - x_i) \delta(y - y_i) dA - \int_A w q dA \end{aligned} \quad (2.5)$$



where  $k_s$  is again a constant to account for the actual nonuniformity of the shearing stresses. Substituting from 2.1 to 2.4 into 2.5 we thus obtain

$$\begin{aligned}\Pi = & \frac{1}{2} \int_A B^T C_b B dA + \frac{1}{2} \int_A \gamma^T C_s \gamma dA + \frac{k_b}{2} \int_A w^2 dA \\ & + \frac{k_a}{2} \int_A w^2 \delta(x - x_a) \delta(y - y_a) dA - \int_A w P_i \delta(x - x_i) \delta(y - y_i) dA \\ & - \int_A M_{x_i} \beta_x \delta(x - x_i) \delta(y - y_i) dA - \int_A M_{y_i} \beta_y \delta(x - x_i) \delta(y - y_i) dA \\ & - \int_A w q dA\end{aligned}\quad (2.6)$$

where

$$C_b = \frac{Et^3}{12(1 - \nu^2)} \begin{bmatrix} 1 & \nu & 0 \\ \nu & 1 & 0 \\ 0 & 0 & \frac{1-\nu}{2} \end{bmatrix}, \quad C_s = \frac{Et k_s}{2(1 + \nu)} \begin{bmatrix} 1 & 0 \\ 0 & 1 \end{bmatrix} \quad (2.7)$$

Equilibrium requires that  $\Pi$  is stationary, i.e.  $\delta\Pi = 0$  where it must be recognized that  $w, \beta_x$  and  $\beta_y$  are independent variables. Hence, in the finite element analysis of an assemblage of the elements, we need to enforce interelement continuity on  $w, \beta_x$  and  $\beta_y$  which can readily be achieved in the same way as in the isoparametric finite element analysis of solids.

Using that the total potential must be stationary, we obtain

$$\begin{aligned}\delta\Pi = & \int_A \delta B^T C_b B dA + \int_A \delta \gamma^T C_s \gamma dA + \int_A \delta w k_b w dA + k_a w \delta w|_{x_a, y_a} \\ & - P_i \delta w|_{x_i, y_i} - M_{x_i} \delta \beta_x|_{x_i, y_i} - M_{y_i} \delta \beta_y|_{x_i, y_i} - \int_A \delta w q dA = 0.\end{aligned}\quad (2.8)$$

which may be regarded as the principle of virtual displacement for the plate-anchor assembly. For finite element analysis we use (refer Bathe [8])

$$w = \sum_{i=1}^n N_i w_i; \quad \beta_x = \sum_{i=1}^n N_i \theta_x^i, \quad \beta_y = \sum_{i=1}^n N_i \theta_y^i \quad (2.9)$$

where the  $N_i$  are the interpolation functions and  $n$  is the number of nodes of the element.  $w_i, \theta_x^i$  and  $\theta_y^i$  are nodal displacements at node 'i' defined as  $U_i$ .

Now substituting  $B = B_b U_i, \quad \gamma = B_s U_i, \quad w = H U_i$

$$B_b = \begin{bmatrix} 0 & \frac{\partial N_i}{\partial x} & 0 \\ 0 & 0 & -\frac{\partial N_i}{\partial y} \\ 0 & \frac{\partial N_i}{\partial y} & -\frac{\partial N_i}{\partial x} \end{bmatrix} \quad (2.10)$$

$$B_s = \begin{bmatrix} \frac{\partial N_i}{\partial y} & 0 & -N_i \\ \frac{\partial N_i}{\partial x} & -N_i & 0 \end{bmatrix} \quad (2.11)$$

$$H = \begin{bmatrix} N_i & 0 & 0 \end{bmatrix} \quad (2.12)$$

We obtain the equation 2.8 in the matrix form by substituting equation 2.10 to equation 2.12 as

$$\begin{aligned} & \left[ \int_A B_b^T C_b B_b dA + \int_A B_s^T C_s B_s dA + \int_A H^T k_b H dA + H^T k_a H|_{x_a, y_a} \right] U \\ & = \int_A q H^T dA + (P_i + M_{x_i} + M_{y_i})|_{x_i, y_i} \end{aligned} \quad (2.13)$$

In Eq. 2.13 the first term on the L.H.S. is the stiffness contribution of the plate element due to bending alone, whereas the second term gives the contribution due to shear deformations in plate. The third term on L.H.S. is stiffness contribution due to elastic base and it is only in the direction of  $w$  at each node. Similarly the fourth term gives the contribution due to anchors in the direction of  $w$  only at the nodes where they are present. The first term on R.H.S. gives the equivalent nodal loads due to distributed load of intensity  $q$  and the last terms represent the concentrated load and moments at the nodes.

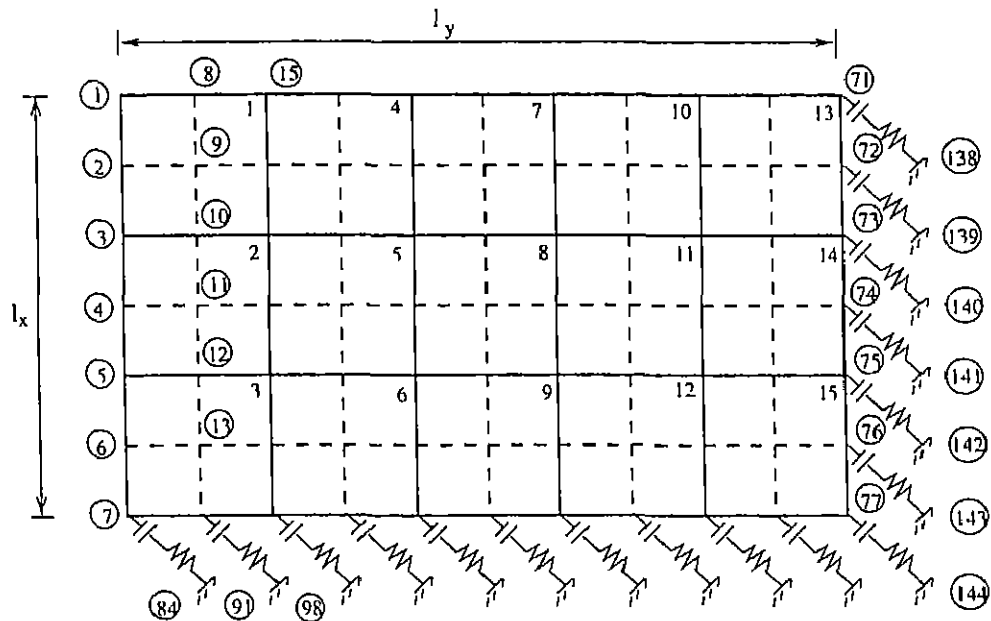
### 2.1.3 Details of the Mathematical Model Adopted:-

The details regarding modeling of the three basic components are as follows

- *Plate.*- The behavior of a plate depends upon number of factors. The following assumptions are made in this regard.

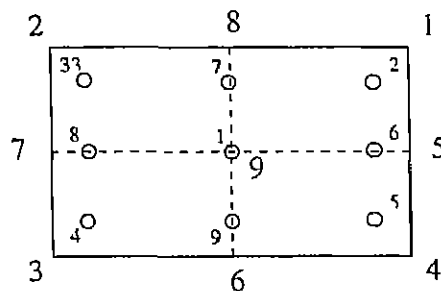
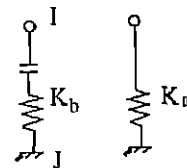
- (1) Plate deflections are small
- (2) There are no restraints on the plate edges caused by embedding in the concrete base.
- (3) Plate material is perfectly elastic-plastic.

A number of finite element models have been suggested by researchers for representing the behavior of plates in bending [22]. As given in Eq. 2.1 to 2.13 due to its simplicity in application and to account for transverse shear stresses, the Mindlin plate element



TYPICAL GRID PATTERN

- Ⓝ - Node Number
- N - Plate Element Number
- K<sub>a</sub> - Anchor Stiffness
- K<sub>b</sub> - Base Stiffness
- - Stress Point Numbers
- N - Node numbers



9 NODED MINDLIN ELEMENT

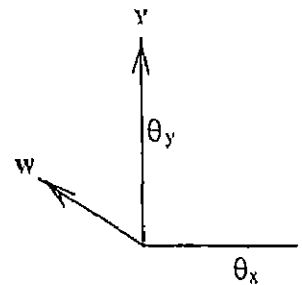


Figure 2 2 Typical Grid Pattern and 9 Noded Mindlin Element

with 3-nodal degrees of freedom has been selected as shown in Fig 2.2. Four-noded elements proved to be overly stiff as the displacement field represented is a bilinear function of  $x$  and  $y$ , which may not represent the actual deformation field in most of the cases, and, thus, a nine-noded quadrilateral element has been adopted for the present study. When Mindlin elements are used for very thin plates, the transverse shear contribution dominates over the bending contribution resulting into mesh locking. To overcome this problem a reduced integration scheme has been used for very thin plates [16]. In general, nodal displacements converge very fast with respect to mesh size but the convergence in stress calculation is rather slow when it is calculated at the center of the element. Near the fixed edges, where the stress gradient is steep, the convergence is even slower. Provision has been made to calculate stresses at a variable number of points within the element (refer Fig 2.2), and this has resulted in early convergence of stresses near fixed edges too.

The plate moment-curvature relationship is linear up to first yield (Von-Mises criterion). It then changes its behavior by reducing the slope (stiffness) to one tenth of the initial value till it becomes fully plastic and will not resist further moment as shown in Fig 2.3. The yield moment,  $M_{yl}$ , and plastic moment capacity,  $M_p$ , are calculated by the expressions given below:

$$M_{yl} = f_y t^2 / 6 \quad (2.14)$$

$$M_p = f_{yl} t^2 / 4 \quad (2.15)$$

where  $f_y$  is the yield stress of plate material in uniaxial tension and  $t$  is the thickness of the plate.

- *Base* - The base has been idealized as a Winkler base [16] in the form of uncorrelated elastic springs attached to each node in the plate having dimensional foundation stiffness  $k_b$  determined using tributary area method as suggested by Diluna and Flaherty [20]

$$k_b = A_c E_c / L \quad (2.16)$$

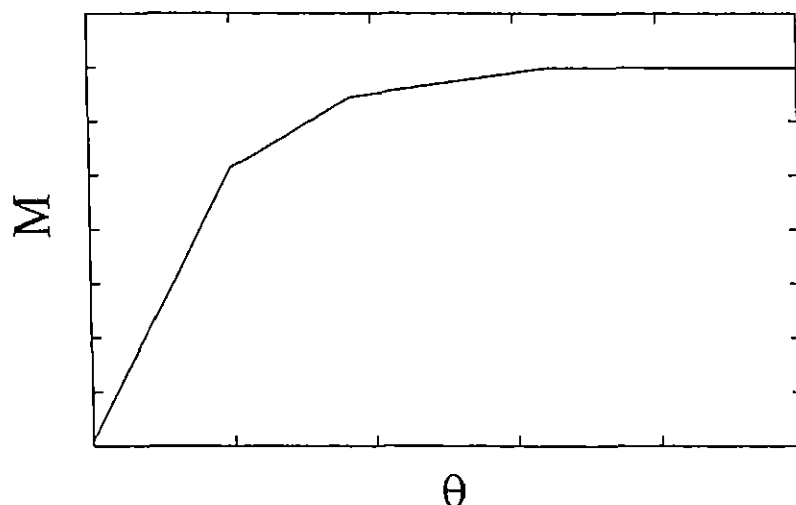


Figure 2.3 Moment-Curvature Relationship for Plates

where,  $A_c$  = tributary area of the concrete base

= 1.0 m per unit area calculation

$E_c$  = modulus of elasticity of concrete

=  $5700(f_{ck})^{0.5}$  [23]

$f_{ck}$  = characteristic compressive strength of concrete

and  $L$  = Equivalent depth of embedment [32]

No reduction in the tributary areas of boundary nodes has been made to compensate for the confining effect of surrounding concrete [13]. The tensionless character of the base has been incorporated by making these springs active in compression only. Only if the node 'i' moves towards node 'j' (refer Fig. 2.2), the spring is introduced and is active, otherwise, it is rendered inactive and deleted in subsequent iterations. The stiffness of base is modeled as piecewise-linear depending on the magnitude of base pressure as shown in Fig. 2.4. Up to a base pressure of 0.50 times the characteristic strength of the base, the stiffness is constant and afterwards it is reduced to one tenth of the initial value [6]. Cracking in concrete base is assumed to be at a pressure of 0.65 times the characteristic strength of the concrete, and crushing is caused when the pressure exceeds the permissible bearing value given in the American Concrete Institute's Building Code Requirements for Reinforced Concrete [1]. The resulting

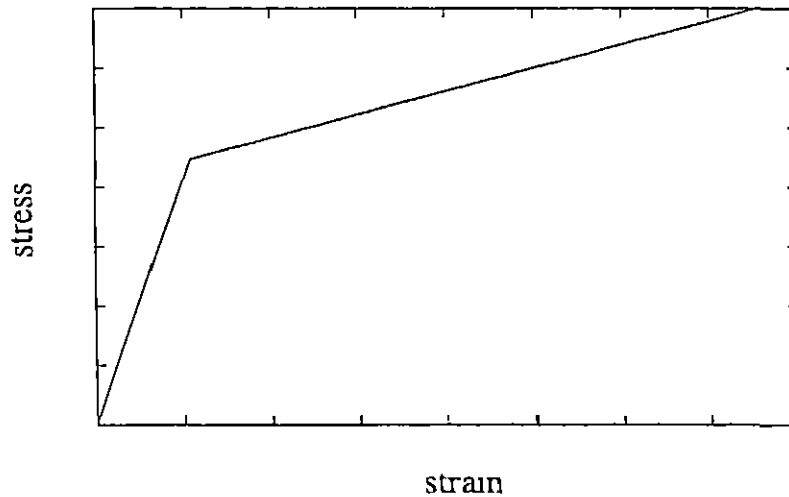


Figure 2.4 Idealised Stress-Strain Curve for Concrete Base

bearing stress at ultimate is

$$f_u = 0.85\Phi f'_c (A_2/A_1)^{0.5} \leq 1.7f'_c \quad (2.17)$$

where,  $f_u$  = permissible bearing stress at failure

$f'_c$  = characteristic strength of concrete

$\Phi$  = strength reduction factor, equal to 0.70

$A_2$  = area of the base plate in contact with base at failure

$A_1$  = area of the base

- *Anchor* - Embedded anchors exhibit non-linear load-deflection behavior when subject to pull-out and/or shearing forces [6,9]. The exact behavior depends on the shape and size of the anchor, properties of the concrete in which the anchor is embedded, and the bonding resistance developed between the concrete and the anchor surfaces. Each anchor is modeled as elastic spring in the specified directions to represent the tensile/compressive and shear resistances offered by the anchors. The value of equivalent spring constant have been derived from the available experimental load-deflection data on J-shaped anchors [9]. If data is not available, the spring constant is assumed to be twice that of anchor steel material alone to account for reduced force along the anchor embedment due to concrete bonding effect [32]. Up to the yield point the stiffness is

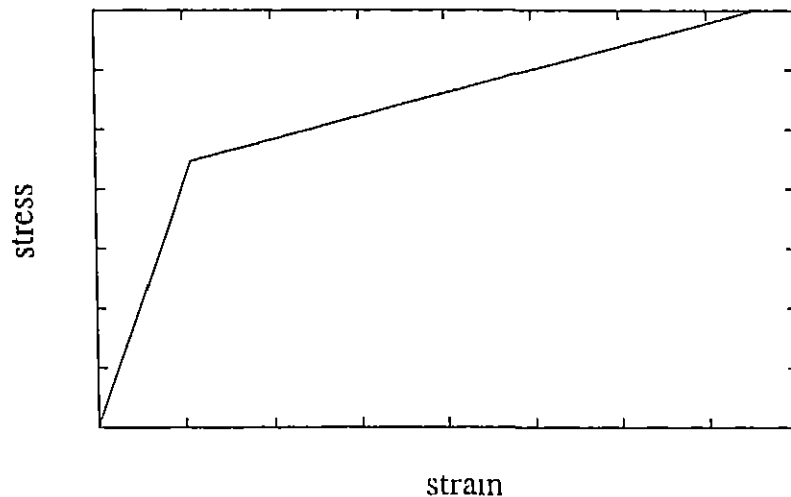


Figure 2.5 Idealised Stress-Strain Curve for Anchors

assumed to be constant and after the yielding has begun it is reduced to one tenth of the initial value till it fails due to excessive deformation. The anchor stiffness in shear is assumed to be half of that in direct tension [9].

- *Attachment.*- Attachment welded to the plate for the purpose of transmitting load to plate is supposed to make the plate highly rigid in the area of contact with the attachment. To account for this increased rigidity of the plate, the thickness of the plate is increased by an arbitrary factor of 10 or more. For the purpose of the present study only rectangular attachments have been considered.

Shear forces coming on the assembly are first resisted by the frictional force on the interface of the plate and the base. A value of coefficient of friction equal to 0.4 is used for concrete and steel interface [10,15]. No slip is caused and anchors are not required to resist shear in case the applied shear is less than frictional resistance. In case the applied shear is more than frictional resistance, anchors in compression are supposed to develop full shear resistance to resist the excess shear force. In case the applied shear exceeds the frictional resistance and shear resistance by anchors in compression, the anchors in tension resist the unresisted shear. The tension anchors are checked for combined shear and tension. The strength of these anchors are limited by the tension/shear interaction relationship of anchors [11,15,30].

# Chapter 3

## Behavior of Assembly : A Parametric Study

### 3.1 Introduction

The behavior and capacity of embedded steel plate-anchor assembly is dependent on the relevant design parameters, e.g., dimensions of the plate, size and number of anchors, characteristic strength of concrete, stress-strain characteristics of the material, size of the attachment and different loadings on the assembly. The important design variables associated are anchor forces, plate stresses, base pressure and rotation of the assembly. It is also pertinent to investigate the relative participation of different components (e.g., plate, concrete base and anchors) of the plate-anchor assembly under common loading conditions. With all these in view, following parametric studies have been performed to derive meaningful information for understanding the realistic behavior and for estimation of assembly capacity.

- Study for the variation in anchor tension due to the variation in base stiffness and anchor stiffness and plate thickness, for eccentric compressive loading on a typical plate-anchor assembly.



- Study for the variation in anchor tension assembly capacity, and associated modes of failure due to the variation in plate thickness, anchor size, anchor material, and grade of base concrete, for tensile loading (with/without eccentricity) on a typical plate-anchor assembly
- Study for the variation in assembly capacity due to the variation in plate thickness, anchor size, anchor material, grade of base concrete for shear loading on a typical plate-anchor assembly.
- Study for the development of strength interaction diagrams (based on assembly failure and assembly collapse) and moment-rotation charts considering variations in plate thickness, plan-dimensions of plate, area of attachment, grade of base concrete, size, locations and number of anchors, for eccentric compressive loading on typical plate-anchor assembly
- Study for the development of strength interaction diagrams (based on assembly failure and assembly collapse) and moment-rotation charts considering variations in plate thickness; plan-dimensions of plate, area of attachment, grade of base concrete, size, locations and number of anchors, for eccentric tensile loading on typical plate-anchor assembly
- Study for the evaluation of the interaction diagrams developed for the cases of eccentric compressive loading, when shear loading is also present on the assembly in combination

### **3.2 Study on Anchor Tension in Plate-Anchor Assemblies subjected to Eccentric Compressive loading.**

Variation of anchor tension in plate-anchor assemblies subjected to eccentric compressive loading, is studied by varying base stiffness, anchor stiffness and plate thickness. For the present study, the various plate thicknesses considered are, 10mm, 12mm,

14mm and 20mm. The base stiffness variation is done by changing the grade of concrete as M25, M30, M35 and M40. The anchor stiffness is varied by using different anchor diameters, 12mm, 14mm, 16mm and 18mm. The base stiffness and anchor-stiffness are calculated using the tributary area method as explained in the previous chapter. The trend for the variation in anchor tension is clearly demonstrated by considering the parametric variation as stated above. The parametric study is carried out using a typical embedded plate-anchor assembly (see Fig. 1.3) having 400mm X 250mm plate with 6 anchors of 12mm diameter, subjected to eccentric compressive load (at eccentricity of 200mm) transferred through an attachment of size 100mm X 100mm.

Following representative cases are studied to make observations regarding the trend in the variation of anchor tensions at collapse of the assembly.

1. Variation of Anchor Tension for Anchor No. 1 with Anchor Stiffness
2. Variation of Anchor Tension for Anchor No. 1 with Base Stiffness
3. Variation of Anchor Tension for Central Anchor with Anchor Stiffness
4. Variation of Anchor Tension for Central Anchor with Base Stiffness

Following observations are made from the studies:

- As evident from Figs. 3.1 and 3.2, it is observed that magnitude of anchor tension in outer anchor increases with increase in anchor stiffness, and decreases with increase in plate thickness, for a particular base-stiffness. It is also observed that the magnitude of anchor tension in outer anchor decreases with increase in base-stiffness, as well as with increase in plate thickness, for a particular anchor-stiffness.

- As observed from Figs 3.3 and 3.4, the magnitude of anchor tension in central anchor increases with increase in anchor stiffness, and decreases with increase in plate thickness, for a particular base stiffness. It is also evident that the magnitude of anchor tension in central anchor increases with increase in base stiffness, and decreases with increase in plate thickness, for a particular anchor stiffness.

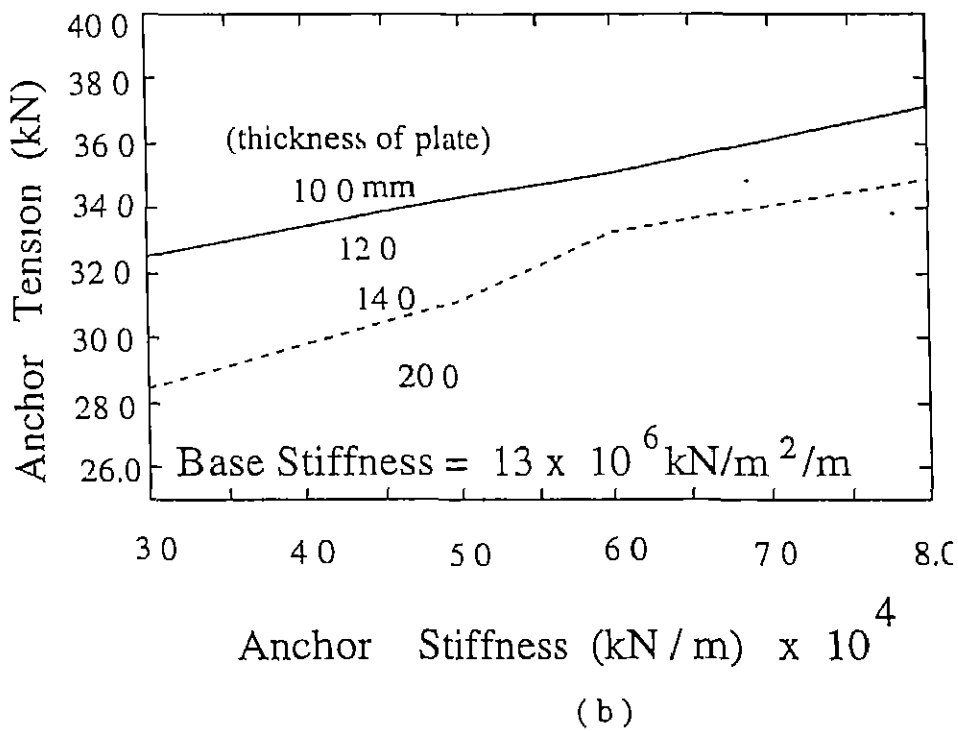
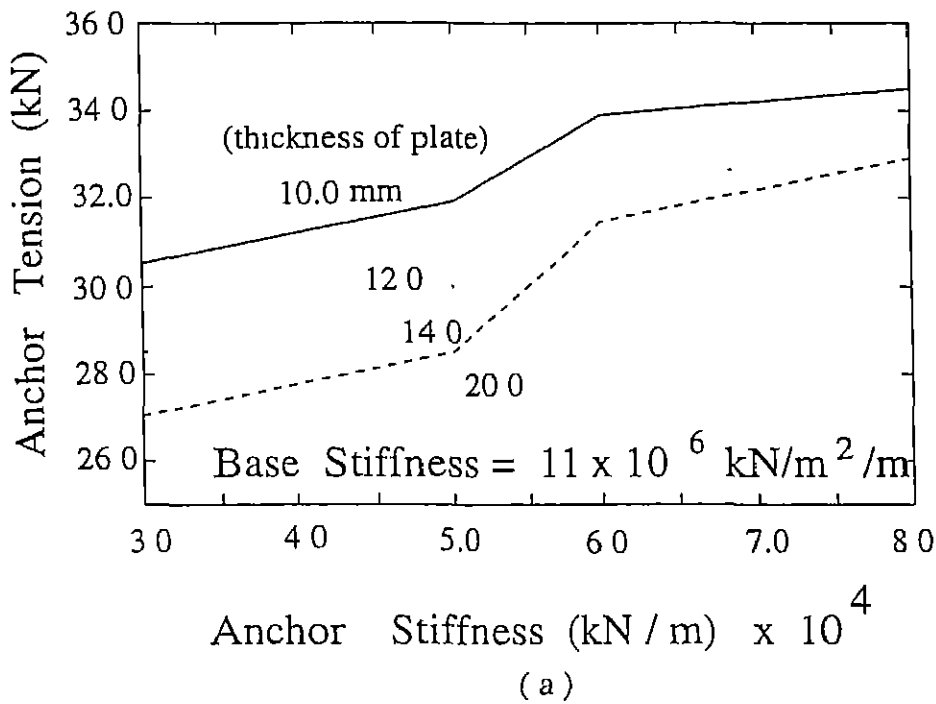


Figure 3.1 Variation of Anchor Tension for Anchor No. 1 with Anchor Stiffness at Collapse

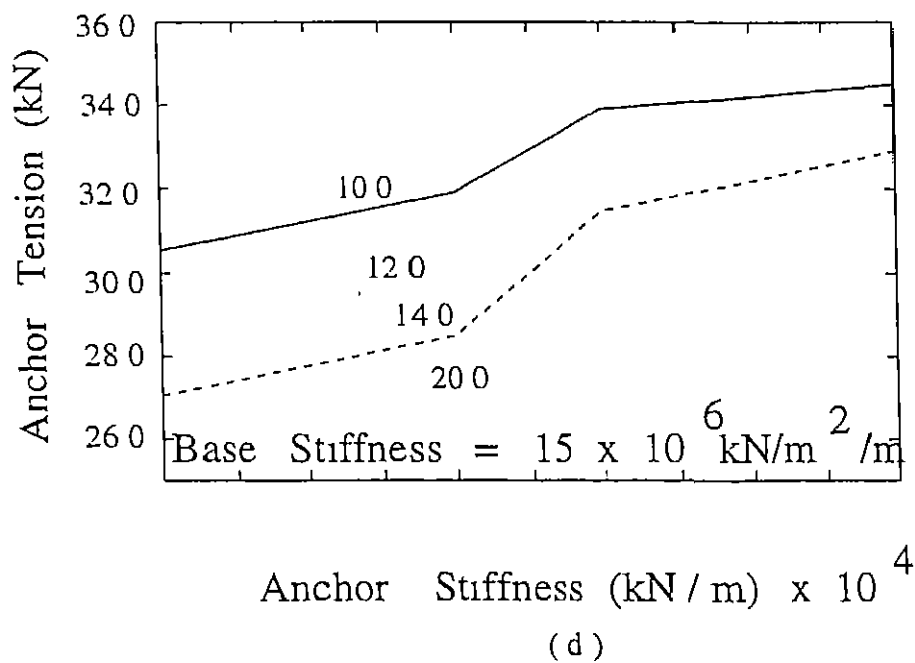
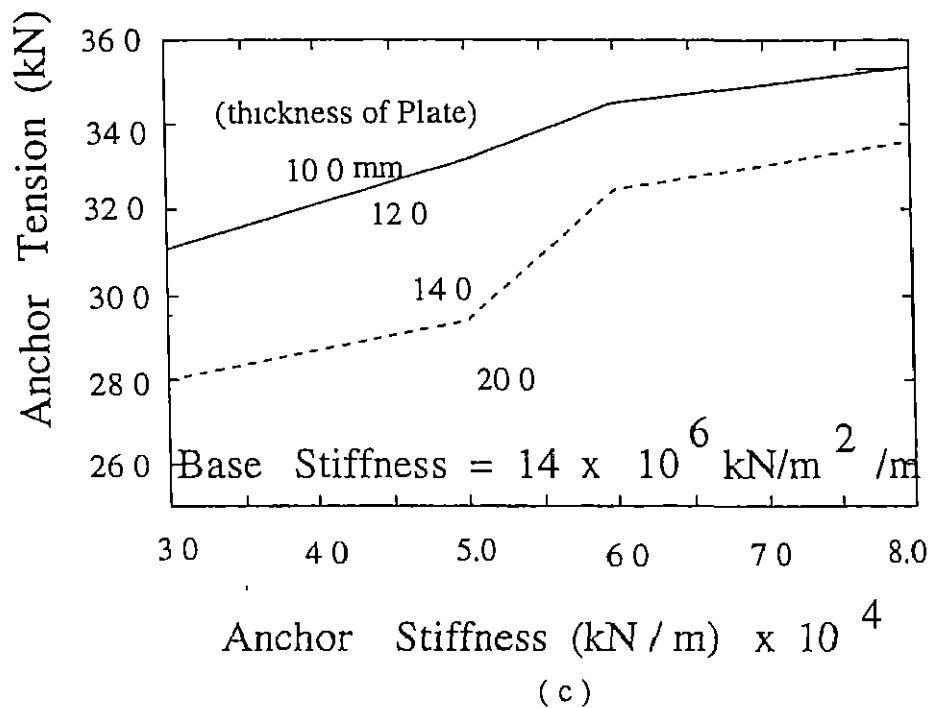


Figure 3.1 Variation of Anchor Tension for Anchor No. 1 with Anchor Stiffness at Collapse

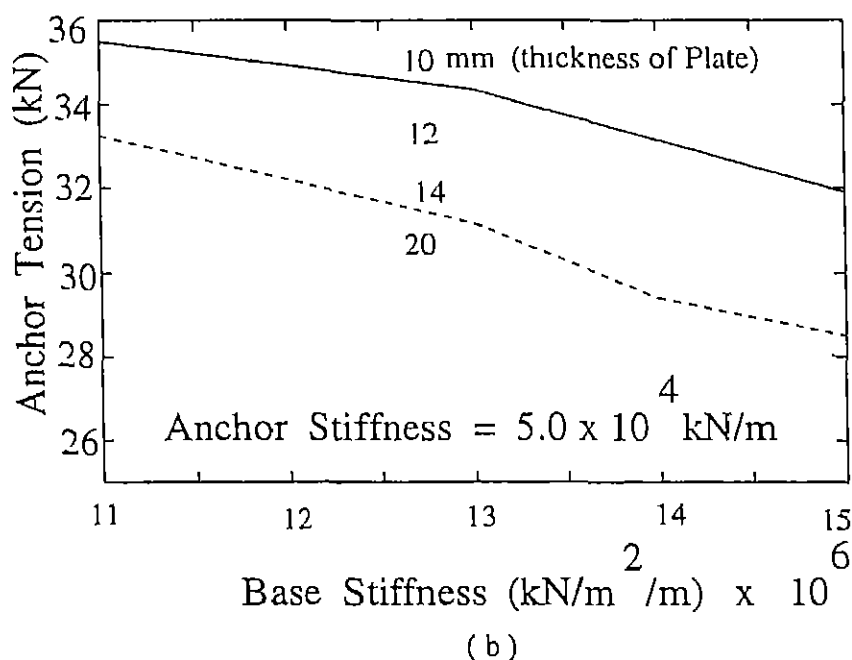
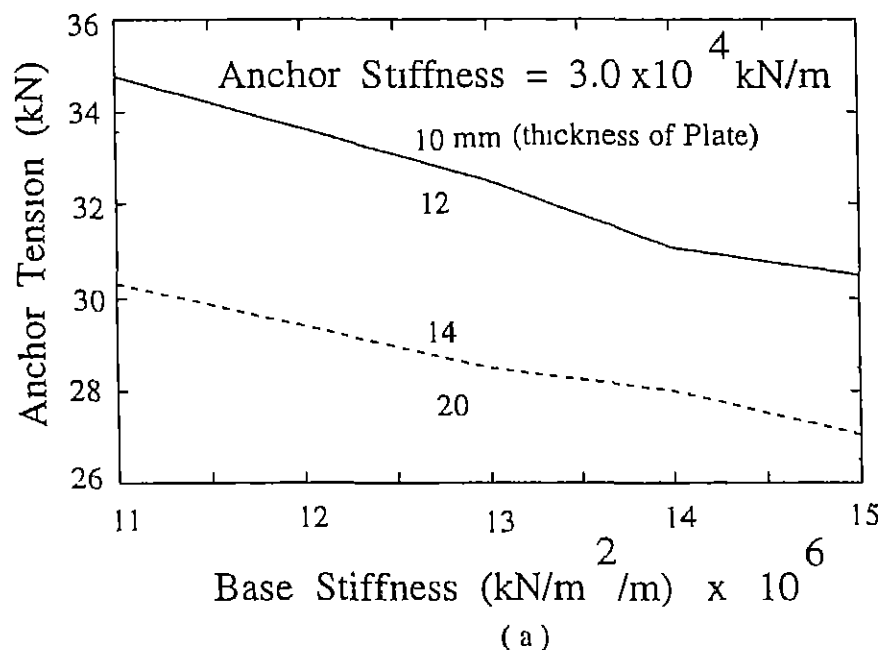


Figure 3 2 Variation of Anchor Tension for Anchor No. 1 with Base Stiffness at Collapse

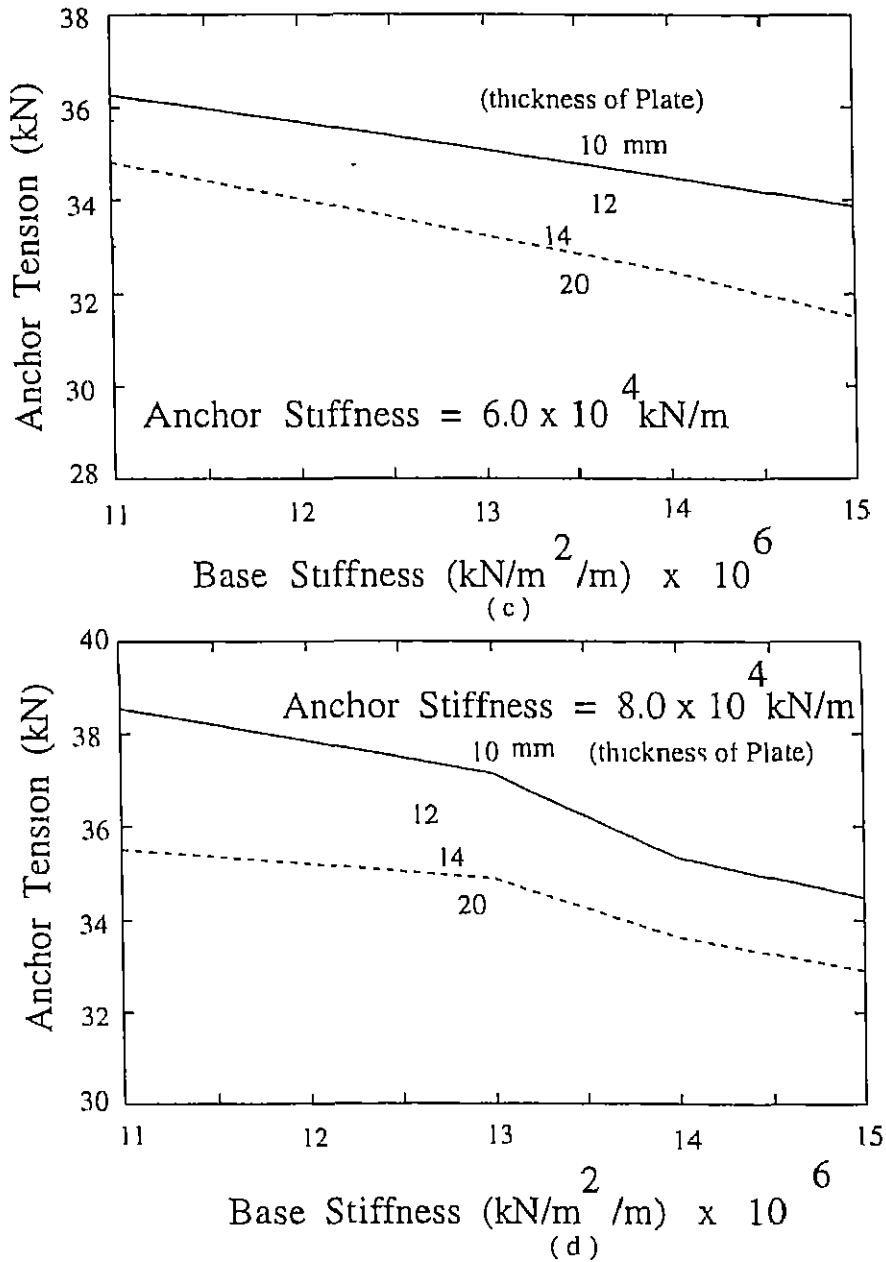


Figure 3.2 Variation of Anchor Tension for Anchor No 1 with Base Stiffness at Collapse

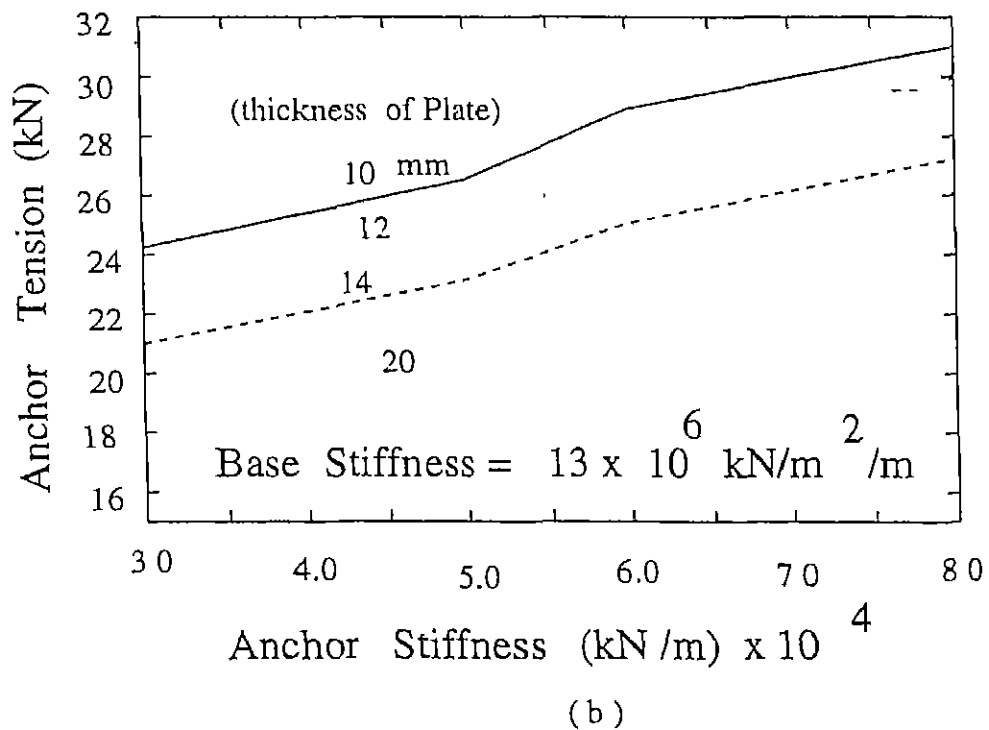
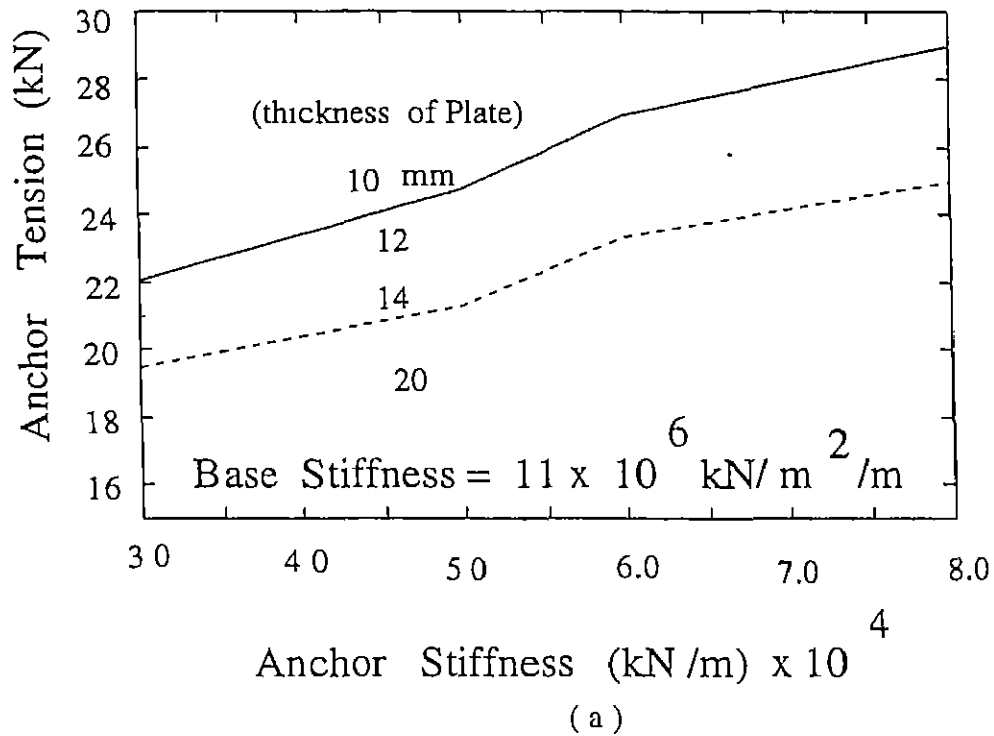


Figure 3.3 Variation of Anchor Tension for Central Anchor with Anchor Stiffness at Collapse



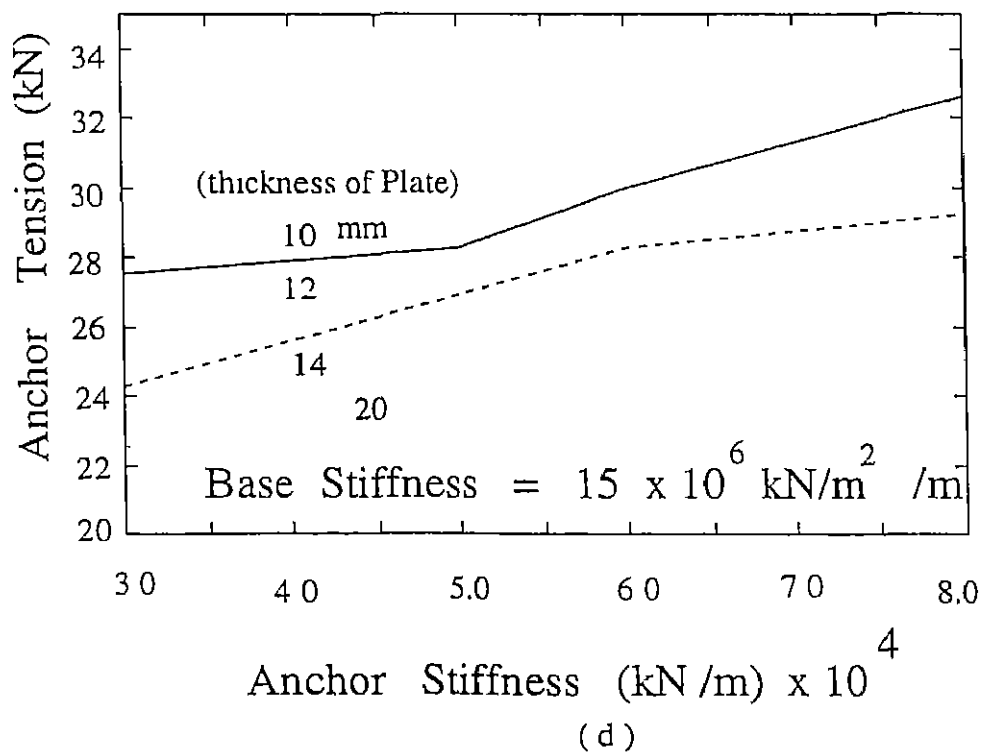
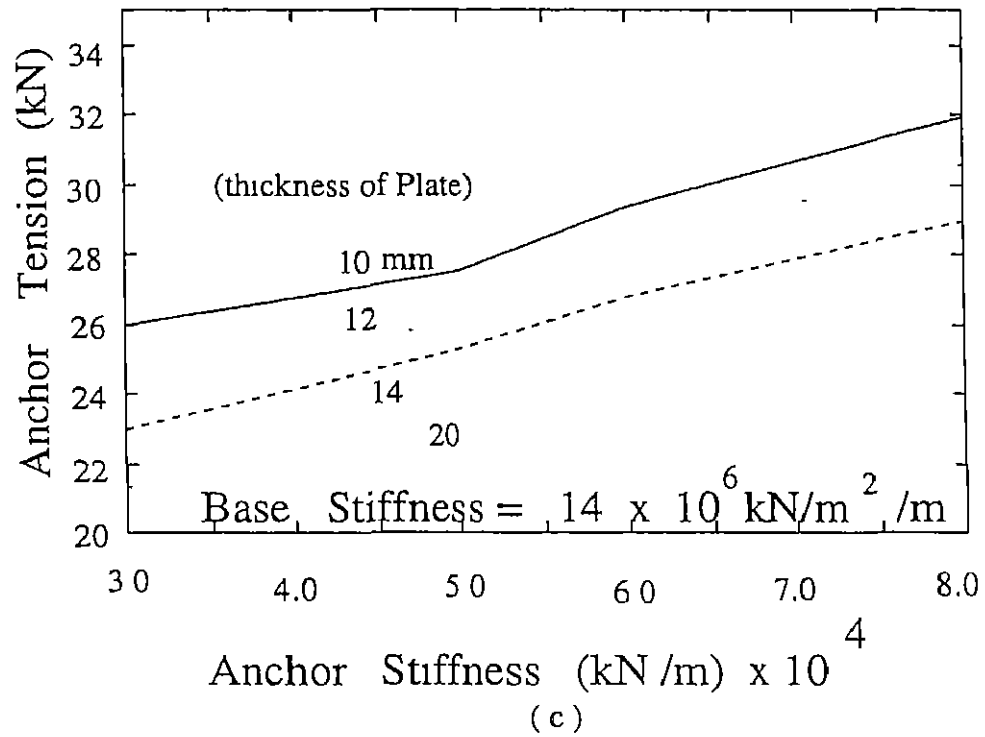


Figure 3.3 Variation of Anchor Tension for Central Anchor with Anchor Stiffness at Collapse

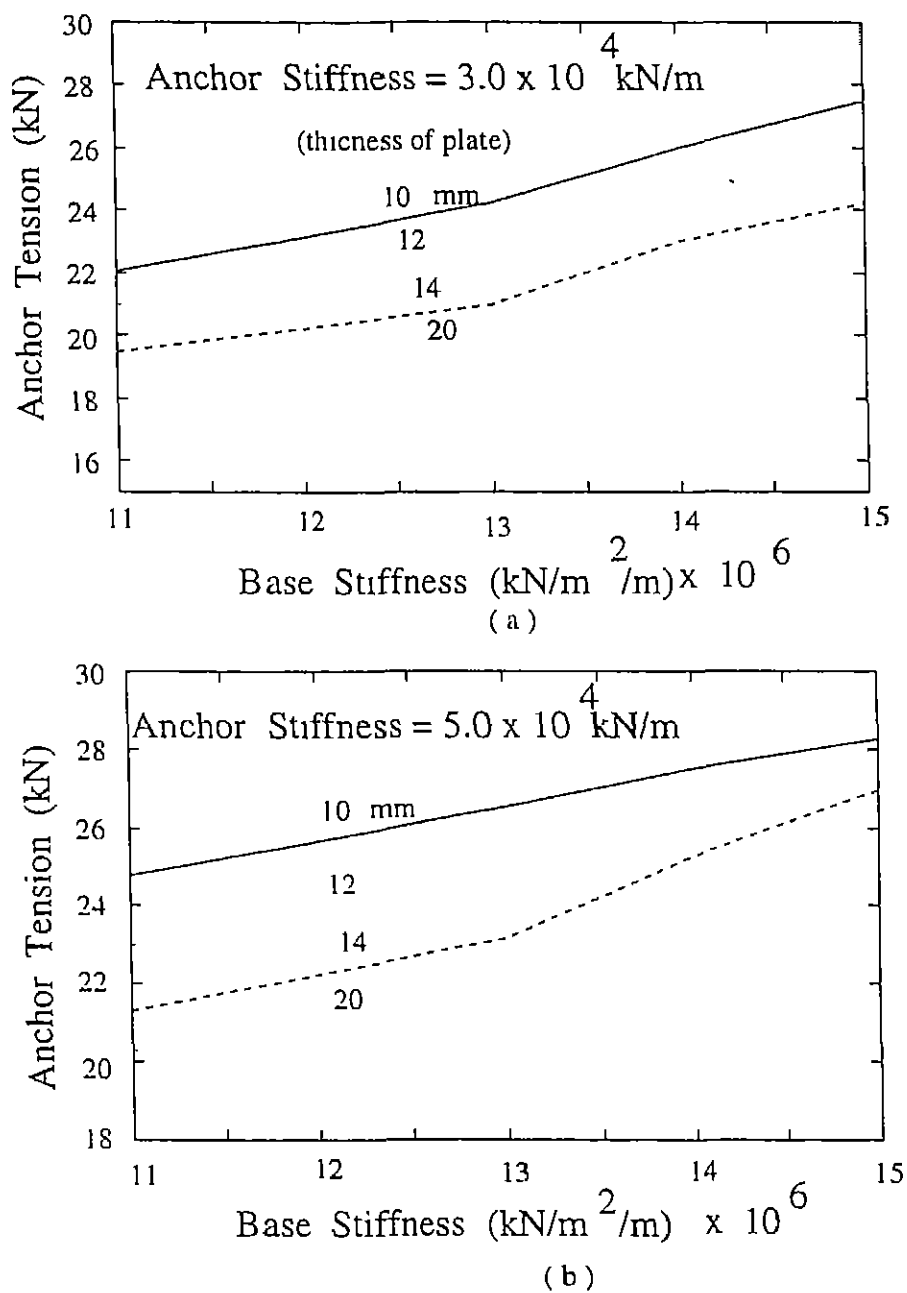


Figure 3.4 Variation of Anchor Tension for Central Anchor with Base Stiffness at Collapse

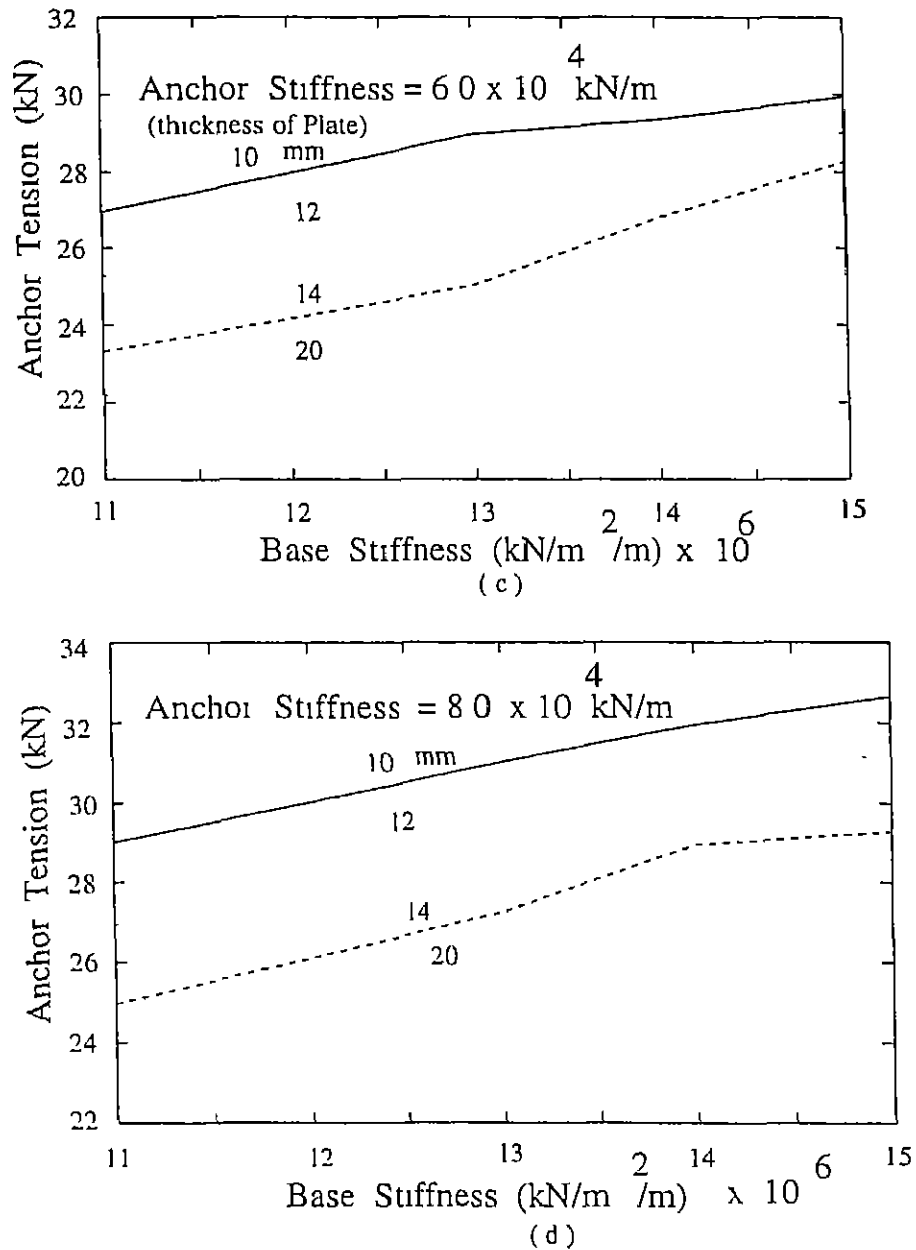


Figure 3.4. Variation of Anchor Tension for Central Anchor with Base Stiffness at Collapse

### 3.3 Study on Anchor Tension and Assembly Capacity in Plate-Anchor Assemblies subjected to Tensile Loading.

Variation of anchor tension, assembly capacity and associated modes of failure in plate-anchor assemblies subjected to eccentric tensile loading, is studied by varying plate thickness, anchor size, anchor material, and grade of base concrete. For the present study, the various plate thicknesses considered are 20mm, 50mm and 100mm. The base stiffness variation is done by changing the grade of concrete as M25, M30 and M40. The anchor stiffness is varied by adopting different anchor diameters, 12mm, 16mm and 24mm. The anchor material is also varied by using materials having yield strengths of  $250 \text{ N/mm}^2$  and  $415 \text{ N/mm}^2$ . The parametric study is carried out using a typical embedded plate-anchor assembly (Fig 1.3) having plate dimensions of 400mm X 250mm with 4 anchors subjected to tensile loading (at eccentricities of 0mm and 100mm) transferred through an attachment of size 100mm X 100mm.

The results of the study are presented in Figs 3.5 (a),(b),(c) and Table 3.1, providing information regarding anchor tension, assembly capacity and associated mode of failure, at collapse.

Following observations are made from the study:

- The magnitude of anchor tension increases with increase in yield strength of anchors for given plate thickness and grade of concrete.
- The variation in the magnitude of anchor tension with increase in plate thickness is not appreciable.
- The magnitude of anchor tension increases with increase in diameter the anchors.
- The increase in the characteristic strength of concrete causes marginal increase in the anchor tension.
- The capacity of the assembly is decreased considerably with increase in the load eccentricity.

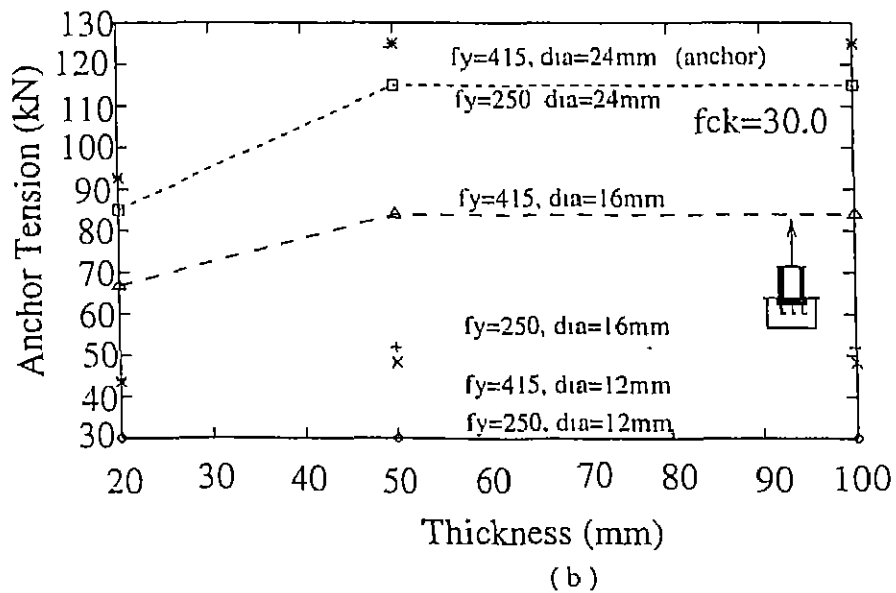
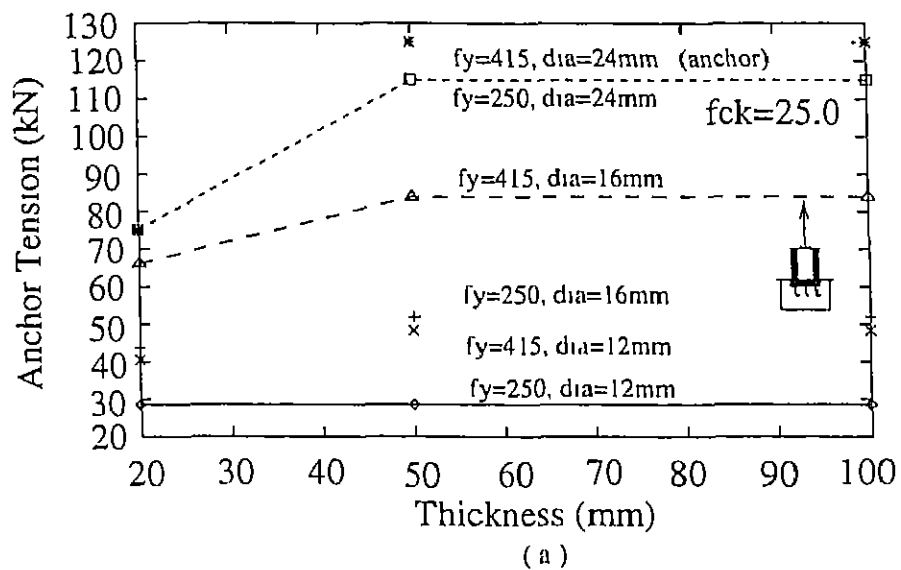
Tensile Capacity of Anchors ( $e=0\text{mm}$ )

Figure 3.5 Anchor Tension at Collapse for Axial Tensile Load

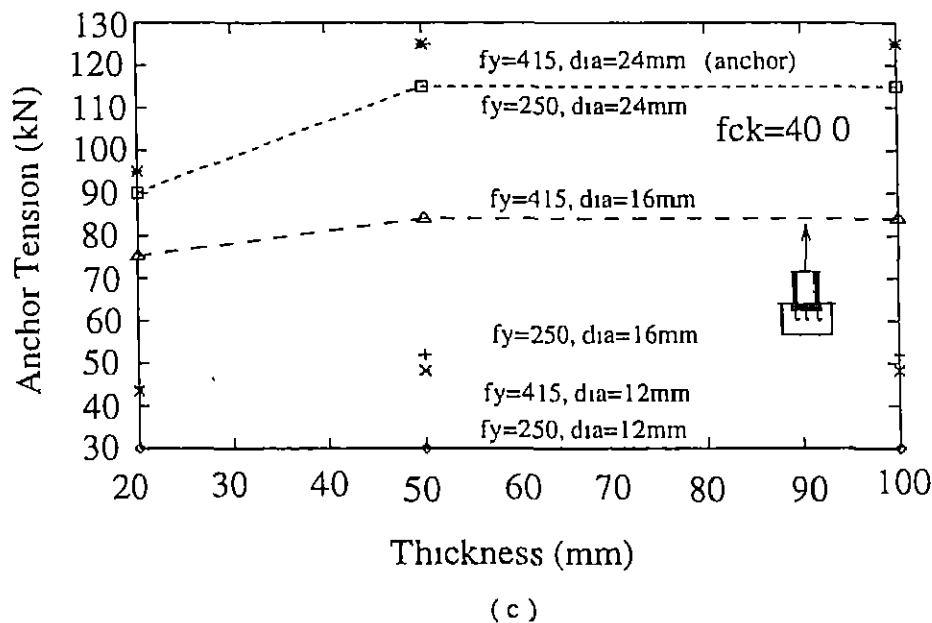


Figure 3.5 Anchor Tension at Collapse for Axial Tensile Load

- In the cases of axial tensile loading (i.e. tensile loading at zero eccentricity), the assembly capacity is marginally lower than the magnitude of total tension in four anchors
- Assembly Collapse is primarily due to the failure of anchors.
- Anchors of lower yield strength and lesser diameter experienced ductile failure at assembly collapse
- Assemblies having thicker plates collapsed with ductile failure of anchors
- Assemblies with smaller plate thickness and larger anchor diameter collapsed with brittle failure of anchors

Table 3.1 Capacity of Plate-Anchor Assembly subjected to Tensile Loading

S No	Plate th mm	$f_{ck}$ (N/mm <sup>2</sup> )	$f_y$ of anchors (N/mm <sup>2</sup> )	Dia of anchors (mm)	Anc. Ten. (kN)	Assembly Capacity(KN)		Type of failure
						e=0 0	e=100 0	
1	20 0	25 0	250 0	12	28 57	114 00	75 00	Anc
2	50 0	25 0	250 0	12	28 57	114 00	75 00	Anc
3	100 0	25 0	250 0	12	28 57	114 00	75 00	Anc
4	20 0	25 0	250 0	16	43 72	160 00	105 00	Con
5	50 0	25 0	250 0	16	52 07	208 00	130 00	Anc
6	100.0	25 0	250.0	16	52.07	208.00	130.00	Anc
7	20 0	25 0	250 0	24	75 21	210 00	142 50	Con
8	50 0	25 0	250 0	24	115 00	457 00	300 00	Anc
9	100 0	25.0	250 0	24	115 00	457 00	300 00	Anc
10	20 0	25 0	415.0	12	40.51	160 00	100 00	Con
11	50.0	25 0	415 0	12	48 32	192 00	120.00	Anc
12	100 0	25 0	415.0	12	48 32	192.00	120.00	Anc
13	20 0	25 0	415.0	16	66.22	176.00	125 00	Con
14	50.0	25.0	415 0	16	84 01	336 00	220 00	Anc
15	100 0	25 0	415 0	16	84 01	336 00	220 00	Anc
16	20 0	25 0	415 0	24	75.16	210 00	150 00	Con
17	50.0	25 0	415 0	24	125 00	457 00	380 00	Anc
18	100.0	25 0	415.0	24	125 00	457 00	380 00	Anc
19	20 0	30 0	250.0	12	30 10	120 00	75.00	Anc
20	50.0	30 0	250 0	12	30.10	120 00	75 00	Anc
21	100 0	30 0	250.0	12	30 10	120 00	75.00	Anc
22	20.0	30 0	250.0	16	44 02	160 00	105 00	Con
23	50 0	30.0	250 0	16	52.01	208.00	130 00	Anc
24	100 0	30.0	250 0	16	52 01	208 00	130 00	Anc
25	20 0	30.0	250.0	24	85.00	210 00	147 50	Con
26	50.0	30 0	250.0	24	115 00	457 00	300 00	Anc
27	100 0	30 0	250 0	24	115 00	457.00	300 00	Anc
28	20.0	30 0	415 0	12	43 52	160 00	100.0	Con
29.	50 0	30 0	415.0	12	48.32	192 00	120.0	Anc
30.	100.0	30.0	415.0	12	48 32	192 00	120.0	Anc
31	20 0	30 0	415.0	16	66 70	176 00	105 00	Con
32	50 0	30 0	415.0	16	84 01	336 00	220.00	Anc
33	100 0	30.0	415 0	16	84 01	336 00	220 00	Anc
34	20 0	30 0	415 0	24	92 70	210.00	167 00	Con
35.	50.0	30.0	415.0	24	125.00	457 00	387 50	Anc
36	100 0	30.0	415 0	24	125.00	457 00	387 50	Anc

table 3 1 (Contd )

S No	Plate th mm	$f_{ck}$ (N/mm <sup>2</sup> )	$f_y$ of anchors (N/mm <sup>2</sup> )	Dia of anchors (mm)	Anc Ten (kN)	Assembly Capacity(KN)		Type of failure
						e=0.0	e=100 0	
37	20 0	40 0	250 0	12	30 09	120 00	75.00	Anc
38	50 0	40 0	250 0	12	30 09	120 00	75 00	Anc
39	100 0	40 0	250 0	12	30 09	120 00	75 00	Anc
40	20 0	40 0	250 0	16	44 28	160 00	105 00	Con
41	50.0	40 0	250 0	16	52 01	208 00	130 00	Anc
42	100 0	40 0	250 0	16	52 01	208.00	130.00	Anc
43	20 0	40 0	250 0	24	90 00	210.00	135 00	Con
44.	50 0	40 0	250 0	24	115.05	457 50	300 00	Anc
45	100 0	40 0	250 0	24	115.05	457 50	300 00	Anc
46	20 0	40.0	415 0	12	43 43	160 00	100.00	Con
47.	50 0	40 0	415 0	12	48 32	192.00	125 00	Anc
48	100 0	40.0	415 0	12	48.32	192.00	125 00	Anc
49	20.0	40.0	415.0	16	75 22	184.05	105.00	Con
50	50 0	40 0	415.0	16	84.01	336 10	220 00	Anc
51	100.0	40 0	415 0	16	84 01	336 10	220 00	Anc
52.	20 0	40 0	415 0	24	95 03	210.00	140 00	Con
53	50.0	40.0	415.0	24	125.10	457 01	380.00	Anc
54	100.0	40 0	415.0	24	125 10	457 01	380 00	Anc

Anc Ten.      Anchor Tension at Collapse

th              Thickness

Anc              Ductile Failure of Anchor

Con.              Brittle Failure of Anchor associated with concrete.



### 3.4 Study on Assembly Capacity in Plate-Anchor Assemblies subjected to Shear Loading.

Variation of the Capacity of plate-anchor assembly subjected to shear loading is studied by varying the plate thickness, anchor size, anchor material and grade of base concrete. For the present study, the various plate thicknesses considered are 20mm, 50mm and 100mm. The base stiffness variation is implemented by changing the grade of concrete as M25, M30 and M40. The anchor stiffness is varied by using different anchor diameters 12mm, 16mm and 24mm. The yield strengths of anchors adopted are  $250 \text{ N/mm}^2$  and  $415 \text{ N/mm}^2$ . The parametric study is carried out using a typical embedded plate-anchor assembly having plate dimensions of 400mm X 250mm with 6 anchors subjected to shear loading transferred through an attachment of size 100mm X 100mm. Two separate cases of shear loading are considered, one acting at the plate level, and, the other one is located at a height of 100mm from the plate top. The plate-anchor assembly considered is illustrated in Fig. 3.6. The Table 3.2 presented has the details of the capacity of the assembly subjected to two shear load cases ( $h=0\text{mm}$  and  $h=100\text{mm}$ ) for different plate thicknesses, characteristic strengths of concrete, yield strength anchors and size of anchors.

In the present study, it is considered that the shear strength of plate-anchor assembly is derived from the frictional resistance offered by the interface between plate and concrete base, and the shear strength provided by the anchors. [45] If the shear strength offered by the friction is greater than the applied shear, then anchors are not required to resist any shear force. If the shear force is greater than the frictional resistance, then the anchors carrying compression start resisting the shear force and the anchors subjected to tension develop their full strength for moment-resistance. If the shear force is greater than the combined resistance offered by friction and compression anchors, then tension anchors will also resist the shear force.

Following observations are made from the results presented in Table 3.2.

- The Capacity of the assembly increases with increase in the diameter of the anchors
- The increase in the characteristic strength of concrete does not have any appreciable effect in respect of increase in the Capacity of the assembly.
- Increase in the yield strength of anchor has demonstrated considerable increase in the Capacity of the assembly
- The increase in plate thickness does not have any influence in increasing the shear resisting capacity of the assembly
- For the cases of shear loading applied at a height ( $h=100\text{mm}$ ) above the plate top, the assembly capacity decreases considerably, compared to the values corresponding to those for the shear loading applied at plate level

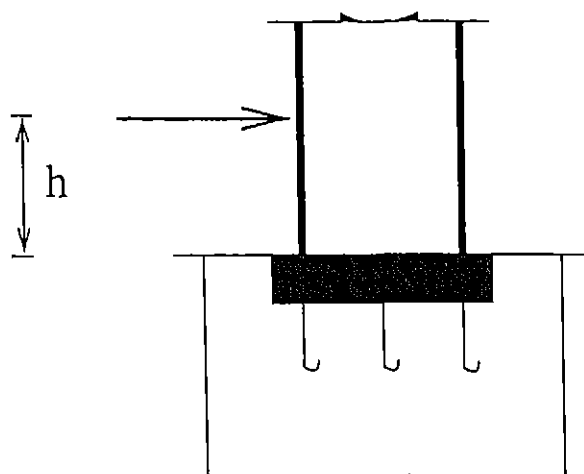


Figure 3.6: Assembly subjected to Shear Loading

table 3.2

S No	Plate th mm	$f_{ck}$ (N/mm <sup>2</sup> )	$f_y$ of anchor (N/mm <sup>2</sup> )	Dia of anchor (mm)	Assembly Cap (kN)	
					e=0 0	e=100 0
1	20 0	25 0	250 0	12	126.67	103 32
2	50 0	25 0	250 0	12	126 67	103 32
3	100 0	25.0	250 0	12	126 67	103 32
4	20 0	25 0	250 0	16	220.00	169 00
5	50.0	25 0	250 0	16	220 00	173 32
6	100 0	25 0	250 0	16	220.00	173 31
7	20 0	25 0	250 0	24	473 35	280.00
8	50 0	25 0	250 0	24	473 35	386 68
9	100 0	25.0	250 0	24	473.35	386 68
10	20 0	25 0	415 0	12	200.00	269 98
11	50.0	25 0	415 0	12	200 00	269 98
12	100 0	25.0	415 0	12	200.00	269 98
13	20 0	25 0	415 0	16	353 48	272 05
14	50 0	25.0	415 0	16	353 48	288 50
15	100 0	25 0	415 0	16	353 48	288 50
16	20 0	25 0	415.0	24	792 00	408.25
17	50.0	25 0	415.0	24	792 00	640 00
18	100 0	25 0	415 0	24	792 00	640 00
19.	20 0	30 0	250 0	12	126 67	105 00
20	50 0	30 0	250.0	12	126 67	105 00
21	100 0	30.0	250 0	12	126.67	105.00
22.	20.0	30 0	250 0	16	220 00	144 00
23.	50.0	30 0	250 0	16	220 00	174.00
24	100 0	30 0	250.0	16	220 00	174 00
25	20 0	30 0	250 0	24	473 35	280.00
26	50 0	30.0	250.0	24	473 35	384.25
27.	100.0	30 0	250.0	24	473 35	384 25
28	20.0	30 0	250 0	12	200.00	168.15
29	50.0	30.0	250 0	12	200 00	168.15
30	100 0	30 0	250.0	12	200 00	168.15
31	20 0	30 0	250 0	16	353 00	234.05
32	50 0	30.0	250.0	16	353 00	288 35
33	100 0	30.0	250 0	16	353 00	288 35
34.	20 0	30 0	250.0	24	792 00	408 00
35	50.0	30 0	250 0	24	792.00	640 25
36	100 0	30.0	250 0	24	792.00	640.25
37	20 0	40 0	250.0	12	126.67	104.00
38	50.0	40.0	250 0	12	126.67	104.00
39	100 0	40.0	250 0	12	126.67	104.00
40.	20 0	40 0	250 0	16	220 00	144.25

table 3.2 (Contd.)

S No	Plate th mm	$f_{ck}$ (N/mm <sup>2</sup> )	$f_y$ of anchor (N/mm <sup>2</sup> )	Dia of anchor (mm)	Assembly Cap.(kN)	
					e=0.0	e=100.0
41	50.0	40.0	250.0	16	220.00	180.85
42	100.0	40.0	250.0	16	220.00	180.85
43	20.0	40.0	250.0	24	473.35	280.00
44	50.0	40.0	250.0	24	473.35	392.25
45	100.0	40.0	250.0	24	473.35	392.25
46	20.0	40.0	250.0	12	200.00	168.00
47	50.0	40.0	250.0	12	200.00	168.00
48	100.0	40.0	250.0	12	200.00	168.00
49	20.0	40.0	250.0	16	353.00	234.25
50	50.0	40.0	250.0	16	353.00	288.00
51	100.0	40.0	250.0	16	353.00	288.00
52	20.0	40.0	250.0	24	792.00	408.00
53	50.0	40.0	250.0	24	792.00	640.00
54	100.0	40.0	250.0	24	792.00	640.00

Note . Assembly Collapse was observed to be primarily due to ductile of anchors

### 3.5 Study for the Development of Strength Interaction Diagrams and Moment-Rotation Charts for Plate-Anchor Assemblies subjected to Eccentric Compressive Loading.

Considering the possible variations in the different design parameters of a plate-anchor assembly subjected to eccentric compressive loading, a study is made for the development of relevant strength interaction diagrams and moment-rotation charts for such assemblies. In order to embrace realistic variations, the study includes the variations in plate thickness, plan dimensions of plate, area of attachment, grade of base concrete,

and size, location and number of anchors. To facilitate the availability of information regarding reserve strength of the assemblies in post-failure phase, failure and collapse interaction diagrams are developed.

The different mild steel plate (yield strength of  $300 \text{ N/mm}^2$ ) thicknesses considered are 10mm, 12mm, 14mm, 16mm, 18mm, 20mm, 25mm, 32mm and 40mm. The compression load eccentricity is increased from zero upto a value such that the loading becomes almost equivalent to a pure moment one, followed by the case of only uni-axial moment. The mild steel anchors (yield strength of  $330 \text{ N/mm}^2$ ) are considered to be placed at any spacings (but, same between consecutive anchors in one direction) in two directions with plate edge distance of twice the diameter of anchor. The ratio of the concrete base area to the plate area is taken as 2.5 considering the same to be commonly adopted in actual application. The ratio of cross-sectional area of single anchor ( $A_{anc}$ ) to the product of the spacings in two directions ( $s_1$  and  $s_2$ ) is taken as 0.0032, this is selected based on observations made while carrying out the study, to facilitate the development/usage of the interaction diagrams. The ratio of area of attachment ( $A_{atch}$ ) to the area of plate ( $A_{plate}$ ) is taken as 0.1 and 0.2. these ratios are considered to be representative for most of the actual cases.

The interaction diagrams and moment-rotation (see Fig. 3.7) charts are presented non-dimensionally. The details regarding the back-ground dimensional analysis are presented in Appendix-II.

The basic details regarding the development of interaction diagrams and moment-rotation charts are typically presented in the following.

Size of the plate ( $D \times B$ ) = 400mm X 250mm

Yield Strength of Plate ( $f_y$ ) = 300 N/mm<sup>2</sup>

Size of attachment ( $d \times b$ ) = 200mm X 100mm

Thickness of plate ( $t$ ) = 10mm

Spacing of anchors in longer direction ( $s_1$ ) = 175mm

Spacing of anchors in shorter direction ( $s_2$ ) = 200mm

Edge distance of anchor ( $d'$ ) = 25mm

Characteristic Strength of concrete ( $f_{ck}$ ) = 25 N/mm<sup>2</sup>

Yield Strength of Anchor ( $f'_y$ ) = 330 N/mm<sup>2</sup>

Area of anchor ( $A_{anc}$ ) = 113.09 mm<sup>2</sup>

$A_{atch}/A_{plate} = 0.2$

$A_{anc}/s_1 s_2 = 0.0032$

S No	Load eccentricity (mm)	Load at Collapse (kN)	Load at Failure (kN)
1	0.00	1919.00	813.88
2	25.00	1560.00	597.82
3	50.00	1360.01	449.82
4	75.00	1050.00	300.11
5	100.00	700.00	217.62
6	125.00	485.00	152.45
7	150.00	372.00	115.11
8	175.00	288.00	92.55
9	200.00	235.00	70.79
10	225.00	206.67	57.03
11	250.00	160.00	47.73
12	275.00	137.50	41.04
13	300.00	129.98	35.99
14	325.00	109.34	31.97
15	350.00	98.67	28.69
16	375.00	92.67	26.03
17	400.00	88.00	25.63
18	425.00	70.00	24.12
19	450.00	62.01	22.45

S No	Moment (kN-m)	Rotation (in rads )	S No	Moment (kN-m)	Rotation (in rads )
1	0 00	.000	24	38 58	00577395
2	7 14	00075349	25	40 01	00631452
3	8 57	.00090427	26	41 44	00690261
4	10 00	00105505	27	42 87	00758288
5.	11.43	00120584	28.	44 30	00845576
6	12 86	00135662	29.	45 73	00952115
7	14.29	00150741	30	47 16	01068330
8	15 72	00165819	31.	48 58	.01187281
9	17 15	00180897	32.	50 01	01307122
10	18 58	00195976	33.	51 44	01431607
11	20 00	00211054	34.	52 87	01573141
12.	21 43	00226133	35.	54 30	01714675
13	22 86	00241211	36	55 73	01859512
14	24 29	00256289	37	57 16	02006501
15	25 72	00274929	38	58.59	.02153490
16	27 15	00297321	39	60 02	02300826
17	28 58	00321243	40.	61 45	.02448162
18	30 01	00348951	41	62.87	.02595497
19	31 44	.00376659	42	64 30	03142830
20	32 87	00405823	43	65 73	.03809560
21	34 29	00441460	44	67 16	04112249
22	35 72	00483092	45	68 59	04268114
23	37 15	00530244	46	70 02	05083060
			47	71 45	06422982

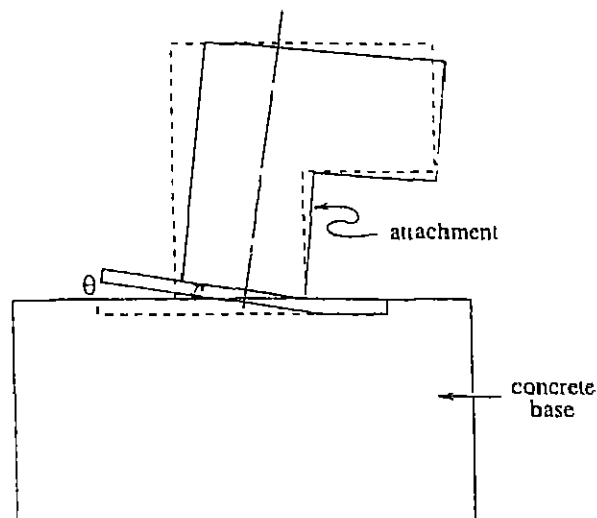


Figure 3 7. Rotation of Assembly

The details and the analysis regarding the interaction diagrams and moment-rotation

charts are presented in the following chapter

### 3.6 Study for the Development of Strength Interaction Diagrams and Moment-Rotation Charts for Plate-Anchor Assemblies subjected to Eccentric Tensile Loading.

Embedded Plate-Anchor Assemblies are commonly subjected to eccentric tensile loading in actual applications. As depicted in case of eccentric compressive loading, a similar study is performed for the development of relevant strength interaction diagrams (failure and collapse) and moment-rotation charts

The material properties and the ratios of different design parameters that were adopted in the case of eccentric compressive loading, are also applicable in the present case. The needed dimensional analysis for presentation of interaction diagrams and moment-rotation charts in non-dimensional form, are furnished in Appendix-II

The basic details regarding the development of interaction diagrams and moment-rotation charts are typically presented in the following

LIBRARY  
KANPUR  
No. A 123314



S No	Load eccentricity (mm)	Load at Collapse (kN)	Load at Failure (kN)
1	0 00	165 00	46 46
2	25 00	154 25	46 35
3	50 00	141 43	46 08
4	75 00	128 32	42 25
5	100 00	115 72	38 38
6	125 00	106 75	35 67
7	150 00	94 28	31 91
8	175 00	87 45	29 81
9	200 00	79.99	27 20
10	225 00	75 27	24 89
11	250 00	70 86	23 75
12	275 00	66 12	22 50
13	300 00	61 72	20 01
14	325 00	57 85	18 89
15	350 00	54 30	18 01
16	375.00	52 67	18.01
17	400 00	50 01	17 14
18	425.00	48 00	16.00
19	450 00	46 25	15.01

S No.	Moment (kN-m)	Rotation (in rads )
1	0 00	000
2.	2 14	00111303
3	2 57	00133577
4	3 00	00155851
5	3 43	00178125
6	3 86	00200399
7	4 29	00222673
8	4 72	00244947
9	5 15	00267221
10	5 57	00289495
11	6.00	.00311769
12	6 43	.00334043
13	6.86	00370506
14	7 29	.00406968
15	7 72	.00445194
16	8 15	00493989
17	8.58	00560378
18	9 01	00647025
19	9 44	.00771378
20	9 86	01023964
21	10 29	01276744
22	10 72	01476372
23	11 15	.02082765
24	11 58	03077335
25	12 01	.03554219

The details and the analysis regarding the interaction diagrams and moment-rotation charts are presented in the following chapter

### 3.7 Study for the Evaluation of the Interaction Diagrams for Plate Anchor Assemblies subjected to Eccentric Compressive Loading and Shear Loading

Considering the different design parameters for possible variations of a plate-anchor assembly, subjected to shear loading combinedly with eccentric compressive loading,

a study is made for the evaluation of the interaction diagrams which were earlier developed for such assemblies subjected to eccentric compressive load. As explained earlier in section 3.4, the shear force is resisted by the frictional resistance offered by the interface between the plate and concrete base unless the anchors are also effective in resisting shear when the applied shear goes beyond the magnitude of frictional resistance

The different mild steel plate (yield strength of  $300 \text{ N/mm}^2$ ) thicknesses considered are 10mm, 12mm, 14mm, 16mm, 18mm, 20mm, 25mm, 32mm and 40mm. The plan dimensions of the plate considered are 400mm X 250mm, with 6 mild steel anchors (yield strength  $330 \text{ N/mm}^2$ ) of 12mm diameter. The load is transferred through an attachment of size 100 mm square. The characteristic strength of base concrete is adopted as  $25 \text{ N/mm}^2$ .

For each thickness of plate, the eccentricity of the compressive load ( $P$ ) is varied and the Shear force ( $H$ ) is applied at the plate level. The ratio of shear force ( $H$ ) to axial compressive load ( $P$ ) is varied for each value of eccentricity for a particular thickness, and the capacity of the assembly is observed. The details of the results of the study are shown in Figs. 3.8-3.12.

Following observations are made from the Figs. 3.8-3.12

- For all the cases, assembly capacity is observed to be constant upto certain ratio of shear force to axial compressive load ( $H/P$ ), beyond which the capacity decreases with increase in the ratio ( $H/P$ ) of shear force to axial compressive load. The value of the specific ratio of shear force to axial compressive load upto which the capacity is constant, increases with increase in compressive load eccentricity, for a given plate thickness.
- For a given plate thickness, at higher compressive load-eccentricities, the assembly capacity remains almost constant.
- There is a trend of convergence of assembly capacity varying within a very narrow band at relatively higher ratios of shear force to axial compressive load ( $H/P$ ).

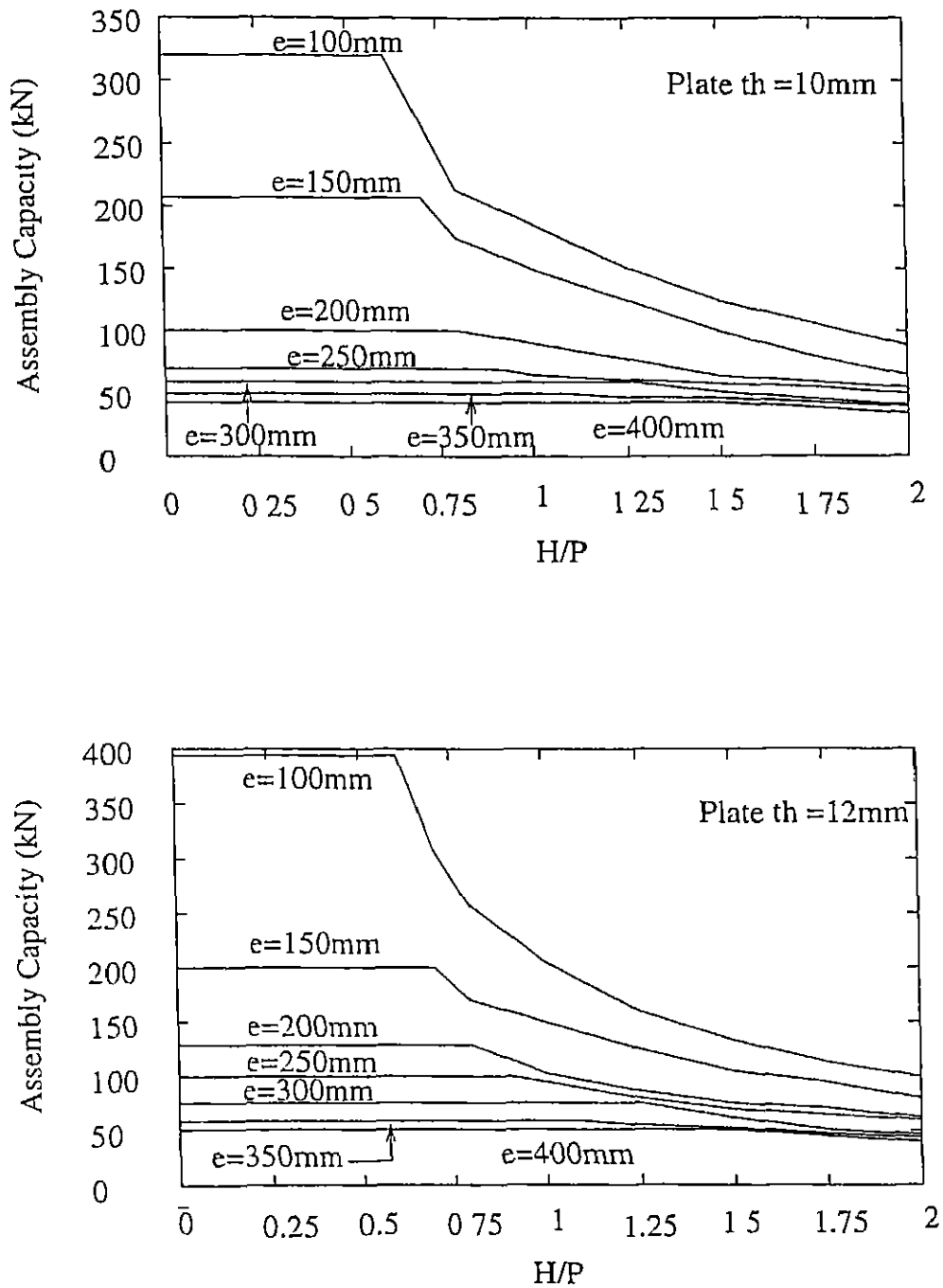


Figure 3.8 Assembly Capacity at Collapse Vs H/P Ratio

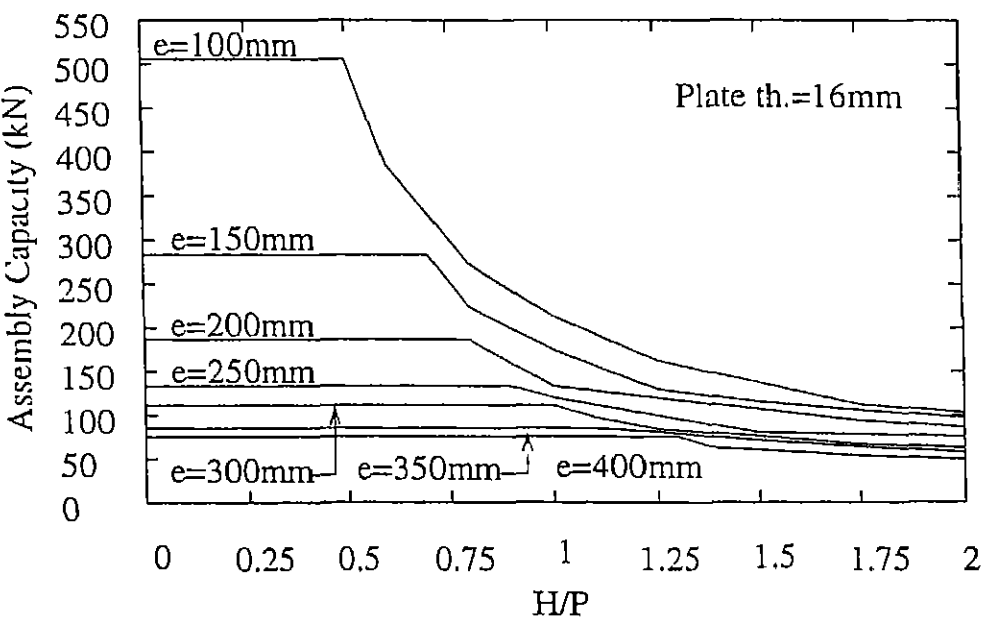
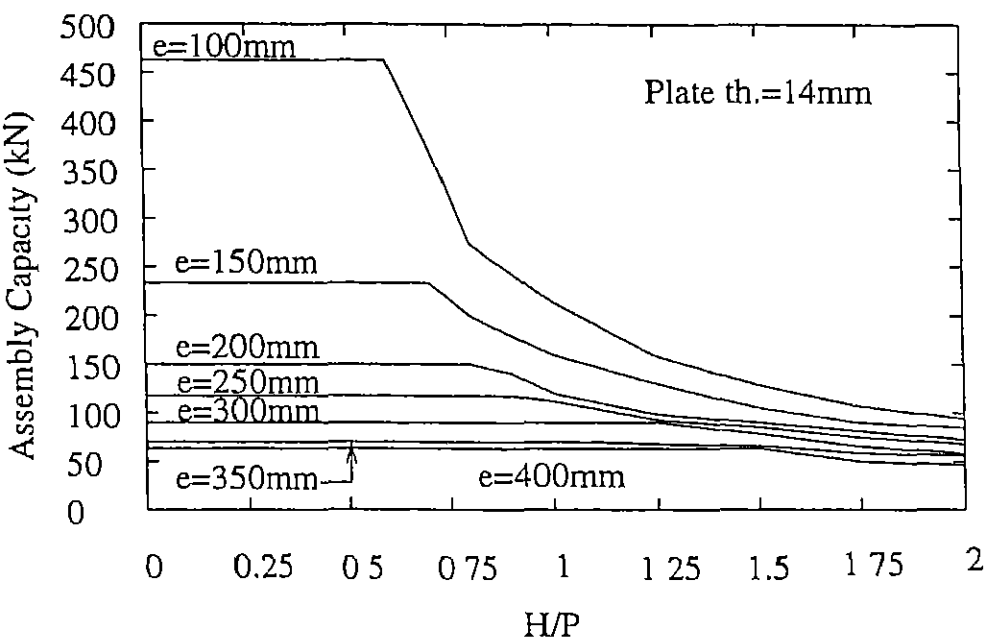


Figure 3 9 Assembly Capacity at Collapse Vs H/P Ratio

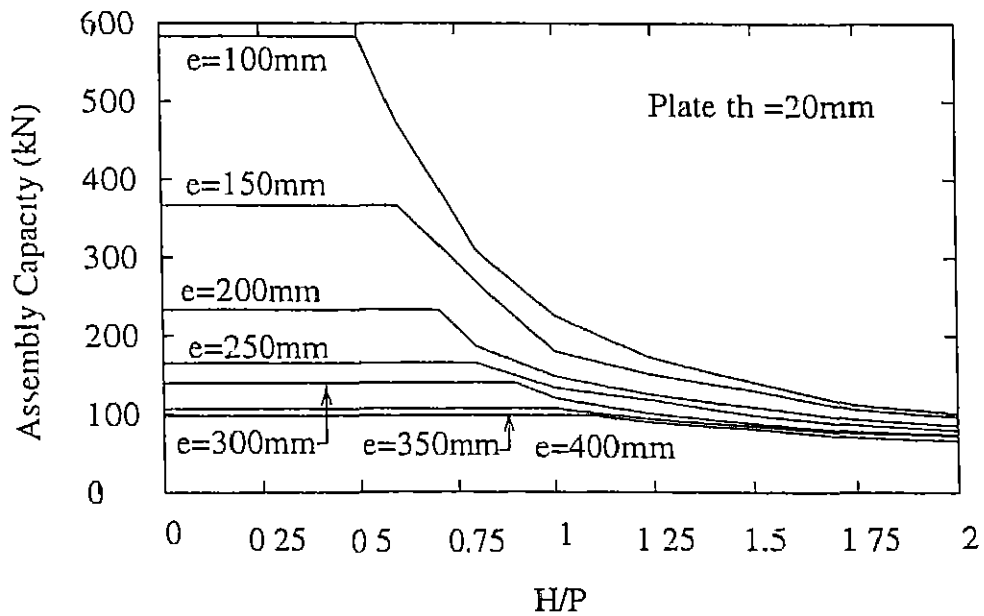
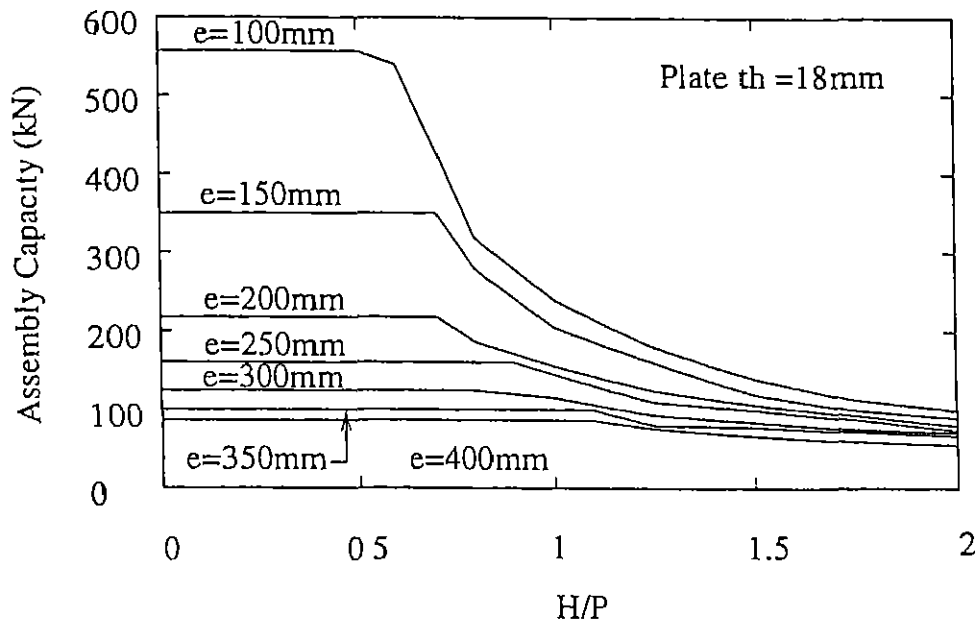


Figure 3 10: Assembly Capacity at Collapse Vs H/P Ratio

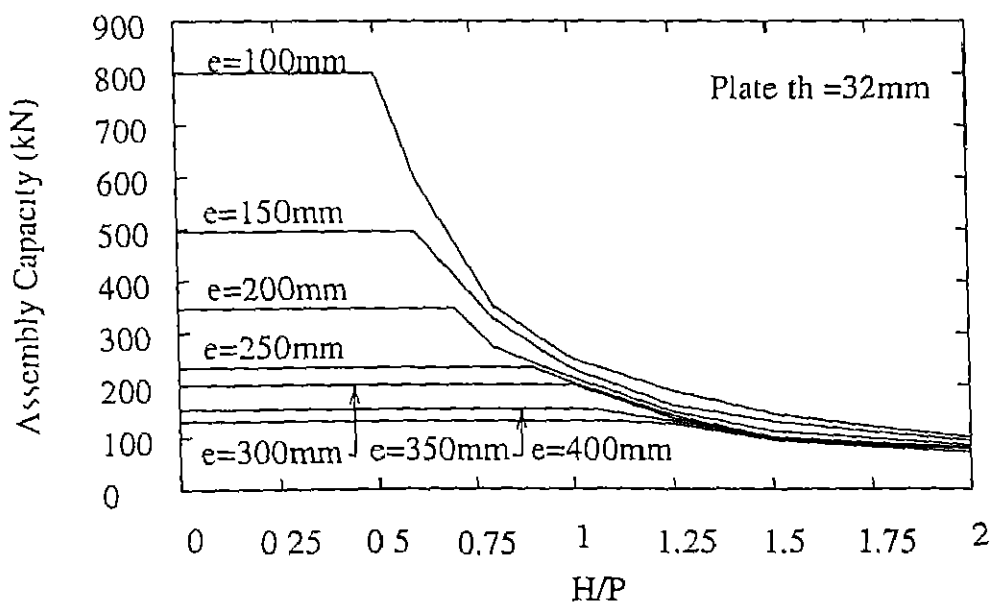
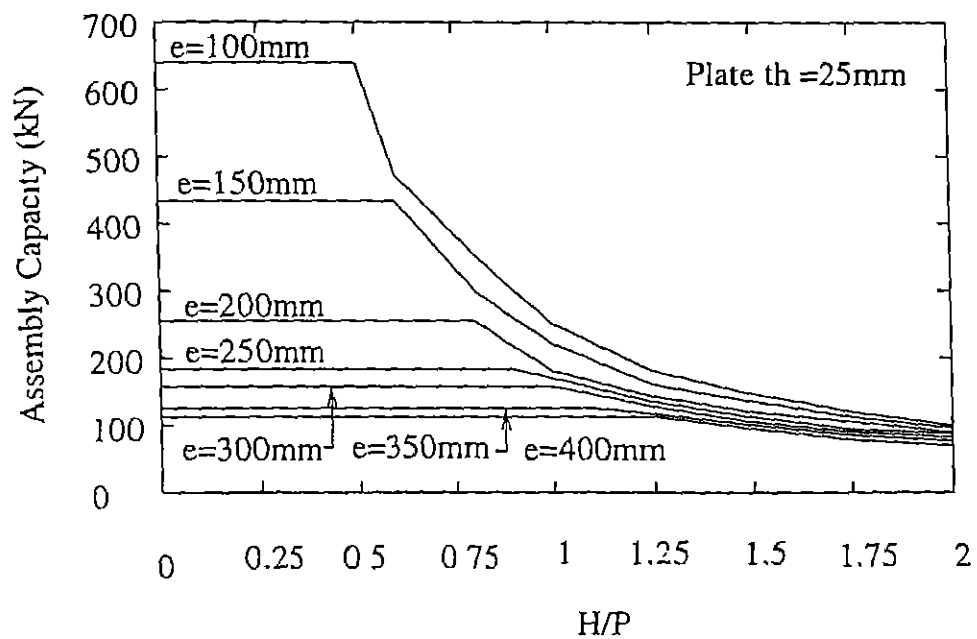


Figure 3.11 Assembly Capacity at Collapse Vs H/P Ratio

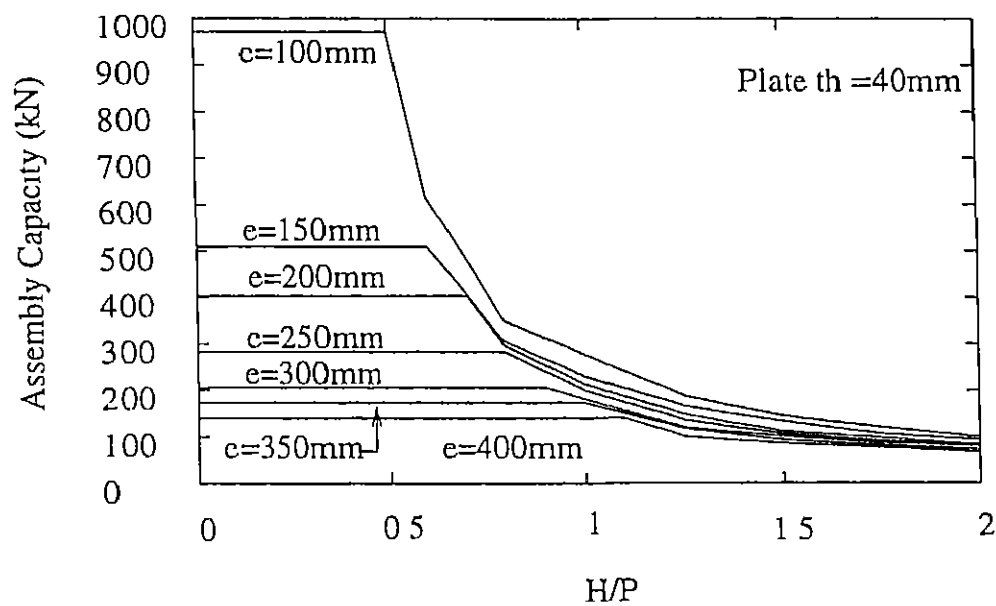


Figure 3 12 Assembly Capacity at Collapse Vs. H/P Ratio



## Chapter 4

# ANALYSIS OF RESULTS

The results of the studies on the plate-anchor assembly subjected to common type of loadings are obtained and presented in the form of strength interaction diagrams and moment-rotation charts. The dimensionless terms obtained after performing the dimensional analysis (for details refer Appendix-II) are used to develop interaction diagrams and moment-rotation charts. The interaction curves are useful for estimation of the capacity of the assembly at failure and at collapse. The moment-rotation charts are useful to estimate the magnitude of the rotation undergone by the assembly due to applied loads. The dimensionless terms (for details see Appendix-II) considered for the interaction diagrams using all the variables of the plate-anchor assembly are.

$$\begin{aligned} t/B, \quad A_{anc}/(s_1 s_2), \quad f_y/f_{ck}, \\ M/(f_{ck} B D^2), \quad P/(f_{ck} B D); \quad A_{atch}/A_{plate}, \\ d'/D, \quad f'_y/f_{ck}, \quad A_{base}/BD \end{aligned}$$

Analysis was carried out for the variation of each dimensionless term while keeping all the others as constants, in order to derive the range of assembly behavior and capacity. After the completion of the analysis, interaction diagrams (as typically shown in Fig. 4.1) are developed from the results of the analysis. As illustrated in Fig. 4.1, all the design parameters are included. Interaction diagrams are developed for different plate

thicknesses. The term  $d'/b$  is taken into consideration by providing an edge distance of twice the diameter of the anchor from the plate edges. Mild steel plates and mild steel J-anchors of yield strength  $300 \text{ N/mm}^2$  and  $330 \text{ N/mm}^2$  respectively are used for all the interaction diagrams. The ratio of area of concrete base to plate is taken as 2.5. The ratio of cross-sectional area of the single anchor to the product of the spacings in two directions is taken as 0.0032. The ratio of area of attachment to the area of plate is taken as 0.1 and 0.2, these ratios are considered to be representative of most of the actual cases. Generally, the ratio of area of attachment to area of plate may range from 0.1 to 0.5, but for the purpose of developing the interaction diagrams and moment-rotation charts, only 0.1 and 0.2 are considered.

## 4.1 Plate-Anchor Assemblies subjected to Eccentric Compressive Loading

As explained in chapter 3, study was performed for plate-anchor assemblies subjected to eccentric compressive loading. The thicknesses considered for the analysis are 10mm, 12mm, 14mm, 16mm, 18mm, 20mm, 25mm, 32mm and 40mm. The interaction diagrams and moment-rotation charts are developed using the dimensional analysis (for details see Appendix-II) for different design parameters as mentioned earlier. These interaction diagrams and moment-rotation charts can be used to analyse/design the plate-anchor assemblies, satisfying the requirements of strength and serviceability conditions. The usage of these interaction diagrams and moment-rotation charts are explained in detail in Appendix-I.

### 4.1.1 Interaction Diagrams

The interaction diagrams at failure and collapse are given in Figs. 4.1 -4.4. From the curves of the Interaction Diagrams, it is observed that for all possible load-eccentricities, the capacity of plate-anchor assembly increases with increase in plate thickness. For

developing a single curve of a particular thickness, the eccentricity is varied at regular intervals (refer section 3.5). The points on  $M/f_{ck}bd^2$  of the interaction diagram denote the capacity of the assembly subjected to pure moment (no axial compressive load). The points on  $P/f_{ck}bd$  of the interaction diagrams indicate the capacity of the assembly subjected to pure axial compressive load. The intermediate points on an interaction curve give the capacities of the assembly in respect of failure/collapse load and moment.

Firstly, the ratio of area of attachment ( $A_{atch}$ ) to area of plate ( $A_{plate}$ ) is taken as 0.1 and the ratio of cross-sectional area of single anchor ( $A_{anc}$ ) to product of spacings in two directions ( $s_1$  and  $s_2$ ) is taken as 0.0032. The interaction diagrams are developed separately for failure and collapse condition of the assembly in order to indicate the reserve strength of the assembly. The failure of the assembly can take place due to cracking of concrete, yielding of plate or yielding of anchors. The failure load of the assembly does not mean the collapse of the structure. The assembly still has the reserve strength after failure has occurred in one or more of the components. The ultimate load at which, the collapse of the assembly occurs can be due to crushing of concrete, failure of anchors or complete yielding of plate along with failure of anchors.

There is no such distinct region in the interaction diagram to explain the type of material failure occurred in the plate-anchor assembly. The collapse of the assembly at zero eccentricity occurs due to crushing of concrete and as the load eccentricity increases, the collapse of the assembly can be due to failure of anchors or complete yielding of plate along with failure of anchors. From the interaction diagrams for both collapse and failure of assembly, it is observed that the capacity of the assembly based on collapse is appreciably higher than that based on failure (for illustration see Appendix-I).

Similar analysis is done for the ratio of area of attachment to area of plate as 0.2 and the ratio of cross-sectional area of single anchor to product of spacings in two directions as 0.0032. The increase in the area of attachment, increases the capacity of the assembly considerably keeping all the other design parameters constant. It is

observed that Assembly Capacity increases with the increase in the ratio of area of attachment to area of plate (illustrated in Appendix-I)

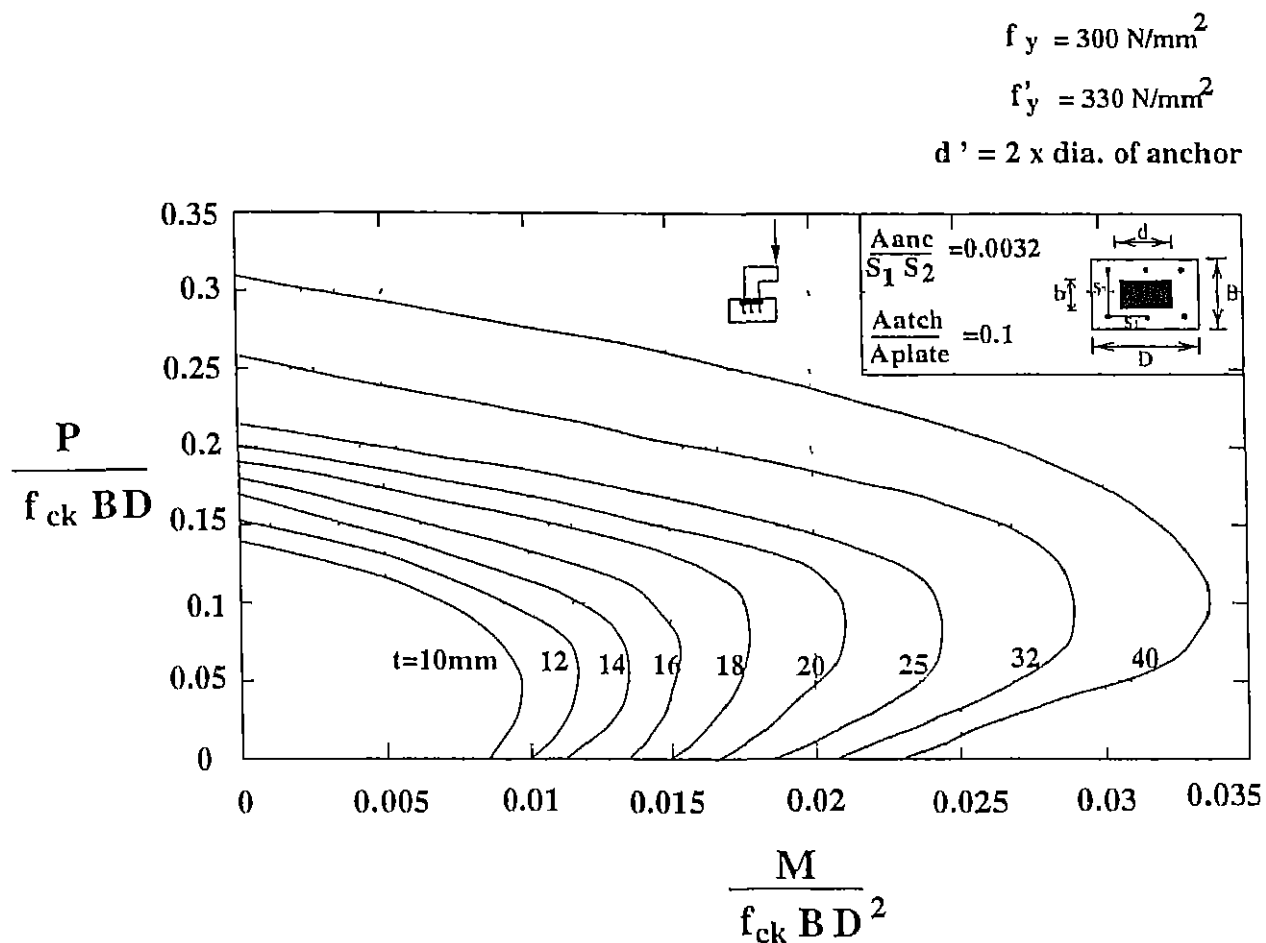


Figure 4.1: Interaction Diagram for Eccentric Compressive loading at Failure

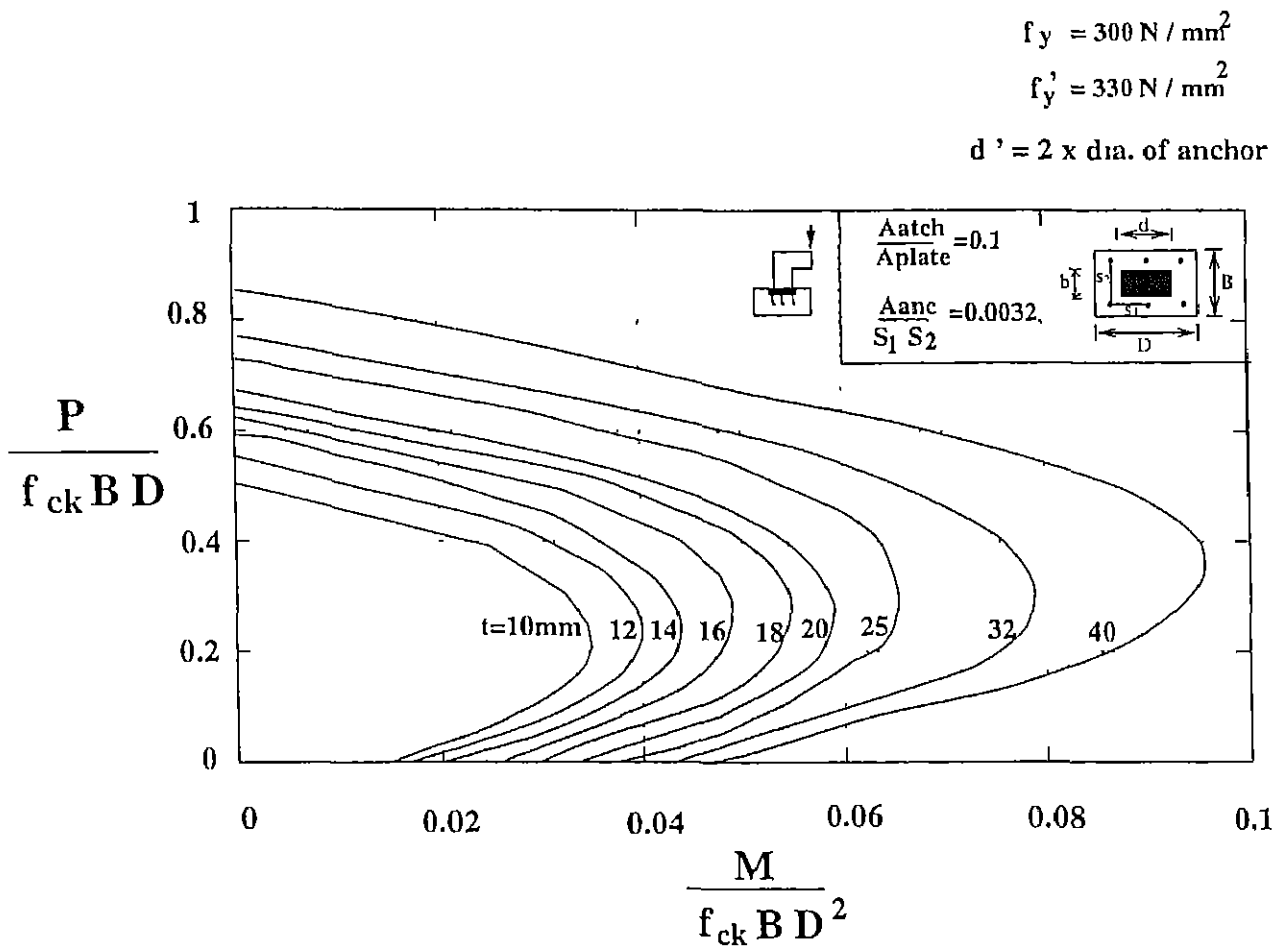


Figure 4.2 Interaction Diagram for Eccentric Compressive loading at Collapse

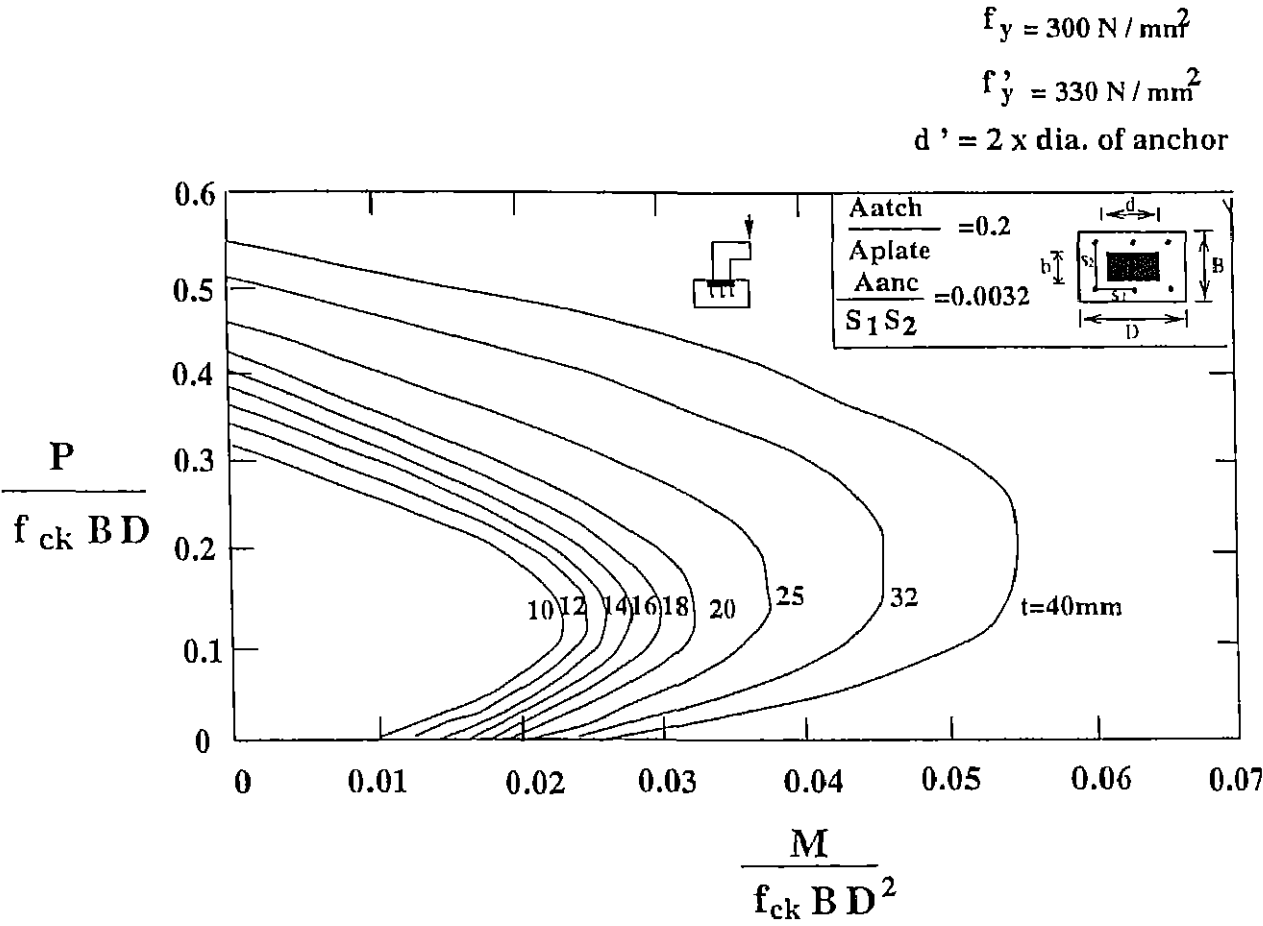


Figure 4.3 Interaction Diagram for Eccentric Compressive loading at Failure

$$f_y = 300 \text{ N/mm}^2$$

$$f'_y = 330 \text{ N/mm}^2$$

$$d' = 2 \times \text{dia. of anchor}$$

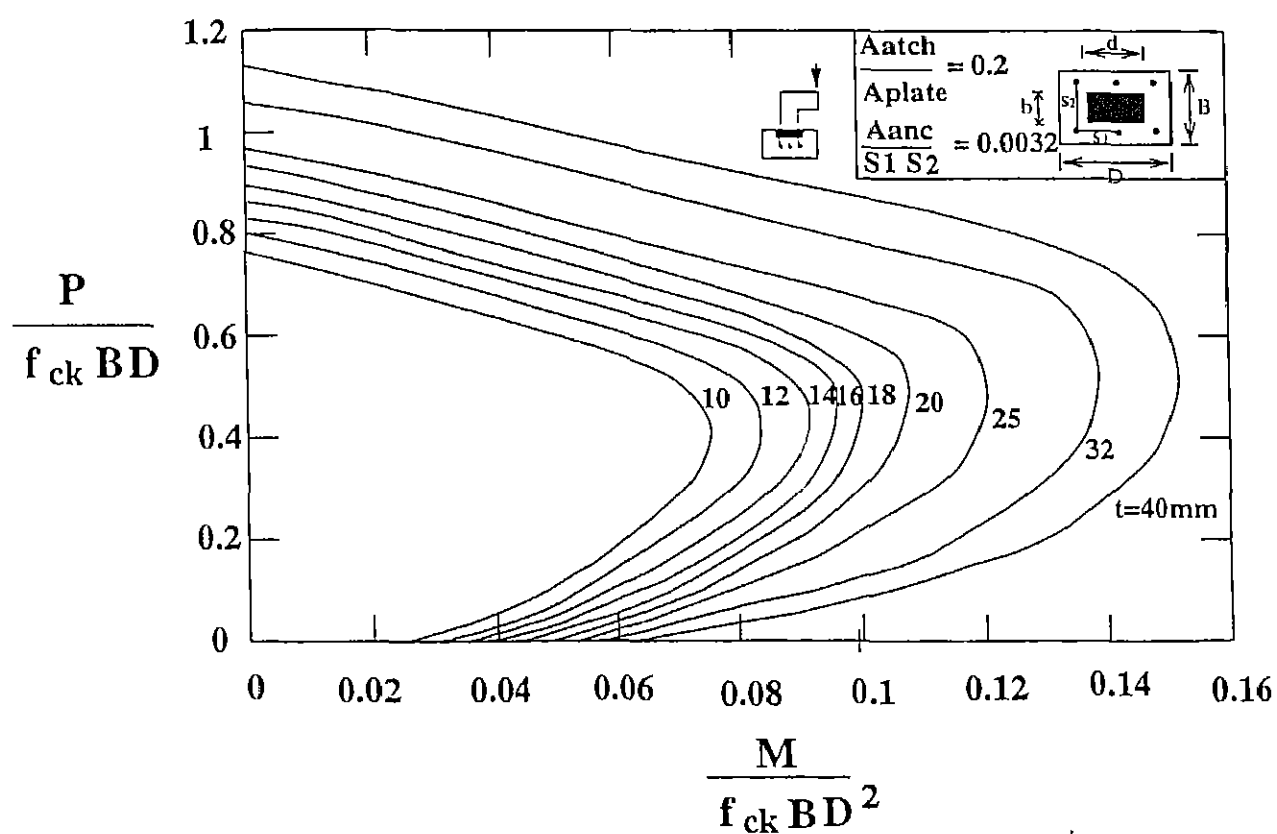


Figure 4.4: Interaction Diagram for Eccentric Compressive loading at Collapse

### 4.1.2 Moment-Rotation Charts

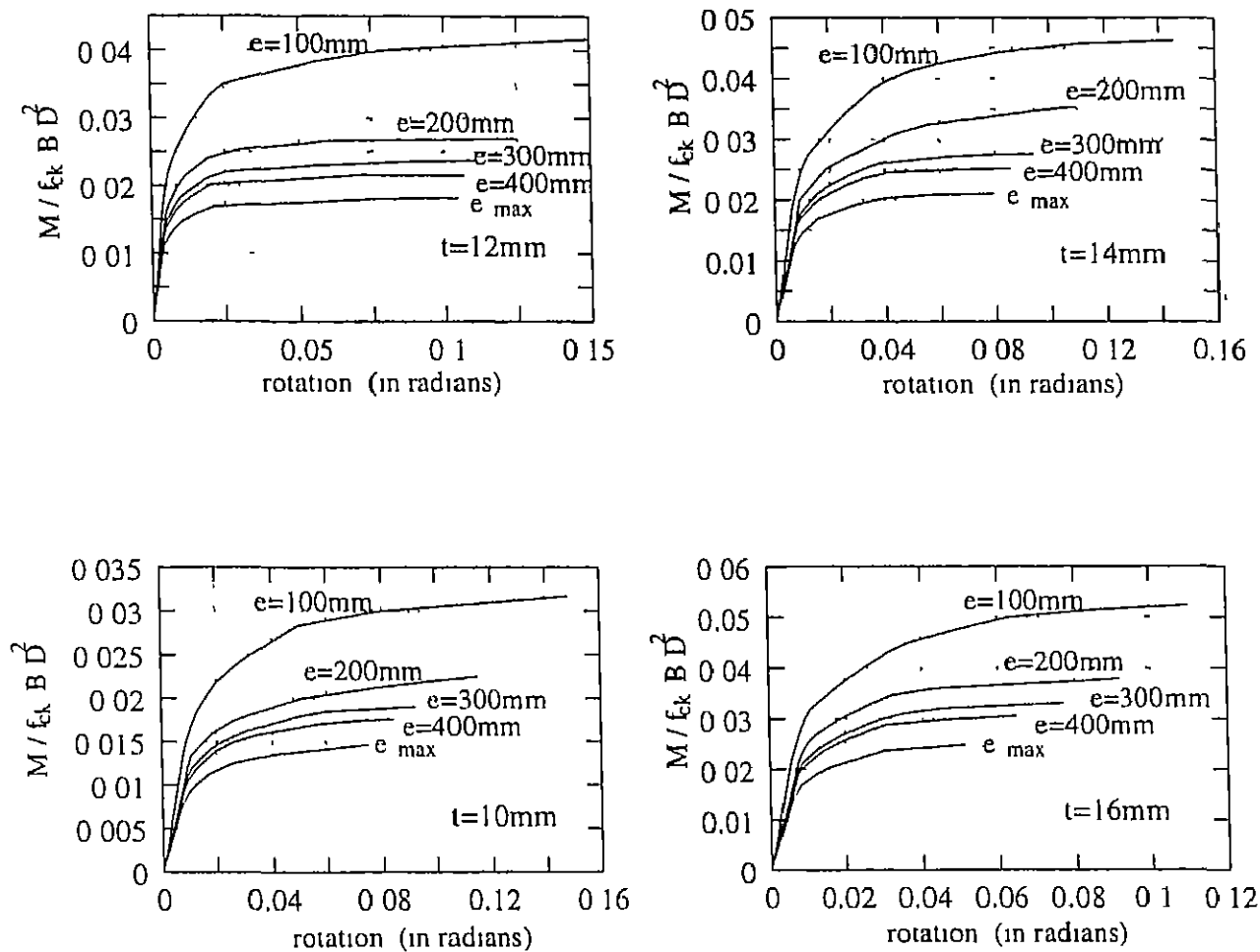
The moment-rotation charts developed in the study are presented in Figs 4.5 and 4.6. The moment-rotation characteristics of the plate-anchor assemblies are important in respect of satisfying the rotational stiffness requirements from the view point of serviceability. The moment-rotation charts are developed for the same design parameters as adopted for the interaction diagrams. The rotation caused due to the eccentric compressive load at every stage of incremental loading till the assembly collapses, is computed. The moment (in terms of dimensionless quantity,  $M/f_{ck}bd^2$ ) -rotation ( $\theta$ ) charts for a given plate thickness are provided considering the incremental variation in load eccentricities from a reasonably low value upto a case of pure moment.

Firstly, a set of charts is provided for different plate thicknesses in Figs 4.5 (a), (b), (c) for the ratios ( $A_{atch}/A_{plate}$ ) and ( $A_{anc}/s_1s_2$ ) as 0.1 and 0.0032, respectively. Subsequently, another set of charts is provided in Figs 4.6 (a), (b), (c) for the ratios ( $A_{atch}/A_{plate}$ ) and ( $A_{anc}/s_1s_2$ ) as 0.2 and 0.0032, respectively.

It is observed that the assembly rotation increases with the increase in load-eccentricity, while keeping the moment same. This is possibly due to the diminishing effect of axial compressive load against rotation with increase in load eccentricity. The assembly rotation gets reduced with increase in plate thickness for the same level of eccentric compression load, this is mainly due to the increase in plate stiffness. It is noted typically that for a given plate-anchor assembly the rate of increase of rotation with respect to increase in moment is relatively much lower initially (till failure of plate/anchor) than the same observed in the post-failure phase of plate/anchor. Also, it is evident that the slope of the moment-rotation curves become increasingly flatter with increase in load-eccentricities.

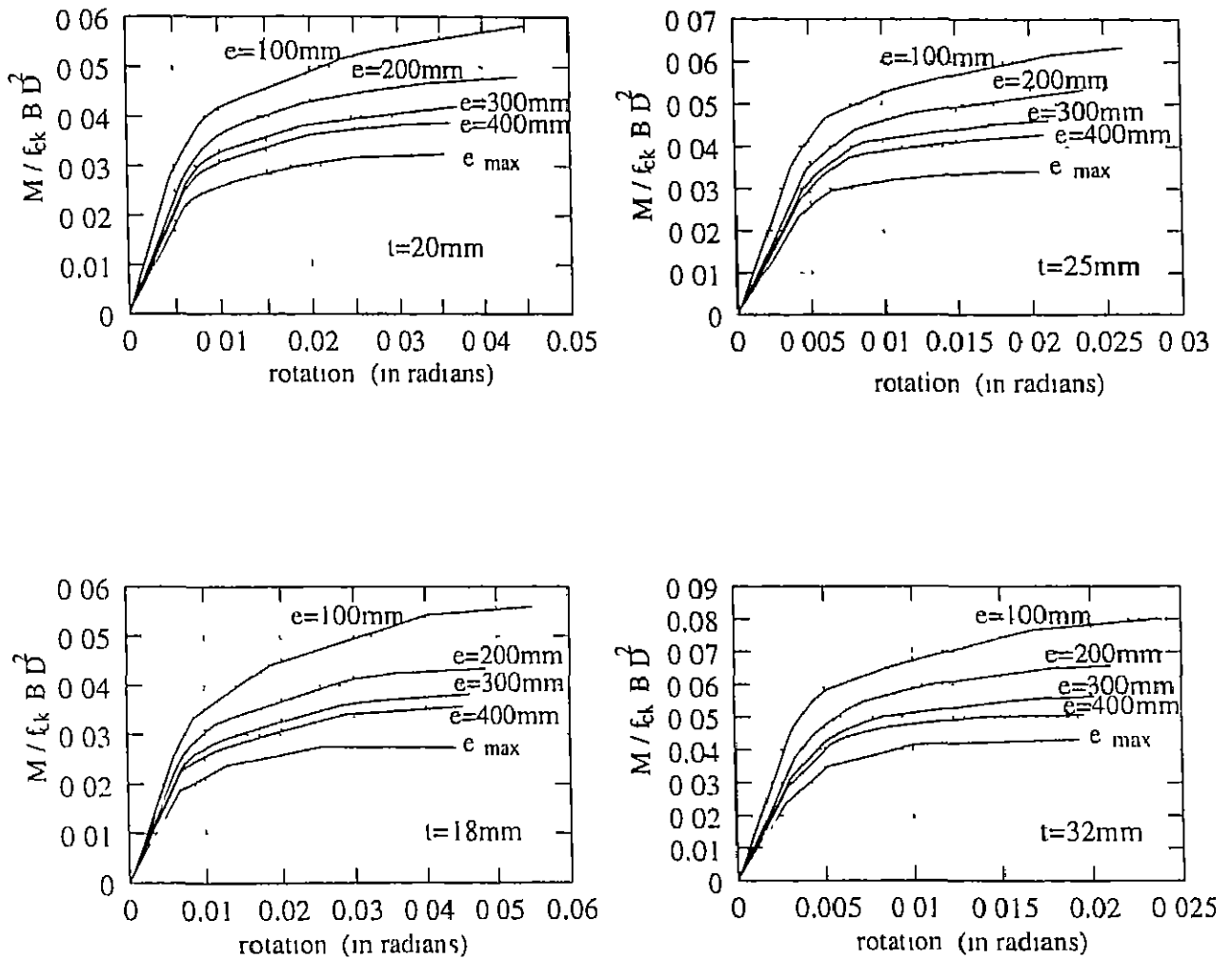
For increase in the value of the ratio ( $A_{atch}/A_{plate}$ ) from 0.1 to 0.2, it is observed that the rotation decreases substantially for the same level of eccentric compressive load, this is possibly due to influence of large area of attachment in enhancing the plate stiffness.





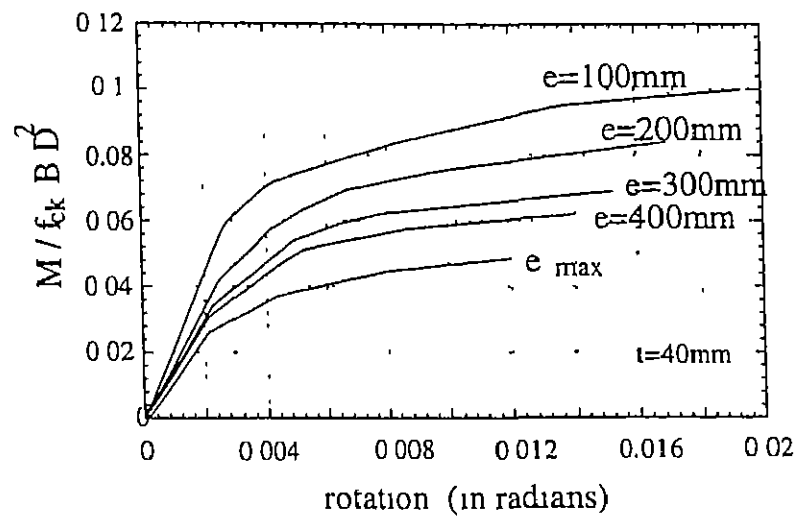
(a)

Figure 4.5 Moment-rotation Charts for Eccentric Compressive loading ( $A_{\text{atch}}/A_{\text{plate}} = 0.1$ )



(b)

Figure 4.5 Moment-rotation Charts for Eccentric Compressive loading ( $A_{\text{atch}}/A_{\text{plate}} = 0.1$ )



(c)

Figure 4.5 Moment-rotation Charts for Eccentric Compressive loading ( $A_{\text{tech}}/A_{\text{plate}} = 0.1$ )

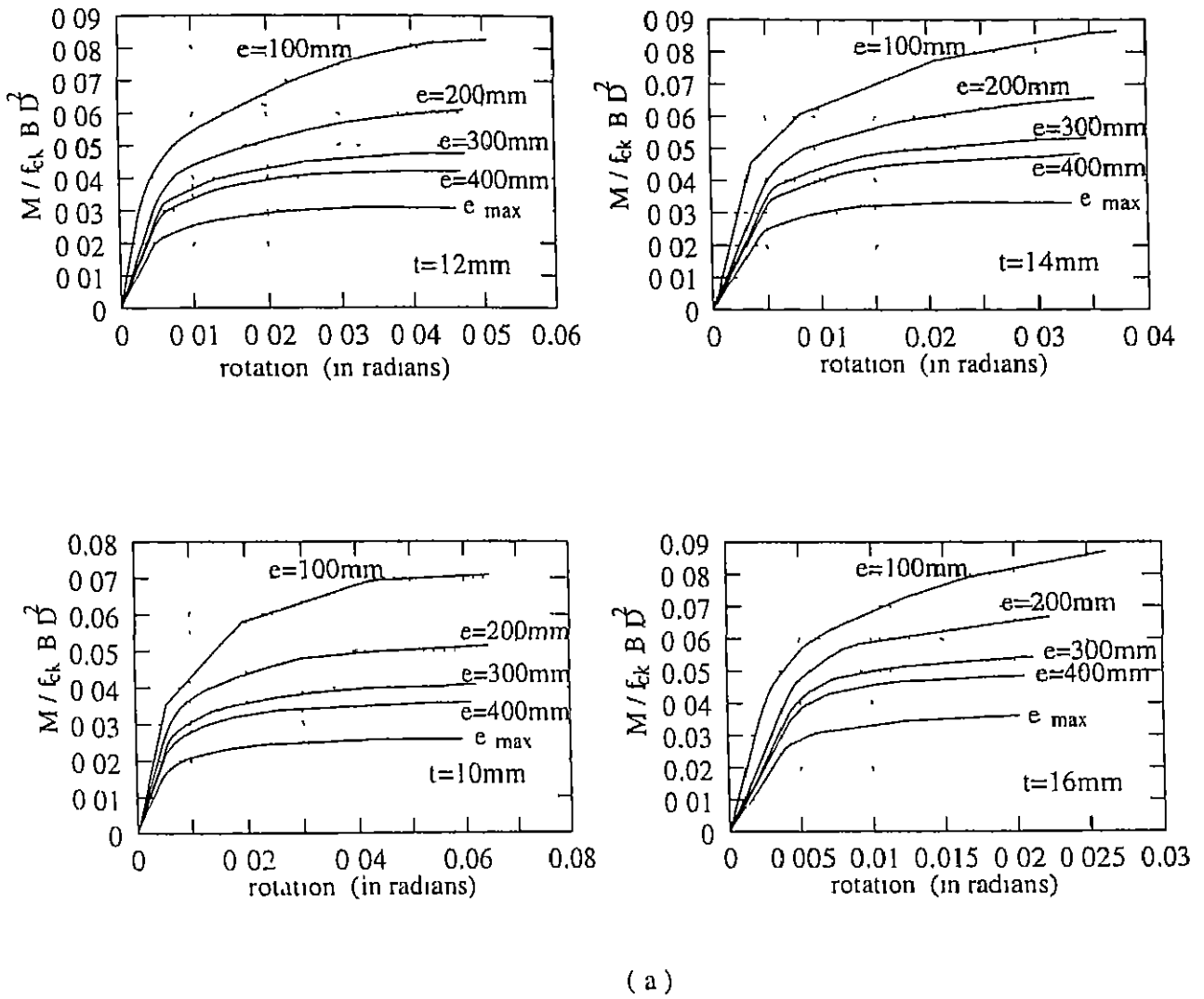


Figure 4.6 Moment-rotation Charts for Eccentric Compressive loading ( $A_{atch}/A_{plate} = 0.2$ )

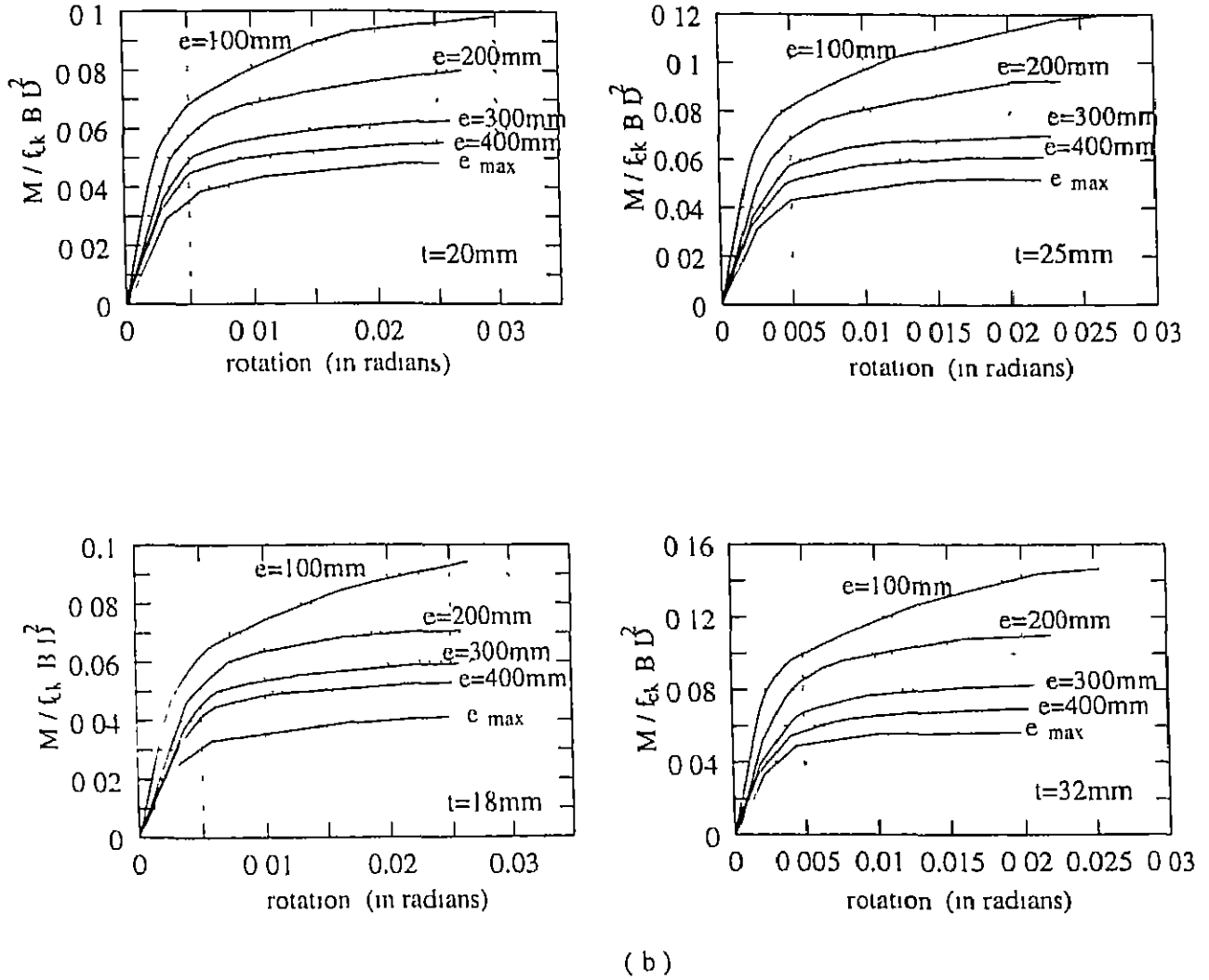
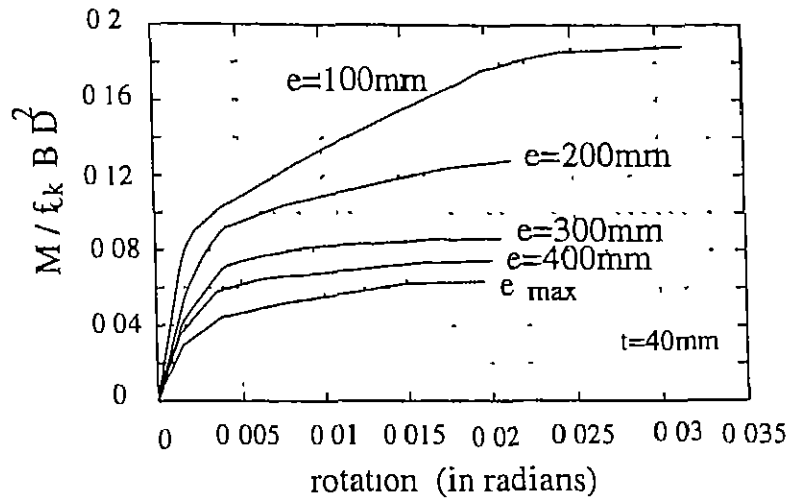


Figure 4 6: Moment-rotation Charts for Eccentric Compressive loading ( $A_{alch}/A_{plate} = 0.2$ )



(c)

Figure 4.6 Moment-rotation Charts for Eccentric Compressive loading ( $A_{\text{atch}}/A_{\text{plate}} = 0.2$ )

## 4.2 Plate-Anchor Assemblies subjected to Eccentric Tensile Loading

As explained in chapter 3, a study was performed for plate-anchor assemblies subjected to eccentric tensile loading. All the design parameters considered are the same as taken for assemblies subjected to eccentric compressive loading. The interaction diagrams and moment-rotation charts are developed using the dimensional analysis (see Appendix-II) for different design parameters as stated earlier. These interaction diagrams and moment-rotation charts are useful in analysing/designing the plate-anchor assemblies satisfying the strength and serviceability criteria. The usage of the interaction diagrams and moment rotation charts are explained in detail in Appendix-I.

### 4.2.1 Interaction Diagrams

The interaction diagrams at failure and collapse are given in Figs 4.7-4.10. From the curves of the interaction diagram, it is observed that for all possible load-eccentricities, the capacity of plate-anchor assembly increases with increase in plate thickness. For developing a single curve, for a particular plate thickness, the eccentricity is varied at regular intervals (refer section 3.6). The points on  $M/f_{ck}bd^2$  axis of the interaction diagram denote the capacity of the assembly subjected to pure moment (no axial compressive load). The points on  $P/f_{ck}bd$  axis of the interaction diagrams indicate the capacity of the assembly subjected to pure axial compressive load. The intermediate points on an interaction curve give the capacities of the assembly in respect of failure/collapse load and moment.

The interaction diagrams are developed separately for failure and collapse conditions of the assembly in order to indicate the reserve strength. The failure of the assembly can occur due to cracking of concrete, yielding of plate or yielding of anchors. Beyond failure, the assembly has its reserve strength till collapse. The ultimate load at which the collapse of the assembly takes place, may be due to the failure of the anchors, or complete yielding of plate along with failure of anchors. Collapse of the assembly due

to the crushing of base concrete is appearing practically impossible, as the moment due to eccentric tensile load is never capable to induce concrete crushing

It is apparent from the interaction diagrams for eccentric compressive loading (see Figs 4.1 - 4.4) and the present ones for eccentric tensile loading, that the load carrying capacity of a plate-anchor assembly is considerably reduced in the case of the latter one (excepting for the case of pure moment). This is possibly due to the fact that in eccentric tensile loading, the participation of the concrete base in resisting the load is insignificant, and the load is mainly resisted by anchors and plate.

When the load eccentricity is zero, the assembly capacity at failure is dictated by yielding of anchors and the same at collapse is due to failure of anchors. As the load eccentricity increases, the moment acting on the system is resisted both by plate and anchors. Unlike the case of assemblies subjected to eccentric compressive loading, in the present case, with increase in load-eccentricity, the magnitude of failure/collapse load decreases while the failure/collapse moment increases continuously upto the case of pure moment. This can be attributed to the increasing influence of load eccentricity (i.e. moment) to cause the failure/collapse of the assembly.

### 4.2.2 Moment-Rotation Charts

The moment-rotation charts developed in the study are presented in Figs. 4.11 and 4.12. The moment (in terms of dimensionless quantity  $M/f_{ck}BD^2$ ) - rotation ( $\theta$ ) charts for a given plate thickness are provided considering the incremental variation in load-eccentricity from a reasonably low value upto a case of pure moment. The moment-rotation charts are developed for the same design parameters as adopted for the interaction diagrams. The rotation caused due to eccentric tensile loading at every stage of incremental loading till the assembly collapses, is computed

Firstly, a set of charts is presented for different plate thicknesses in Figs. 4.11 (a), (b), (c) for the ratios  $(A_{anch}/A_{plate})$  and  $(A_{anc}/s_1s_2)$  as 0.1 and 0.0032 respectively. Subsequently, another set of charts is presented in Figs. 4.12 (a), (b), (c) for the ratios  $(A_{anch}/A_{plate})$  and  $(A_{anc}/s_1s_2)$  as 0.2 and 0.0032, respectively.



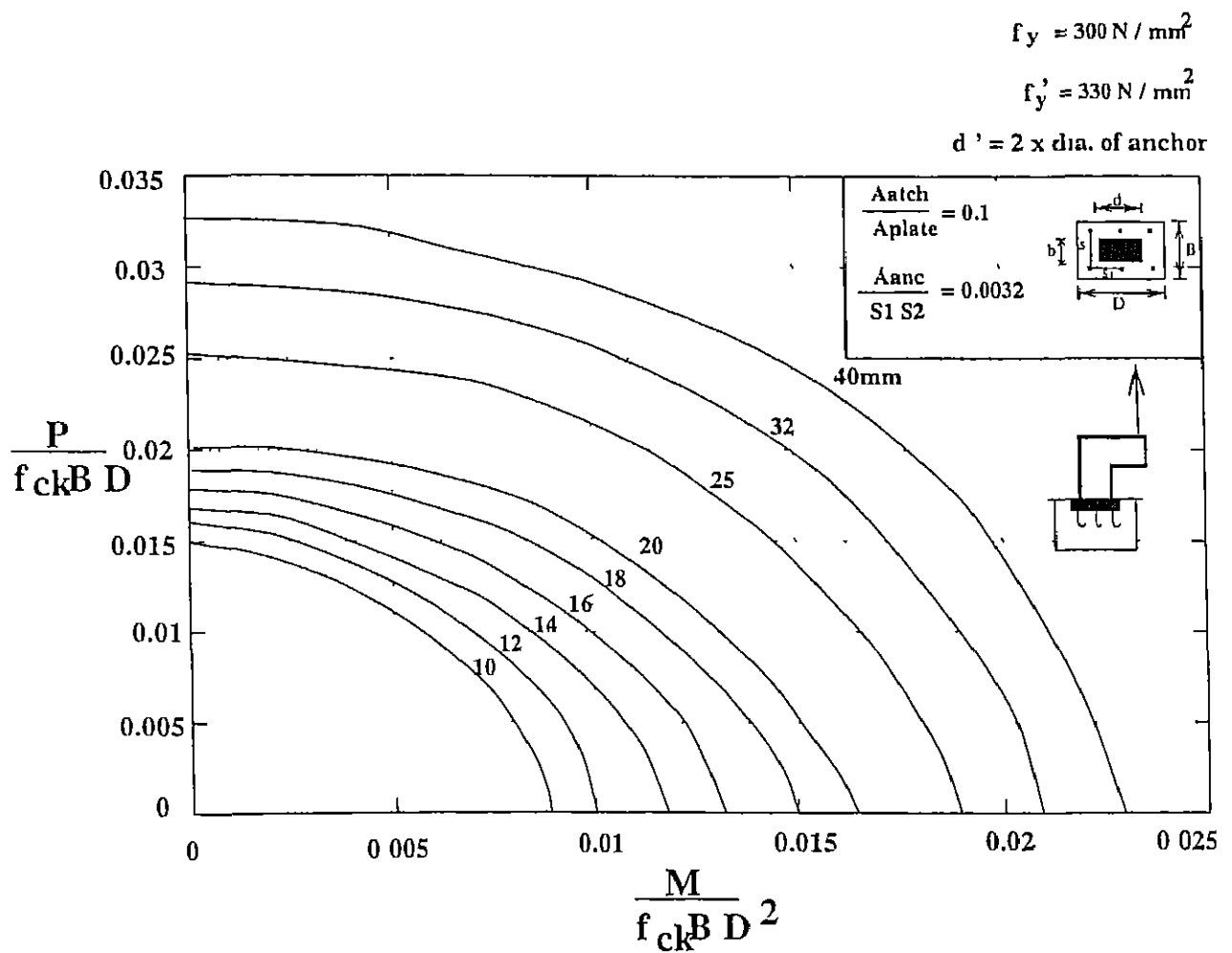


Figure 4.7 Interaction Diagram for Eccentric Tensile loading at Failure

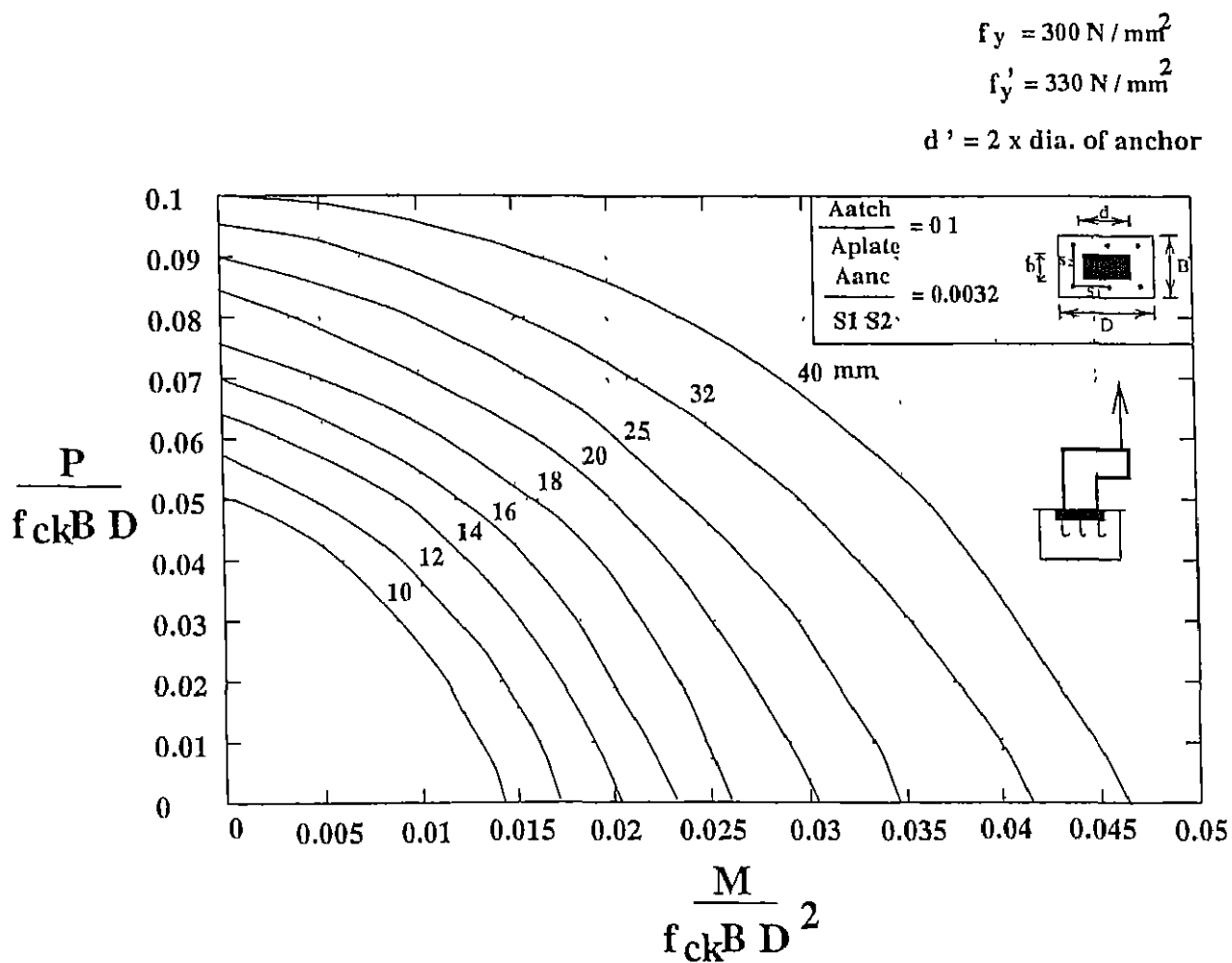


Figure 4.8 Interaction Diagram for Eccentric Tensile loading at Collapse

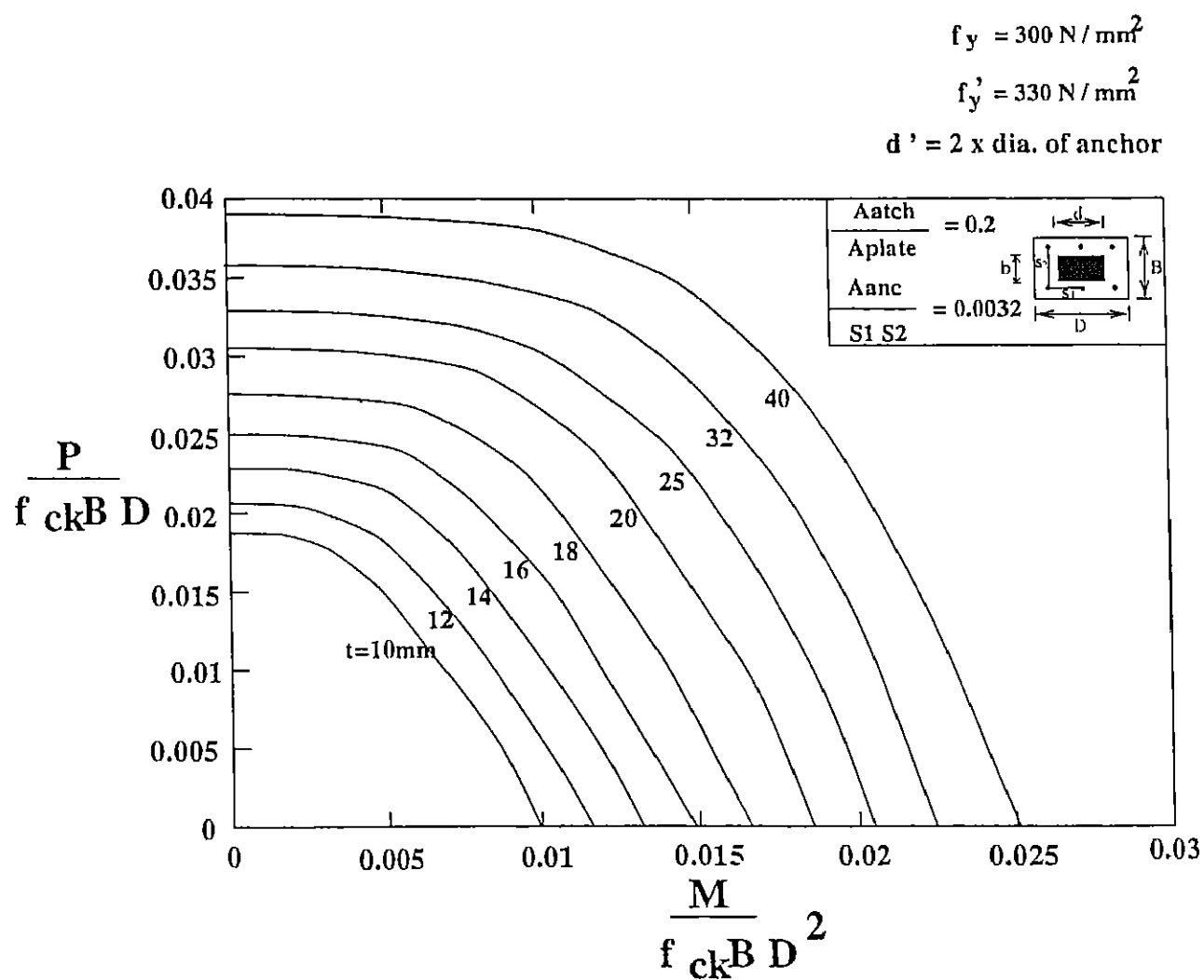


Figure 4.9: Interaction Diagram for Eccentric Tensile loading at Failure

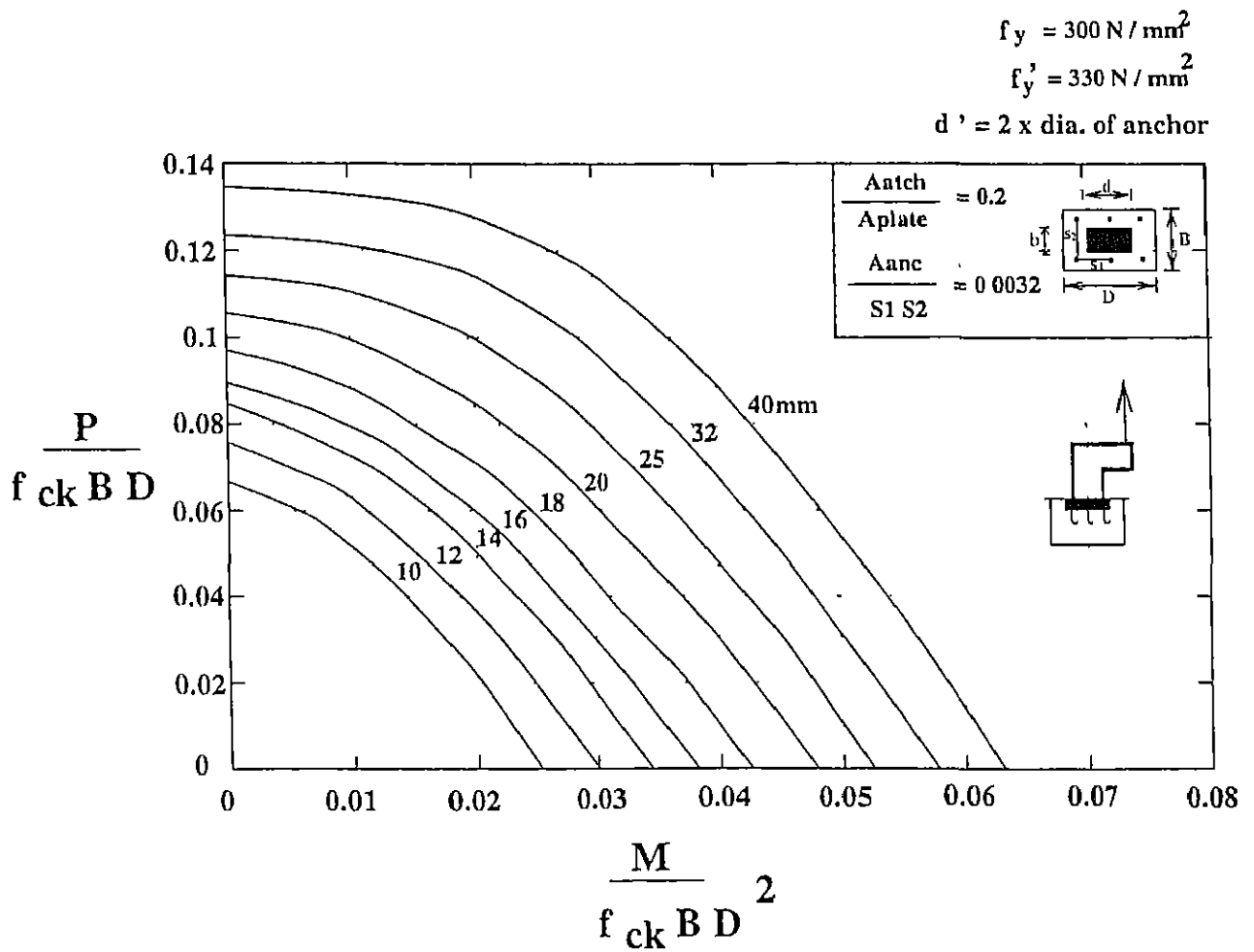
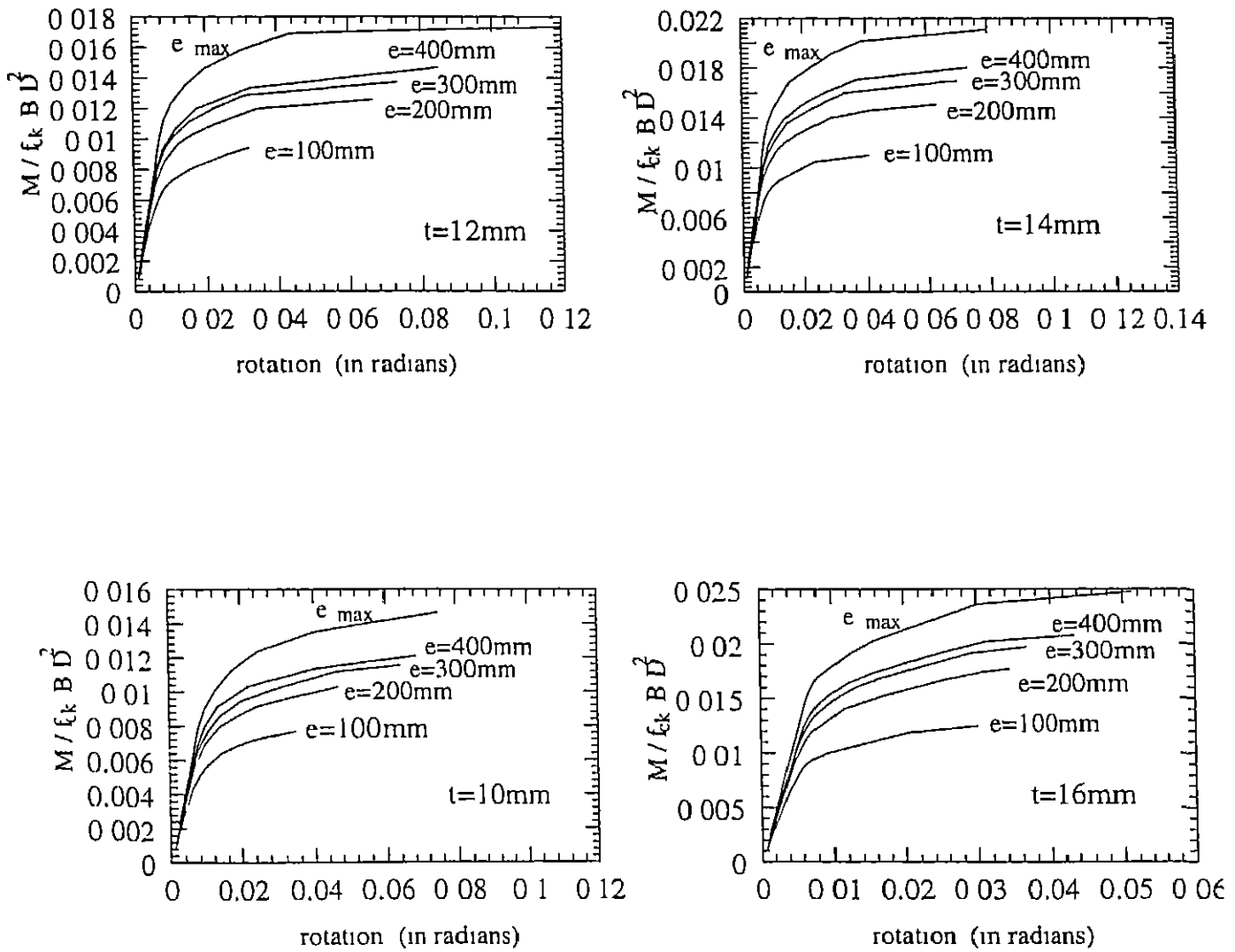


Figure 4.10: Interaction Diagram for Eccentric Tensile loading at Collapse

It is observed that the assembly rotation decreases with the increase in load eccentricity while keeping the moment same, which is reverse to the case of eccentric compressive loading. When the load is compressive, the anchor tension is due to moment acting on the system only, whereas in case of tensile loading, the anchor tension is caused due to both axial tensile force and moment. As the load eccentricity increases, the effect of axial tensile force in causing rotation decreases as compared to the effect of moment acting on the system. It is to be noted that for a particular plate-anchor assembly, the moment rotation curve for pure moment condition (i.e.  $e = e_{max}$  case) lies in the middle of the curves of the curves for eccentric compressive loading (lying above the pure moment curve) and the curves for eccentric tensile loading (lying below the pure moment curve), as illustrated typically in Fig. 4.13.)

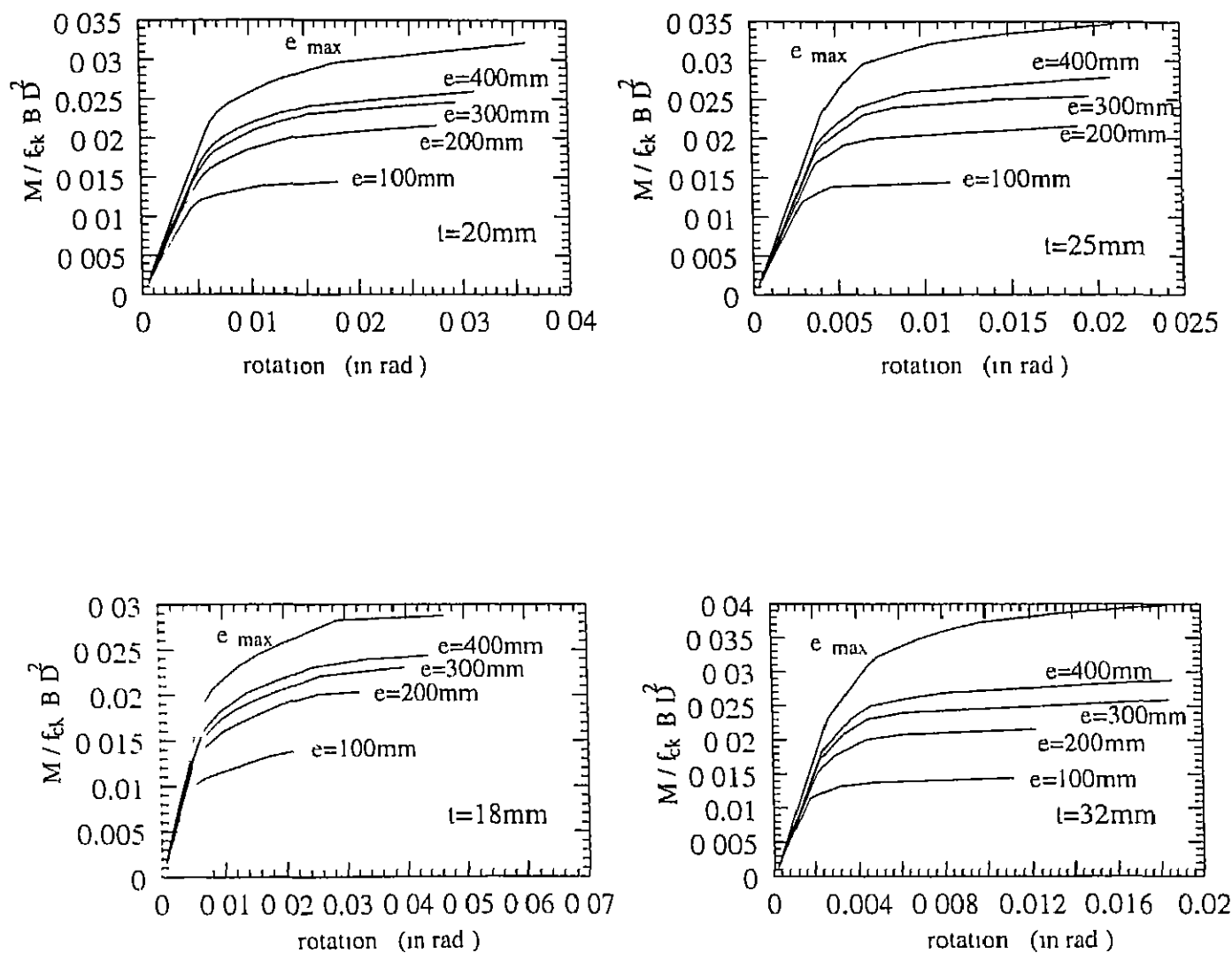
As the thickness increases, the rotation of the assembly decreases, for the same value of moment of a curve of particular load eccentricity. Also, it is apparent that the slope of the moment-rotation curves become increasingly flatter with decrease in load-eccentricity.

For increase in the value of the ratio ( $A_{atch}/A_{plate}$ ) from 0.1 to 0.2, it is observed that the rotation decreases substantially for the same level of eccentric tensile loading, and this is possibly due to the influence of larger area of attachment in enhancing the plate stiffness.



(a)

Figure 4.11: Moment-rotation Charts for Eccentric tensile loading ( $A_{\text{atch}}/A_{\text{plate}} = 0.1$ )



(b)

Figure 4.11. Moment-rotation Charts for Eccentric tensile loading ( $A_{atch}/A_{plate} = 0.1$ )

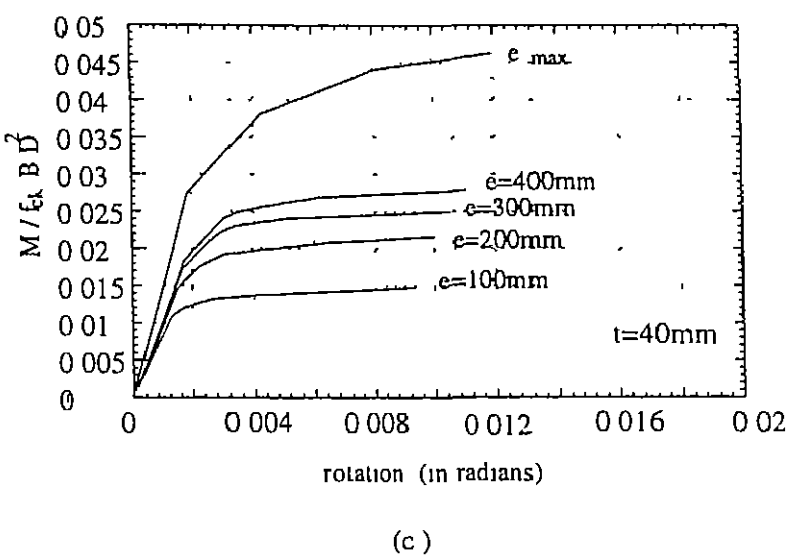
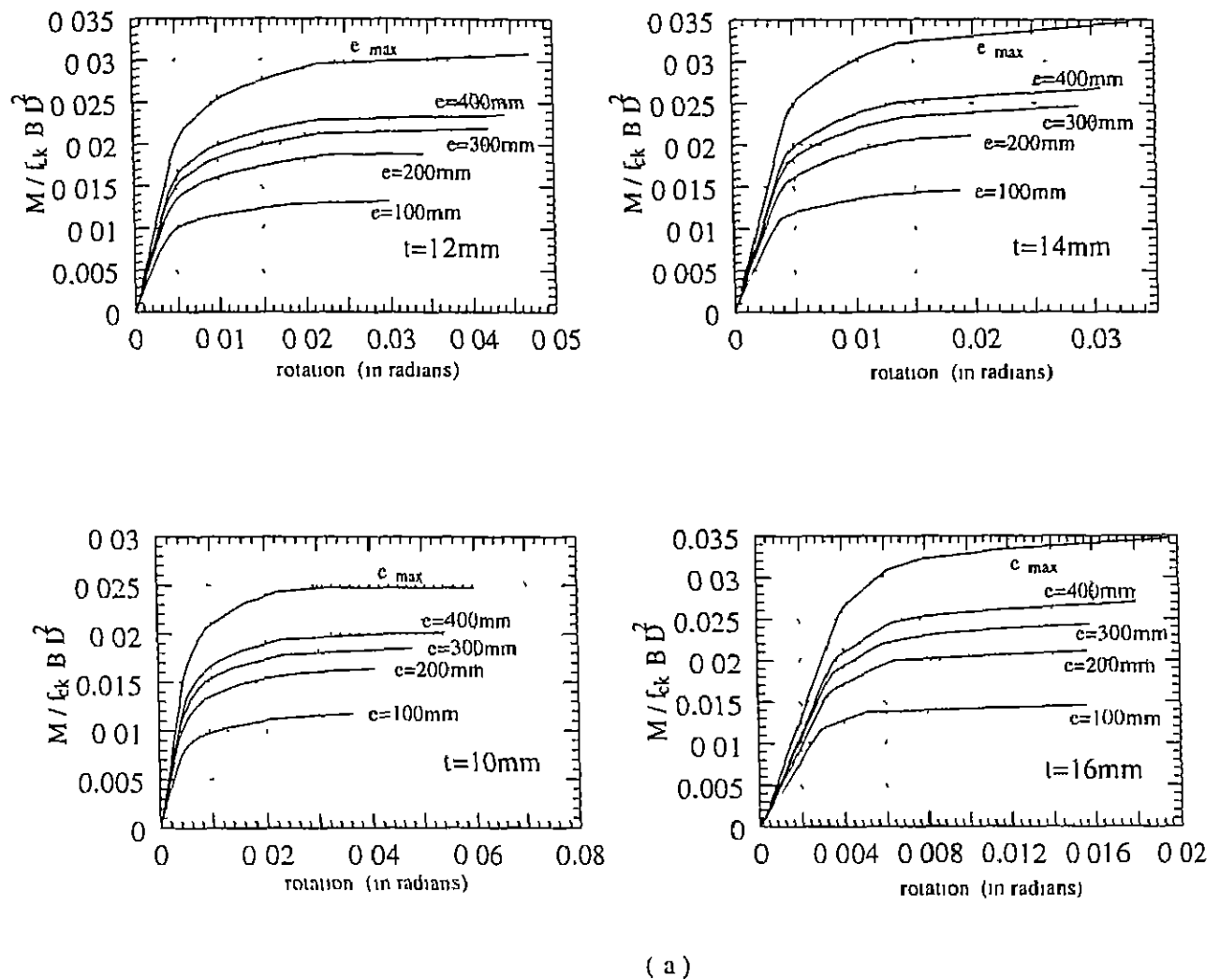
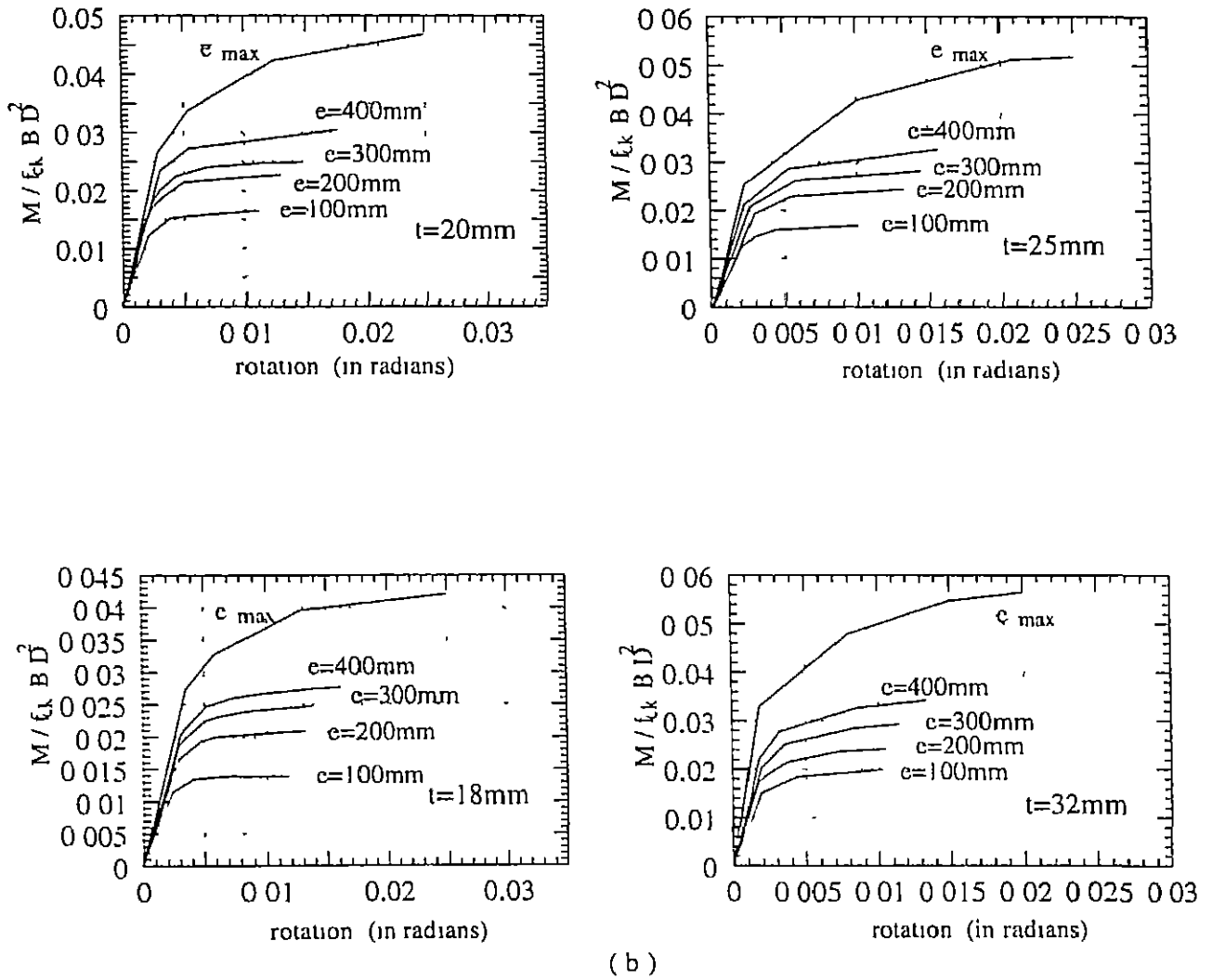


Figure 4.11: Moment-rotation Charts for Eccentric tensile loading ( $A_{atch}/A_{plate} = 0.1$ )



Figure 4.12 Moment-rotation Charts for Eccentric tensile loading ( $A_{alch}/A_{plate} = 0.2$ )

Figure 4.12. Moment-rotation Charts for Eccentric tensile loading ( $A_{\text{attach}}/A_{\text{plate}} = 0.2$ )

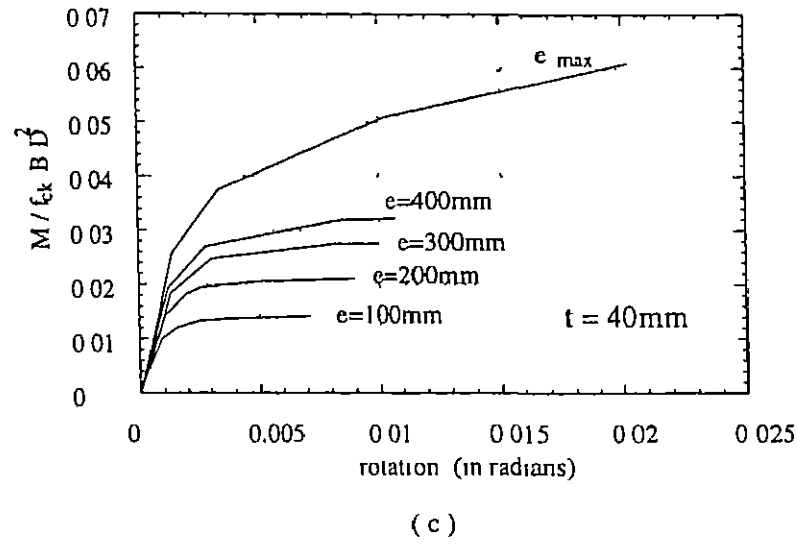


Figure 4.12 Moment-rotation Charts for Eccentric tensile loading ( $A_{atch}/A_{plate} = 0.2$ )

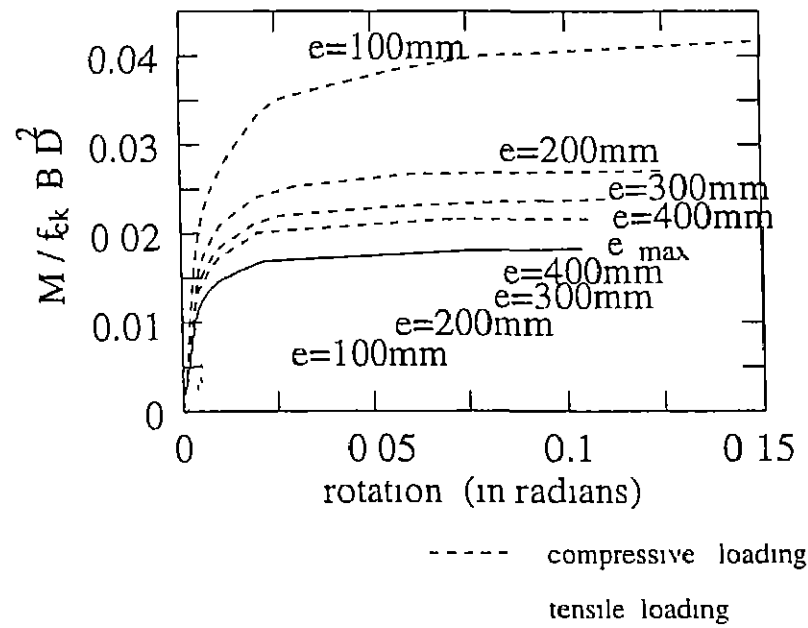


Figure 4.13 Moment-rotation Chart for Eccentric Compressive and Tensile Loading

### 4.3 Evaluation of Interaction Diagrams for Eccentric Compressive Loading combined with Shear Loading.

The results of the assembly subjected to shear force in addition to axial compressive load and uniaxial moment are presented in the previous chapter. The objective of the study was to evaluate the already developed strength interaction diagrams for eccentric compressive loading for the condition when the plate-anchor assembly is also subjected to shear load in combination.

It is observed that the capacity of the assembly remains constant upto some ratio of shear force to axial load for different load eccentricities. As the load eccentricity increases, the assembly capacity remains constant for higher values of ratio of shear force to axial load. When the load is purely axial, the horizontal resistance due to friction is  $\mu P$  ( $\mu$  is coefficient of friction between plate and concrete base). When the moment is acting additionally, the assembly undergoes rotation. When the frictional resistance alone is not capable to resist the shear, the anchors participate in resisting the shear force. As stated in Section 3.7 of chapter 3, up to a specific value of H/P ratio for a given assembly, the interaction diagrams (refer Figs. 4.1-4.4) can be adopted without any modification. The individual values of the H/P ratio for different assemblies are obtainable from Figs. 3.8-3.12.

### 4.4 Deflected Shapes and Stress Contours

The deflected shape of the embedded plate of the assembly is presented in Fig. 4.14. The deflected shapes are obtained for different eccentricities for a particular size of the plate. The typical stress contours for equivalent stress at different eccentricities are presented in Fig. 4.15.

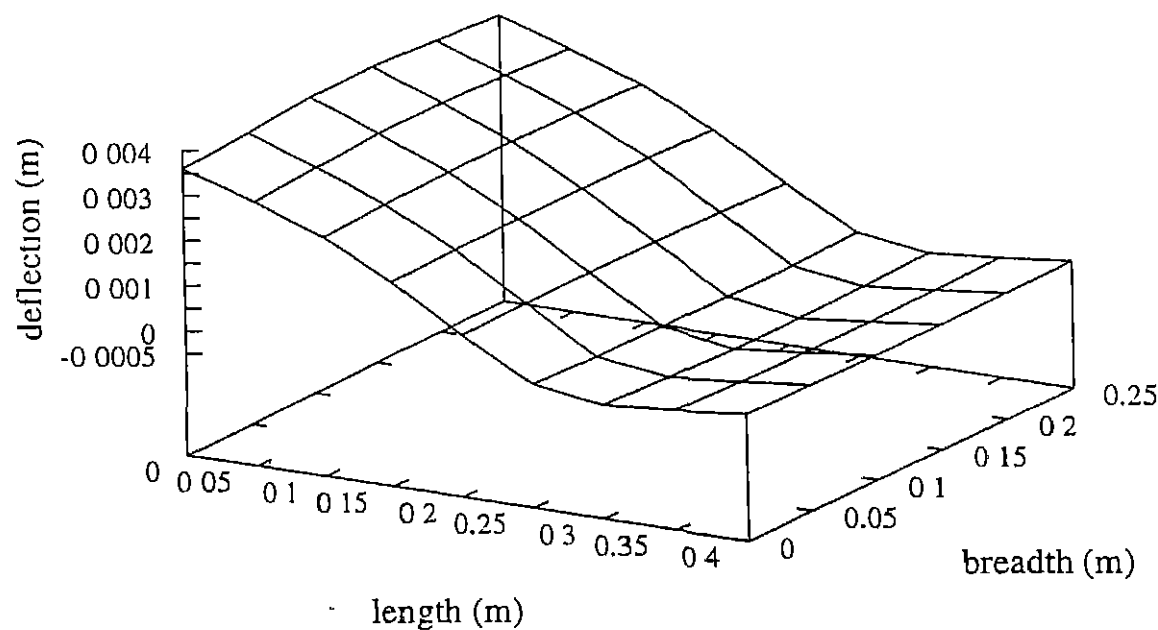
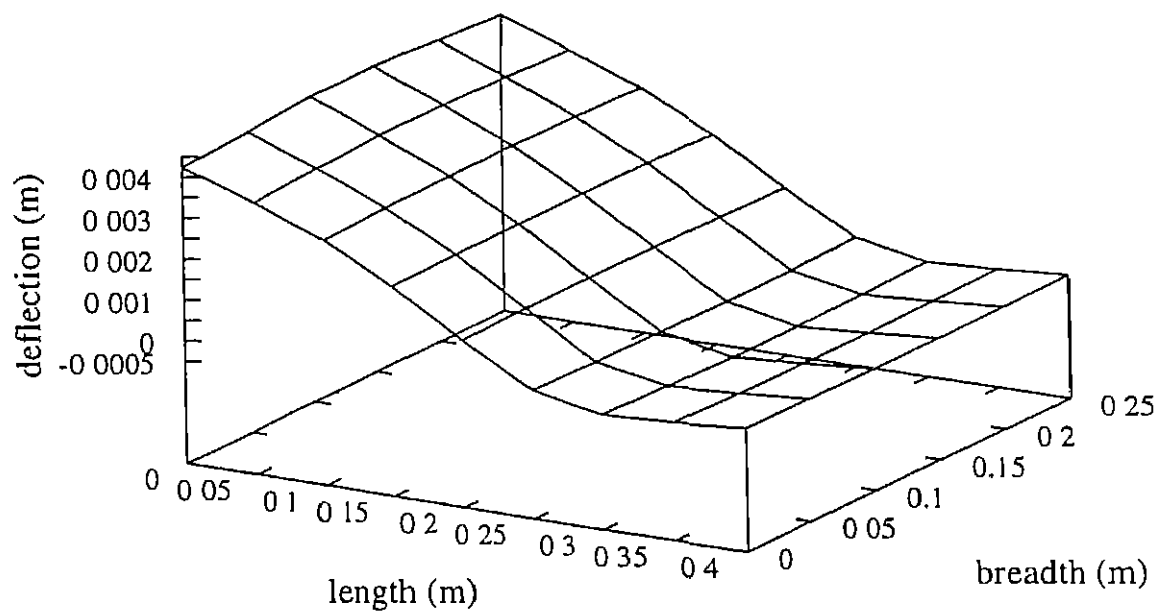


Figure 4.14 Typical Deflected Shapes of Embedded Plate

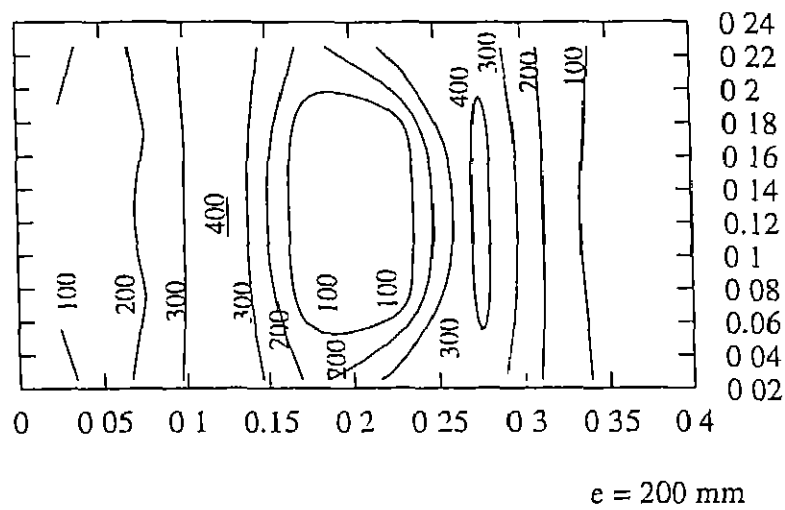
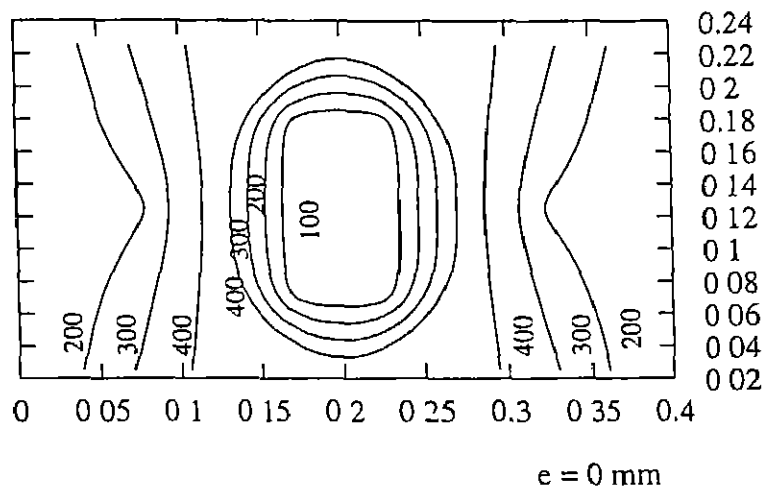


Figure 4 15: Typical Contours for Equivalent Stress

# Chapter 5

## Summary and Conclusions

### 5.1 Summary

In many Engineering applications, the cast-in-place embedded steel plates are used to support machines, equipment, pipelines etc. The plate-anchor assembly consists of steel plate, anchors and concrete base. The behavior of embedded plate anchor assembly has been studied using the mathematical model developed. The model estimates the load carrying capacity of the assembly and also provides other pertinent information regarding the assembly behavior during its loading history.

The behavior and capacity of plate-anchor assembly is dependent on relevant design parameters, e.g. dimensions of the plate, size, location and number of anchors, characteristic strength of concrete, yield strength of plate and anchors, stress-strain characteristics of materials, size of attachment and different loadings on the assembly. The factors mentioned above have an influence on the anchor forces, plate stresses, base pressure and rotation of the assembly.

A study is performed to observe the behavior of anchors due to variation in base stiffness, anchor stiffness and plate thickness for eccentric compressive loading. The behavior of anchors and assembly capacity subjected to tensile loading, is studied. A similar type of study is carried out for shear loading also. A study is made for the development of the interaction diagrams and moment-rotation charts for eccentric

compressive loading and eccentric tensile loading. Evaluation of interaction diagrams developed for the case of eccentric compressive loading, is made when shear loading is also present on the assembly in combination. Dimensional analysis is performed to develop the interaction diagrams and moment-rotation charts. Interaction diagrams and moment-rotation charts are developed adopting different ratios of dimensionless terms. The curves of the interaction diagram are useful to estimate the magnitude of the assembly capacity at failure and at collapse. The moment-rotation charts are useful to estimate the magnitude of rotation undergone by the assembly.

## 5.2 Conclusions

Following are the conclusions made from the present study

- Anchor stiffness and Base stiffness of the plate-anchor assembly influence the magnitude of anchor tension considerably.
- The increase in anchor stiffness increases the magnitude of anchor tension and increase in plate thickness decreases the magnitude of anchor tension.
- For tensile loading, increase in yield strength of anchors increases the magnitude of anchor tension, whereas, the increase in plate thickness does not have appreciable effect in the increase of anchor tension.
- Anchors of lower yield strength experience ductile anchor failure when the diameter of anchors are small.
- In case of shear loading, increase in diameter and yield strength of anchors cause increase in the assembly capacity.
- Thicker plates cause increase in assembly capacities for both eccentric compressive and tensile loading.
- In case of eccentric compressive loading, the failure of the assembly may be due to cracking of concrete, yielding of plate or yielding of anchors, and the collapse



of the assembly may be due to crushing of concrete, complete yielding of plate along with failure of anchors or failure of anchors only

- At low eccentricities of compressive loading, the failure/collapse will be due to cracking/crushing of concrete.
- At higher eccentricities of compressive loading, the failure may be due to yielding of anchors or yielding of plate and the collapse may be due to complete yielding of plate along with failure of anchors or failure of anchors only
- The capacity of the assembly at collapse is much higher than the failure load of the assembly
- Increase in area of attachment increases the assembly capacity considerably
- Increase in load eccentricity increases the assembly rotation considerably, in case of eccentric compressive loading
- Increase in thickness of the plate reduces the rotation of the assembly
- Increase in area of attachment reduces the rotation of the assembly
- The rate of increase of rotation with respect to increase in moment is relatively much lower initially (till failure of plate/anchor) than the same observed in post-failure phase of the plate/anchor
- In case of eccentric tensile loading, the failure of assembly can occur due to cracking of concrete, yielding of plate or yielding of anchors. The collapse of the assembly may be due to failure of anchors or complete yielding of anchors along with failure of anchors
- At low eccentricities of tensile loading, the assembly failure/collapse is dictated by yielding/failure of anchors
- The load carrying capacity decreases considerably in case of eccentric tensile loading in comparison to eccentric compressive loading
- In eccentric tensile loading, the rotation caused decreases with the increase in eccentricity

- Thicker plates and increase in area of attachment, decrease the rotation of the assembly in eccentric tensile loading.
- In case of eccentric compressive loading combined with shear loading, the capacity of the assembly remains constant upto some ratio of shear force to axial load for different load eccentricities
- For combined loading of eccentric compressive loading and shear force, the assembly capacity remains constant for higher values of ratio of shear force to axial compressive load
- There is a trend of convergence of assembly capacity varying within a very narrow band at relatively higher ratios of shear force to axial compressive load.
- The strength interaction diagrams and moment-rotation charts developed in the present study can be used for analysis/design of plate-anchor assemblies

### 5.3 Future Scope of Work

The model developed has the capability of predicting the behavior of the assembly, when subjected to bi-axial moments. Interaction diagrams and moment-rotation charts can be developed for bi-axial moments also. The interaction diagrams and moment-rotation charts are presently developed for some limited ratios of the design parameters. More interaction diagrams and moment-rotation charts may be provided to have better design guidelines. The moment-rotation charts can be modified with the help of regression analysis to have a characteristic curve or equation instead of providing curves for different eccentricities and thickness. Study can be performed for assemblies subjected to a combination of tension and shear.

# Bibliography

- [1] ACI 318-77(1977) " *Building Code Requirements for Reinforced Concrete*," American Concrete Institute, Detroit, Mich
- [2] ACI 349 (1990) " *Code requirements for Nuclear Safety Related Concrete Structures (ACI 349-90) and Commentary (ACI 349R-90)*
- [3] AISC (1978). " *Specifications for the design, Fabrication and Erection of Structural Steel Buildings, with commentary* ", American Institute of Steel Construction, New york, 235 pp.
- [4] ASCE (1984) " *State-of-the-Art Report on Steel Embedments*", ASCE Nuclear Structures and Materials Committee. Materials and Structural Design Committee ASCE, June 1984
- [5] Al-Khariat, H. and West, H H (1986) " *Analysis of plates by the Initial-Value Method* ", Computers and Structures, 24(3), 475-484
- [6] Armentrout, Daryl R and Burdette, Edwin G . " *Analysis of Behavior of steel liner anchorages.* ", Journal of the Structural Division, Proceedings of the American Society of Civil Engineers, Vol 108, No ST7, pp 1451-1463, July 1982
- [7] Bathe. Klaus-Jurgen, Wilson, Edward L , and Peterson, Fred L (1974) " *A Structural Analysis Program for Static and Dynamic Response of Linear Systems.* ". SAP Manual.
- [8] Bathe. Klaus-Jurgen, (1990) " *Finite Element Procedures in Engineering Analysis* ", 2nd Ed , Prentice Hall
- [9] Brown Russel H , and Whitlock. A Rhett (1983), " *Strength of Anchor Bolts in Grouted Concrete Masonry* ", Jr of Structural Engg., ASCE, Vol 109, No 6, pp 1362-1374, June 1983.
- [10] Cannon, R W , Godfrey, D A and Moreadith, F L (1981), " *Guide to the Design of Anchor Bolts and Other Steel Embedments* ", Concrete International, July 1981
- [11] Cannon, R W (1992). " *Flexible Base plates Effects of plate Flexibility and preload on Anchor Loading and Capacity,* ", ACI Structural Journal, Vol 89, No 3, pp 315-324
- [12] Celep. Zekai (1988) " *Rectangular plates resting on tensionless elastic foundation* ". Jr of Engg Mech Div., ASCE. 114(12), 2083-2092

- [13] Chakrabarti S K and Tripathi, R P (1992) " *Design of Embedded Steel Plates in Reinforced Concrete Structures* ", Structural Engineering Review, Vol 4, No 1, pp 81-91
- [14] Cohn, M Z and Maier, G (1992) " *Engineering Plasticity by Mathematical Programming* ". Proceedings of the NATO Advanced Study Institute, University of Waterloo, August 2-12
- [15] Cook, R A and Klingner, R E (1992) " *Ductile Multiple Anchor Steel To Concrete Connections* ", Jr of Str Engg, ASCE, 118(6), 1645-1655
- [16] Cook, Robert D (1974), " *Concepts and application of finite element analysis* ", Wiley, New York
- [17] Dewolf, J T (1978) " *Axially loaded column base plates* ", Jr of Str Div., ASCE, 104(ST5), 781-794
- [18] Dewolf, J T and Sarisly, E F (1978) " *Axially loaded Base Plates- Effect of Concrete Base Depth* ", Report No 78-119, Civil Engineering Department, University of Connecticut, Storrs, Conn, Aug. 1978
- [19] Dewolf, J T. and Sarisly, E F. (1980) " *Column Base plates with axial loads and moments* ", Jr of Str. Mech Div, ASCE, Vol 106, No ST11
- [20] Diluna, L.J. and Flaherty, J A (1979) " *An assessment of the effect of plate flexibility on the design of moment resisting base plates* ", paper contributed by the Pressure Vessels and Piping Division of the ASME for presentation at the Pressure Vessels and Piping Conference, San Francisco, California. 25-29 June 1979
- [21] McGraw, W (1968), " *steel structures* ", Prentice Hall, London
- [22] Hrabok, M M and Hruby, T M (1984) " *A review and catalogue of plate bending finite elements* ", Computers and Structures 19(3), 479-495
- [23] IS 456, (1978) " *Indian Code of practice for Plain and Reinforced Concrete* ", Indian Standard Institution, New Delhi India, 1978
- [24] Kallol, Joseph J (1993), " *An Experimental Investigation of the behavior of Plate Anchor Assembly Embedded in Concrete* ". M Tech Thesis, Department of Civil Engg, Indian Institute of Technology, Kanpur, July, 1993
- [25] Klingner, R E and Mendonca, J.A (1982). " *Tensile Capacity of Short Anchor Bolts and Welded Struts A Literature Review* ", ACI Journal, July-Aug, 1982
- [26] Klingner, R E and Mendonca, J A (1982). " *Shear Capacity of Short Anchor Bolts and Welded Struts A Literature Review* ", ACI Journal, Sept-Oct, 1982
- [27] Kamiya, N (1977) " *Circular plates resting on bimodulus and no tension foundations* ". Jr of Engg Mech Div., ASCE, 103(6), 1161-1164
- [28] McGuire, W (1968), " *Steel Structures* ", Prentice Hall, London
- [29] Mishra R C and Chakrabarti, S K (1995). " *Rectangular Plates Resting on Tensionless Elastic Foundation* ", Jr of Engg Mech, ASCE, p 385-387 April 1996
- [30] PCI Design Handbook (1970), " *Precast and Prestressed Concrete* ", 2nd Ed., Prestressed Concrete Institute Chicago

- [31] Reissner, E (1958) *A Note on Deflections of Plates on a Visco-elastic foundations*, Jr of Applied Mech, Trans ASME, 1958, p 144-145
- [32] Salmon, Charles G, Schenker, L, and Johnston B G (1957), *Moment -Rotation Characteristics of Column Anchorage* ", Transcation, ASCE, Vol 122, 1957, pp 132-154
- [33] Save, M A and Massonnet, C E (1972) " *Plastic analysis and design of plates, shells and disks* ", North-Holland Pub 1972
- [34] Shull, H E and Hu, L W (1963) " *Load carrying capacities of simply supported rectangular plates* ", Trans of ASME, Jr of Apphed Mech 30(12), 617
- [35] Sinha, S N (1963) " *Large Deflection of plates on elastic foundations* ", Jr Engg Mech Div Proc ASCE, 89(EM1), 1-24
- [36] Szilard, R (1974) " *Theory and analysis of plates* ", Prentice Hall, 1st ed
- [37] Thambiratnam, David P and Paramasivam, P. (1986) " *Base plates under axial loads and moments* ", Jr of Str Engg, ASCE. 112(5), 1166-1181
- [38] Timoshenko, S. P and Krieger, W " *Theory of plates and Shells* ", McGraw Hill Book Co .2nd ed ,1970
- [39] Turvey, G J (1984). " *Effect of shear deformation on the yielding of circular plates* ", Computers and Structures , 18(2), 307-310
- [40] Ueda, T, Kitipornchai, S, and Ling, K. (1990), " *Experimental Investigation of Anchor Bolts under shear* ", Journal of Structural Engineering, American Society of Civil Engineers, Vol.116, No 4, April, 1990
- [41] Villaggio, P (1983) " *A free boundary value problem in plate theory* ", Jr of App Mech Trans, ASME, 50(2), 297-302
- [42] Winkler (1970) " *On foundations that react in compression only* ", Jr of App Mech. Div Trans., ASME, 37(4), 1019-1030
- [43] Weitsman, Y (1970) " *On foundations that react in compression only* " Jr of App Mech. Div Trans, ASME, 37(4), 1019-1030
- [44] Yuan, Fuh Gwo et al (1992) " *Improved rectangular elements for shear deformable Plates* ", Jr of Engg Mech, ASCE, Vol 118, No 2
- [45] R C Mishra (1995), " *Non-Linear Modelling of Embedded Plate Prediction of Capacity and Behavior* ", Ph.D Thesis Department of Civil Engg, Indian Institute of Technology, Kanpur, July, 1995

# Appendix-I

The usage of the interaction diagram and the moment-rotation charts, that are developed in the present study are demonstrated through the following design examples for embedded plate-anchor assemblies

$A_{atch}$  = Area of Attachment,

$A_{plate}$  = Area of Plate,

$A_{anc}$  = Area of Anchor,

$s_1, s_2$  = Spacing of Anchors in either direction,

$P$  = Axial Load,

$M$  = Uni-axial Moment,

$f_{ck}$  = Characteristic Strength of Concrete

$f_y$  = Yield Strength of Plate,

$f'_y$  = Yield Strength of Anchor,

$B, D, t$  = Dimensions of the Plate,

$\theta$  = Rotation of the Assembly,

Example 1 ( For a Plate-Anchor Assembly subjected to Eccentric Compressive Loading )

Design of an embedded plate-anchor assembly with base-concrete of characteristic strength  $25 \text{ N/mm}^2$ , steel plate of yield strength  $300 \text{ N/mm}^2$  and M.S. anchors of

yield strength  $330 \text{ N/mm}^2$  subjected to an eccentric compressive load of  $1000 \text{ kN}$  at an eccentricity of  $100 \text{ mm}$  at failure

$$P = 1000 \text{ kN}$$

$$M = P \times e$$

$$= 1000 \times 0.1$$

$$= 100 \text{ kNm}$$

Assuming  $A_{atch}/A_{plate} = 0.1$  and  $A_{anc}/s_1 s_2 = 0.0032$  and using the interaction diagram for failure load. (Fig 4.1)

Consider a plate size of  $600 \text{ mm} \times 400 \text{ mm}$

$$M/f_{ck} B D^2 = 100.0 / (25000 \times 0.4 \times 0.6^2)$$

$$= 0.0277$$

$$P/f_{ck} B D = 1000.0 / (25000 \times 0.4 \times 0.6)$$

$$= 0.167$$

From the interaction diagram provided for the ratios mentioned earlier, a thickness of  $40 \text{ mm}$  is obtained

$$\text{Plate dimensions} = 600 \text{ mm} \times 400 \text{ mm} \times 40 \text{ mm}$$

$$\text{Area of Attachment} = 0.1 \times 600 \times 400$$

$$= 24000 \text{ mm}^2$$

$$\text{Assuming the Anchor diameter} = 12 \text{ mm}$$

$$\text{Edge distance } d' = 2 \times 12$$

$$= 24 \text{ mm say } 25 \text{ mm}$$

$$s_2 = (400 - 25 - 25) / 2$$

$$= 175 \text{ mm}$$

$$\begin{aligned}
 s_1 &= A_{anc}/s_2 \times 0.0032 \\
 &= 113.00/(175 \times 0.0032) \\
 &= 201 \text{ mm}
 \end{aligned}$$

Provide 4 anchors in long direction at a spacing of 183 mm c/c and at an edge distance of 25 mm

Now, for the designed plate-anchor assembly, the capacity at collapse can be estimated using the interaction diagram (Fig 4.2) as per the following .

Dimensions of Plate from failure load criteria = 600 mm x 400 mm x 40 mm

From the envelope of 40mm thick plate in Fig 4.2 (interaction diagram at collapse for eccentric compressive loading)

$$\begin{aligned}
 f_{ck}BD &= 25000 \times 0.4 \times 0.6 \\
 &= 6000 \text{ kN}
 \end{aligned}$$

$$\begin{aligned}
 f_{ck}BD^2 &= 25000 \times 0.4 \times 0.6^2 \\
 &= 3600 \text{ kN-m}
 \end{aligned}$$

$$\begin{aligned}
 \text{Selecting } P/(f_{ck}BD) &= 0.4 \\
 P &= 0.4 \times 6000 \\
 &= 2400 \text{ kN}
 \end{aligned}$$

$$\begin{aligned}
 \text{Corresponding } M/(f_{ck}BD^2) &= 0.0094 \\
 M &= 0.0094 \times 3600 \\
 &= 338.4 \text{ kN-m}
 \end{aligned}$$

$$\begin{aligned}
 M/P &= (338.4/2400.0) \\
 &= 0.141 > 0.1
 \end{aligned}$$

$$\begin{aligned}
 \text{Hence, Selecting } P/(f_{ck}BD) &= 0.5 \\
 P &= 0.5 \times 6000
 \end{aligned}$$



$$= 3000 \text{ kN}$$

$$\text{Corresponding } M/(f_{ck}BD^2) = 0.00833$$

$$M = 0.00833 \times 3600$$

$$= 300.0 \text{ kNm}$$

$$M/P = (300.0/3000.0)$$

$$= 0.1$$

We can observe that the size of plate 600 mm x 400 mm x 40 mm has the capacity equal to three times the failure load at collapse

For the same loading condition, the ratios considered are different i.e. ( $A_{atch}/A_{plate}=0.2$  and  $A_{anc}/s_1s_2=0.0032$ ), the interaction diagram used is for failure load (Fig. 4.3) subjected to loads,  $P=1000 \text{ kN}$  and  $M=100 \text{ kNm}$

Consider a plate size of 500 mm X 300 mm

$$\begin{aligned} M/f_{ck}BD^2 &= 100.0/(25000 \times 0.3 \times 0.5^2) \\ &= 0.053 \end{aligned}$$

$$\begin{aligned} P/f_{ck}BD &= 1000.0/(25000 \times 0.3 \times 0.5) \\ &= 0.267 \end{aligned}$$

From the interaction diagram provided for the ratios mentioned earlier, a thickness of 40 mm is obtained

$$\text{Plate dimensions} = 500 \text{ mm} \times 300 \text{ mm} \times 40 \text{ mm}$$

$$\begin{aligned} \text{Area of Attachment} &= 0.2 \times 500 \times 300 \\ &= 30000 \text{ mm}^2 \end{aligned}$$

$$\text{Assuming the Anchor diameter} = 12 \text{ mm}$$

$$\text{Edge distance } d' = 2 \times 12$$

$$\begin{aligned}
 &= 24 \text{ mm, say } 25 \text{ mm} \\
 s_2 &= (300 - 25 - 25) \\
 &= 250 \text{ mm} \\
 s_1 &= A_{anc}/s_2 \times 0.0032 \\
 &= 113.00/(250 \times 0.0032) \\
 &= 141.25 \text{ mm}
 \end{aligned}$$

Provide 4 anchors in long direction at a spacing of 140 mm c/c with an edge distance of 40 mm

Now, for the designed plate-anchor assembly, the capacity at collapse can be estimated using the interaction diagram (Fig 4.4) as per the following

Dimensions of Plate from failure load criteria = 500 mm x 300 mm x 40 mm

From the envelope of 40mm thick plate in Fig 4.4 (interaction diagram at collapse for eccentric compressive loading)

$$\begin{aligned}
 f_{ck}BD &= 25000 \times 0.3 \times 0.5 \\
 &= 3750 \text{ kN} \\
 f_{ck}BD^2 &= 25000 \times 0.3 \times 0.5^2 \\
 &= 1875 \text{ kN-m}
 \end{aligned}$$

$$\begin{aligned}
 \text{Selecting } P/(f_{ck}BD) &= 0.6 \\
 P &= 0.6 \times 3750 \\
 &= 2250 \text{ kN}
 \end{aligned}$$

$$\begin{aligned}
 \text{Corresponding } M/(f_{ck}BD^2) &= 0.15 \\
 M &= 0.15 \times 1875 \\
 &= 281.25 \text{ kN-m} \\
 M/P &= (281.25/2250.00)
 \end{aligned}$$

$$\begin{aligned}
 &= 0.125 > 0.1 \\
 \text{Hence, Selecting } P/(f_{ck}BD) &= 0.7 \\
 P &= 0.7 \times 3750 \\
 &= 2625 \text{ kN} \\
 \text{Corresponding } M/(f_{ck}BD^2) &= 0.14 \\
 M &= 0.14 \times 1875 \\
 &= 262.5 \text{ kNm} \\
 M/P &= (262.5/2625) \\
 &= 0.1
 \end{aligned}$$

We can observe that the size of plate 500 mm x 300 mm x 40 mm has much higher collapse load than the failure load

For the same designed plate-anchor assembly, the estimation of assembly rotation at failure and at collapse, can be made as per the following .

From strength criteria, for a load  $P=1000 \text{ kN}$  and  $M=100 \text{ kNm}$  at failure, a plate is designed having dimensions 600 mm x 400 mm x 40mm, considering the ratios ( $A_{atch}/A_{plate}=0.1$  and  $A_{anc}/s_1s_2=0.0032$ )

$$M/f_{ck}BD^2 = 0.0277 \text{ (calculated earlier)}$$

$$e = 100 \text{ mm}$$

For the same ratios, the maximum rotation can be obtained from moment-rotation charts provided. For thickness of 40 mm and the ratios mentioned above, the moment-rotation chart is provided in Fig. 4.5 (c). The rotation possible for the plate is 0.0015 radians.

Now, for this designed plate-anchor assembly, the rotation at collapse can be estimated

using the moment-rotation chart Fig. 4.5 (c) The moment resisted by the plate 600 mm x 400 mm x 40 mm at collapse is 300 kN-m

$$\begin{aligned} M/f_{ck}BD^2 &= 300\,00/(25000.0 \times 0.4 \times 0.6^2) \\ &= 0.0833 \end{aligned}$$

The rotation possible for the plate is 0.0102 radians

For the ratios of  $A_{atch}/A_{plate}=0.2$  and  $A_{anc}/s_1s_2=0.0032$ , and the plate dimensions from strength criteria are 500 mm x 300 x 40 mm, the moment-rotation charts is provided in Fig. 4.6 (c) for thickness 40mm

$$\begin{aligned} M/f_{ck}BD^2 &= 100\,0/(25000.0 \times 0.3 \times 0.5^2) \\ &= 0.053 \end{aligned}$$

The rotation possible for the plate is 0.001 radians

Now, for this designed plate-anchor assembly, the rotation at collapse can be estimated using the moment-rotation chart Fig. 4.6 (c) The moment resisted by the plate 500 mm x 300 mm x 40 mm at collapse is 262.50 kN-m

$$\begin{aligned} M/f_{ck}BD^2 &= 262\,50/(25000.0 \times 0.3 \times 0.5^2) \\ &= 0.14 \end{aligned}$$

The rotation possible for the plate is 0.012 radians

Example 2 ( For a Plate-Anchor Assembly subjected to Eccentric Tensile Loading.)

Design of an embedded plate-anchor assembly with base-concrete of characteristic strength  $25 \text{ N/mm}^2$ , steel plate of yield strength  $300 \text{ N/mm}^2$  and M.S anchors of yield strength  $330 \text{ N/mm}^2$  subjected to an eccentric tensile load of  $150 \text{ kN}$  at an eccentricity of  $100 \text{ mm}$  at failure

$$P = 150 \text{ kN}$$

$$M = P \times e$$

$$= 150 \times 0.1$$

$$= 15 \text{ kNm}$$

Assuming  $A_{atch}/A_{plate} = 0.1$  and  $A_{anc}/s_1 s_2 = 0.0032$  and using the interaction diagram for failure load (Fig 4.7)

Consider a plate size of  $600 \text{ mm} \times 400 \text{ mm}$

$$M/f_{ck}BD^2 = 15.0/(25000 \times 0.4 \times 0.6^2)$$

$$= 0.0041$$

$$P/f_{ck}BD = 150.0/(25000 \times 0.4 \times 0.6)$$

$$= 0.025$$

From the interaction diagram provided for the ratios mentioned earlier, a thickness of  $25 \text{ mm}$  is obtained

Plate dimensions

$600 \text{ mm} \times 400 \text{ mm} \times 25 \text{ mm}$

Area of Attachment

$= 0.1 \times 600 \times 400$

$$\begin{aligned}
 &= 24000 \text{ mm}^2 \\
 \text{Assuming the Anchor diameter} &= 12 \text{ mm} \\
 \text{Edge distance } d' &= 2 \times 12 \\
 &= 24 \text{ mm, say } 25 \text{ mm} \\
 s_2 &= (400 - 25 - 25)/2 \\
 &= 175 \text{ mm} \\
 s_1 &= A_{anc}/s_2 \times 0.0032 \\
 &= 113.00/(175 \times 0.0032) \\
 &= 201 \text{ mm}
 \end{aligned}$$

Provide 4 anchors in long direction at a spacing of 183 mm c/c and at an edge distance of 25 mm

Now, for the designed plate-anchor assembly, the capacity at collapse can be estimated using the interaction diagram (Fig. 4.8) as per the following :

Dimensions of Plate from failure load criteria = 600 mm x 400 mm x 25 mm

From the envelope of 25mm thick plate in Fig. 4.8 (interaction diagram at collapse for eccentric tensile loading)

$$\begin{aligned}
 f_{ck}BD &= 25000 \times 0.4 \times 0.6 \\
 &= 6000 \text{ kN} \\
 f_{ck}BD^2 &= 25000 \times 0.4 \times 0.6^2 \\
 &= 3600 \text{ kN-m} \\
 \text{Selecting } P/(f_{ck}BD) &= 0.05 \\
 P &= 0.05 \times 6000 \\
 &= 300 \text{ kN} \\
 \text{Corresponding } M/(f_{ck}BD^2) &= 0.024
 \end{aligned}$$

$$\begin{aligned}
 M &= 0.024 \times 3600 \\
 &= 86.40 \text{ kNm} \\
 M/P &= (86.40/300.00) \\
 &= 0.288 > 0.1
 \end{aligned}$$

Hence, Selecting  $P/(f_{ck}BD) = 0.075$

$$\begin{aligned}
 P &= 0.075 \times 6000 \\
 &= 450 \text{ kN}
 \end{aligned}$$

Corresponding  $M/(f_{ck}BD^2) = 0.0125$

$$\begin{aligned}
 M &= 0.0125 \times 3600 \\
 &= 45 \text{ kNm} \\
 M/P &= (45.0/450.0) \\
 &= 0.1
 \end{aligned}$$

We can observe that the size of plate 600 mm x 400 mm x 25 mm has the capacity equal to three times the failure load at collapse

For the same loading condition, the ratios considered are different i.e. ( $A_{slab}/A_{plate}=0.2$  and  $A_{slab}/s_1s_2=0.0032$ ), the interaction diagram used is for failure load (Fig. 4.9) subjected to loads,  $P=150 \text{ kN}$  and  $M=15 \text{ kNm}$

Consider a plate size of 600 mm X 400 mm

$$\begin{aligned}
 M/f_{ck}BD^2 &= 15.0/(25000 \times 0.4 \times 0.6^2) \\
 &= 0.0041 \\
 P/f_{ck}BD &= 150.0/(25000 \times 0.4 \times 0.6) \\
 &= 0.025
 \end{aligned}$$

From the interaction diagram provided for the ratios mentioned earlier, a thickness of 16 mm is obtained

Plate dimensions	600 mm x 400 mm x 16 mm
Area of Attachment	$= 0.2 \times 600 \times 400$ $= 48000 \text{ mm}^2$
Assuming the Anchor diameter	$= 12 \text{ mm}$
Edge distance $d'$	$= 2 \times 12$ $= 24 \text{ mm, say } 25 \text{ mm}$
$s_2$	$= (400 - 25 - 25)/2$ $= 175 \text{ mm}$
$s_1$	$= A_{anc}/s_2 \times 0.0032$ $= 113.00/(175 \times 0.0032)$ $= 201 \text{ mm}$

Provide 4 anchors in long direction at a spacing of 183 mm c/c with an edge distance of 25 mm

Now for the designed plate-anchor assembly, the capacity at collapse can be estimated using the interaction diagram (Fig 4.10) as per the following .

Dimensions of Plate from failure load criteria  $= 600 \text{ mm} \times 400 \text{ mm} \times 16 \text{ mm}$

From the envelope of 16mm thick plate in Fig 4.4 (interaction diagram at collapse for eccentric tensile loading)

$$f_{ck}BD = 25000 \times 0.4 \times 0.6$$

$$= 6000 \text{ kN}$$

$$f_{ck}BD^2 = 25000 \times 0.4 \times 0.6^2$$

$$= 3600 \text{ kNm}$$

$$\text{Selecting } P/(f_{ck}BD) = 0.08$$

$$P = 0.08 \times 6000$$



$$\begin{aligned}
 &= 480 \text{ kN} \\
 \text{Corresponding } M/(f_{ck}BD^2) &= 0.01 \\
 M &= 0.01 \times 3600 \\
 &= 36 \text{ kNm} \\
 M/P &= (36.0/480.0) \\
 &= 0.075 < 0.1 \\
 \text{Hence, Selecting } P/(f_{ck}BD) &= 0.075 \\
 P &= 0.075 \times 6000 \\
 &= 450 \text{ kN} \\
 \text{Corresponding } M/(f_{ck}BD^2) &= 0.0125 \\
 M &= 0.0125 \times 3600 \\
 &= 45 \text{ kNm} \\
 M/P &= (45.0/450.0) \\
 &= 0.1
 \end{aligned}$$

We can observe that the size of plate 600 mm x 400 mm x 16 mm has the capacity equal to thrice the failure load at collapse of the assembly

For the same designed plate-anchor assembly, the estimation of assembly rotation at failure and at collapse, can be made as per the following

From strength criteria for a load  $P=150 \text{ kN}$  and  $M=15 \text{ kNm}$  at failure, a plate is designed having dimensions 600 mm x 400 mm x 25mm, considering the ratios ( $A_{atch}/A_{plate}=0.1$  and  $A_{anc}/s_1s_2=0.0032$ ).

$$\begin{aligned}
 M/f_{ck}BD^2 &= 0.0041 \text{ (calculated earlier)} \\
 e &= 100 \text{ mm}
 \end{aligned}$$

For the same ratios, the maximum rotation can be obtained from moment-rotation

charts provided. For thickness of 25 mm and the ratios mentioned above, the moment-rotation chart is provided in Fig. 4.11 (b). The rotation possible for the plate is 0.001 radians.

Now, for this designed plate-anchor assembly, the rotation at collapse can be estimated using the moment-rotation chart Fig. 4.11 (b). The moment resisted by the plate 600 mm x 400 mm x 25 mm at collapse is 45 kNm.

$$\begin{aligned} M/f_{ck}BD^2 &= 45.00/(25000.0 \times 0.4 \times 0.6^2) \\ &= 0.0125 \end{aligned}$$

The rotation possible for the plate is 0.005 radians.

For the ratios of  $A_{anch}/A_{plate}=0.2$  and  $A_{anc}/s_1s_2=0.0032$ , and the plate dimensions from strength criteria are 600 mm x 400 x 16 mm, the moment-rotation chart is provided in Fig. 4.12 (a) for thickness 16mm.

$$\begin{aligned} M/f_{ck}BD^2 &= 15.0/(25000.0 \times 0.4 \times 0.6^2) \\ &= 0.0041 \end{aligned}$$

The rotation possible for the plate is 0.0004 radians.

Now, for this designed plate-anchor assembly, the rotation at collapse can be estimated using the moment-rotation chart Fig. 4.12 (a). The moment resisted by the plate 600 mm x 400 mm x 16 mm at collapse is 45 kNm.

$$\begin{aligned} M/f_{ck}BD^2 &= 45.0/(25000.0 \times 0.4 \times 0.6^2) \\ &= 0.0125 \end{aligned}$$

The rotation possible for the plate is 0.004 radians

Example 3 ( For a Plate-Anchor Assembly subjected to Eccentric Compressive Loading along with Shear load )

Design of an embedded plate-anchor assembly with base-concrete of characteristic strength  $25 \text{ N/mm}^2$ , steel plate of yield strength  $300 \text{ N/mm}^2$  and M S anchors of yield strength  $330 \text{ N/mm}^2$  subjected to an eccentric compressive load of  $800 \text{ kN}$  at an eccentricity of  $100 \text{ mm}$  in combination with a shear force of  $320 \text{ kN}$  at Collapse

Axial Compressive Load (P) =  $800 \text{ kN}$

Shear Force (H) =  $320 \text{ kN}$

Ratio of H/P =  $320/800$   
= 0.4

M =  $P \times e$   
=  $800 \times 0.1$   
=  $80 \text{ kNm}$

Referring Figs 3.8-3.12, the embedded plate has to be designed for  $e=100\text{mm}$ ,  $H/P$  as 0.4, and  $P=800 \text{ kN}$ . A size of 32 mm thick plate of dimensions  $400 \text{ mm} \times 250 \text{ mm}$  is obtained from Fig 3.11

Dimensions of the Plate =  $400 \text{ mm} \times 250 \text{ mm} \times 32 \text{ mm}$

The same design can be obtained from the interaction diagram provided in Fig 4.2 (at collapse). Considering the size of plate as 400 mm x 250 mm

$$\text{Axial Compressive Load (P)} = 800 \text{ kN}$$

$$\text{Moment (M)} = 80 \text{ kNm}$$

$$\begin{aligned} P/(f_{ck}BD) &= 800.0 / (25000 \times 0.25 \times 0.40) \\ &= 0.32 \end{aligned}$$

$$\begin{aligned} M/(f_{ck}BD^2) &= 80.0 / (25000 \times 0.25 \times 0.40^2) \\ &= 0.08 \end{aligned}$$

For the above values, the thickness obtained is 32 mm from the interaction diagram and the plate dimensions are 400 mm x 250 mm x 32 mm

From the Fig 3.11, for H/P ratio as 1.0 developed for 32mm, it is observed that the Assembly Capacity is 250 kN i.e. P=250 kN, H=250 kN and e=100mm

$$\begin{aligned} M &= P \times e \\ &= 250 \times 0.1 \\ &= 25 \text{ kNm} \end{aligned}$$

From the interaction diagram (Fig 4.2),

$$\begin{aligned} P/(f_{ck}BD) &= 250.0 / (25000 \times 0.25 \times 0.4) \\ &= 0.1 \end{aligned}$$

$$\begin{aligned} M/(f_{ck}BD^2) &= 25.0 / (25000 \times 0.25 \times 0.4^2) \\ &= 0.025 \end{aligned}$$

The thickness obtained from the interaction diagram is 10mm i.e., the plate dimensions are 400 mm x 250 mm x 10 mm

This indicates that for higher ratios of  $H/P$  ( as mentioned in Section 3.7 ), interaction diagrams which are developed for eccentric compressive loading cannot be used, when shear force is acting combinedly with eccentric compressive loading

## Appendix-II

The dimensional analysis deals with the process of involving all the important factors of a physical phenomenon in a systematically organised manner in the form of dimensionless terms. After doing the dimensional analysis, the problem is generalised and the need for a particular system of units is eliminated. The various parameters involved in the plate-anchor assemblies are stated below and the dimensions of these quantities are stated in brackets in Force-Length-Time (F-L-T) system.

$t$  = thickness of the plate  $[L]$

$B$  = breadth of the plate  $[L]$

$D$  = length of the plate  $[L]$

$A_{atch}$  = Area of the attachment  $[L^2]$

$A_{base}$  = Area of concrete base  $[L^2]$

$A_{plate}$  = Area of plate  $[L^2]$

$A_{anc}$  = Area of anchor  $[L^2]$

$s_1, s_2$  = spacing of anchors in either directions of the plate  $[L]$

$f_y$  = yield strength of plate  $[FL^{-2}]$

$f'_y$  = yield strength of anchor  $[FL^{-2}]$

$f_{ck}$  = characteristic strength of concrete  $[FL^{-2}]$

$d'$  = edge distance of anchors from plate boundary  $[L]$

$P$  = Axial Load  $[F]$

$M$  = Moment  $[FL]$

The dimensional analysis is done with the help of Buckingham's  $\pi$ -theorem. The

number of primary dimensions among all the parameters are only two, namely the Force and the Length. The total number of parameters are 14

$$\begin{aligned}
 \text{total number of parameters}(m) &= 14 \\
 \text{Number of primary variables}(n) &= 2 \\
 \text{Number of dimensionless terms} &= m - n \\
 &= 12
 \end{aligned}$$

$$\pi = [\text{repeating variable}]^p [\text{repeating variable}]^q [\text{non-repeating variable}]$$

Considering the breadth of plate ' $B$ ' and characteristic strength of concrete ' $f_{ck}$ ' as repeating variables,  $p$  and  $q$  are the constants to be determined to establish a relationship between various parameters. Among other variables, each one is taken as non-repeating in turn and various primary dimensions of the equation are equated to zero in each turn. In each of the equations below, the first term on the R H S is the primary dimension of the breadth of the plate, the second term is the characteristic strength of concrete ' $f'_{ck}$ ' and the third term represents the primary dimension of the non-repeating variable ' $t$ '. The details of the non-repeating variables are shown in brackets for all the equations

$$\pi_1 = [L]^p [FL^{-2}]^q [L] \quad (\text{thickness } 't' )$$

$$p - 2q + 1 = 0, \quad q = 0, \quad p = -1, \quad \pi_1 = t/B \quad (.1)$$

$$\pi_2 = [L]^p [FL^{-2}]^q [L] \quad (\text{length of plate } 'd' )$$

$$p - 2q + 1 = 0; \quad q = 0; \quad p = -1, \quad \pi_2 = d/B, \quad (.2)$$

$$\pi_3 = [L]^p [FL^{-2}]^q [L^2] \quad (\text{Area of attachment } 'A_{atch}' )$$

$$p - 2q + 2 = 0, \quad q = 0, \quad p = -2; \quad \pi_3 = A_{att}/B^2 \quad (.3)$$

$$\pi_4 = [L]^p [FL^{-2}]^q [L^2] \quad (\text{Area of plate } 'A_{plate}')$$

$$p - 2q + 2 = 0, \quad q = 0, \quad p = -2, \quad \pi_4 = A_p/B^2 \quad (4)$$

$$\pi_5 = [L]^p [FL^{-2}]^q [L^2] \quad (\text{Area of base } 'A_{base}')$$

$$p - 2q + 2 = 0, \quad q = 0, \quad p = -2, \quad \pi_5 = A_{base}/B^2 \quad (5)$$

$$\pi_6 = [L]^p [FL^{-2}]^q [L^2] \quad (\text{Area of anchor } 'A_{anc}')$$

$$p - 2q + 2 = 0, \quad q = 0, \quad p = -2, \quad \pi_6 = A_{anc}/B^2 \quad (6)$$

$$\pi_7 = [L]^p [FL^{-2}]^q [L] \quad (\text{Spacing of anchor } 's_1')$$

$$p - 2q + 1 = 0, \quad q = 0, \quad p = -1; \quad \pi_7 = s_1/B \quad (7)$$

$$\pi_8 = [L]^p [FL^{-2}]^q [L] \quad (\text{Spacing of anchor } 's_2')$$

$$p - 2q + 1 = 0, \quad q = 0, \quad p = -1, \quad \pi_8 = s_2/B \quad (8)$$

$$\pi_9 = [L]^p [FL^{-2}]^q [FL^{-2}] \quad (\text{yield strength of plate } 'f_y')$$

$$p - 2q - 2 = 0, \quad q + 1 = 0, \quad q = -1; \quad p = 0, \quad \pi_9 = f_y/f_{ck} \quad (9)$$

$$\pi_{10} = [L]^p [FL^{-2}]^q [L] \quad (\text{edge distance } 'd')$$

$$p - 2q + 1 = 0, \quad q = 0; \quad p = -1; \quad \pi_{10} = d/B \quad (10)$$

$$\pi_{11} = [L]^p [FL^{-2}]^q [F] \quad (\text{Axial Load } 'P')$$

$$p - 2q = 0; \quad q + 1 = 0; \quad q = -1, \quad p = 0. \quad \pi_{11} = P/(f_{ck}B^2) \quad (11)$$



$$\pi_{12} = [L]^p [FL^{-2}]^q [FL] \quad (\text{Moment } M))$$

$$p - 2q + 1 = 0, \quad q + 1 = 0; \quad q = -1; \quad p = 3, \quad \pi_{12} = M/(f_{ck}B^3) \quad (.12)$$

The product or reciprocal of  $\pi$  terms are also non-dimensional. The various  $\pi$ -terms involved in the analysis are -

$$\begin{aligned} \pi_1 &= t/b, & \pi_2 &= d/b; & \pi_3 &= A_{atch}/b^2, & \pi_4 &= A_p/B^2; \\ \pi_5 &= A_{base}/B^2, & \pi_6 &= A_{anc}/B^2, & \pi_7 &= s_1/B; & \pi_8 &= s_2/B; \\ \pi_9 &= f_y/f_{ck}, & \pi_{10} &= d'/B, & \pi_{11} &= P/(f_{ck}B^2), & \pi_{12} &= M/(f_{ck}B^3) \end{aligned}$$

Considering the importance of different parameters, the product and division of different  $\pi$ -terms are done to have a realistic relation between the parameters

$$\begin{aligned} \pi_{11}/\pi_2 &= P/(f_{ck}BD) \\ \pi_{12}/\pi_2^2 &= M/(f_{ck}BD^2) \\ \pi_6/(\pi_7\pi_8) &= A_{anc}/(s_1s_2) \\ \pi_3/\pi_4 &= A_{atch}/A_{plate} \end{aligned}$$

123314

**Date Slip** 123314

This book is to be returned on the  
date last stamped.

[illegible]

CE-1997-M-PAN-BEH